



Prediction and Mitigation of Methane Explosions Effects for Improved Protection of Mine Infrastructure and Critical Equipment

(EXPRO)

FINAL REPORT

Prediction and Mitigation of Methane Explosions Effects for Improved Protection of Mine Infrastructure and Critical Equipment (EXPRO)

European Commission

Directorate-General for Research and Innovation

Directorate D - Industrial Technologies

Unit D.4 — Coal and Steel

Contact Hervé Martin

E-mail RTD-PUBLICATIONS@ec.europa.eu

European Commission

B-1049 Brussels

Manuscript completed in 2019.

This document has been prepared for the European Commission however it reflects the views only of the authors, and the Commission cannot be held responsible for any use which may be made of the information contained therein.

More information on the European Union is available on the internet (<http://europa.eu>).

Luxembourg: Publications Office of the European Union, 2019

PDF

ISBN 978-92-79-98308-5

ISSN 1831-9424

doi: 10.2777/609898

KI-NA-29-525-EN-N

© European Union, 2019.

Reuse is authorised provided the source is acknowledged. The reuse policy of European Commission documents is regulated by Decision 2011/833/EU (OJ L 330, 14.12.2011, p. 39).

For any use or reproduction of photos or other material that is not under the EU copyright, permission must be sought directly from the copyright holders.

All pictures, figures and graphs © Central Mining Institute, RFCR-CT-2014-00005 EXPRO

European Commission

Research Fund for Coal and Steel

Prediction and Mitigation of Methane Explosions Effects for Improved Protection of Mine Infrastructure and Critical Equipment (EXPRO)

Krzysztof Cybulski

Central Mining Institute, Plac Gwarków 1, PL-40-166 Katowice, Poland

Zdzislaw Dyduch, Robert Hildebrandt, Jacek Skiba, Ksawery Graboś
Główny Instytut Górnictwa (GIG), ul. Podleska 72, 43-190 Mikołow - Poland Name

José Luis Fuentes-Cantillana, Pedro Morillo, Florencio Fernández
Asociación Para La Investigación y Desarrollo Industrial de Los Recursos Naturales (AITEMIN),
c\ Margarita Salas 14, ES-28918 Leganés (Madrid) - Spain

Benjamin Truchot, Emmanuel Leprette

Institut National de l'Environnement Industriel et des Risques (INERIS), Parc Technologique ALATA.
BP 2. F 60550 Verneuil-en-halatte - France

Marcin Małachowski, Andrzej Turek

Instytut Technik Innowacyjnych EMAG (EMAG), ul. Leopolda 31, 40-189 Katowice - Poland

Fernando Ordás, Luis Manuel Álvarez

Fundación Santa Bárbara (FSB), C/ Aguilonjos s/n 24310 La Ribera de Folgoso (León) - Spain

Klaudiusz Szczerba

Polska Grupa Górnicza (PGG), ul. Powstancow 30, PL-40-039 Katowice - Poland

Maksym Shyshoy, Vadim Miroshnichenko, Aleksey Zhukovskiy
DTEK Energy (DTEK), Ukraine, 01032, Str. Leo Tolstoy 57 - Ukraine

Grant Agreement RFFC-CT-2014-00005
01/07/2014 to 31/12/2017

Final report

Directorate-General for Research and Innovation

1 TABLE OF CONTENTS

| | |
|---|-----------|
| 1 TABLE OF CONTENTS | 3 |
| 2 FINAL SUMMARY | 7 |
| 3 SCIENTIFIC AND TECHNICAL DESCRIPTION OF THE RESULTS | 11 |
| 3.1 OBJECTIVES OF THE PROJECT | 11 |
| 3.2 COMPARISON OF INITIALLY PLANNED ACTIVITIES AND WORK ACCOMPLISHED | 11 |
| 3.3 DESCRIPTION OF ACTIVITIES AND DISCUSSION..... | 12 |
| 3.3.1 <i>WP2 – Development and calibration of explosion numerical models.....</i> | 12 |
| 3.3.2 <i>WP3 – Development of fast air pressure monitoring system</i> | 48 |
| 3.3.3 <i>WP4 – Validation of explosion mitigation systems</i> | 77 |
| 3.3.4 <i>WP5 – Integration of results and dissemination</i> | 77 |
| 3.4 CONCLUSIONS | 78 |
| 3.5 EXPLOITATION AND IMPACT OF THE RESEARCH RESULTS | 80 |
| 4 LIST OF ACRONYMS AND ABBREVIATIONS..... | 83 |
| 5 LIST OF REFERENCES | 85 |

List of figures

| | |
|--|----|
| Figure 1. Some key phenomena of the flame propagation in a tube | 13 |
| Figure 2. Comparison with experiments..... | 15 |
| Figure 3. Comparison with experiments..... | 17 |
| Figure 4. Comparison with experiments..... | 18 |
| Figure 5. Comparison with experiments..... | 18 |
| Figure 6. Comparison with experiments..... | 20 |
| Figure 7. Comparison with experiments..... | 20 |
| Figure 8. Pressure-time history, 20 dm ³ sphere, XiCoef=0.5; XiShape=1.0; u' coeff. 0,9..... | 22 |
| Figure 9. Pressure-time history, 5 m ³ chamber, EMB test condition | 22 |
| Figure 10. Laminar burning velocity SL as a function of equivalence ratio Ø - SCOPE model..... | 23 |
| Figure 11. Pressure-time history – comparison of laminar burning velocities models for homogeneous (Guilder model) and non-homogeneous (SCOPE model) cases..... | 23 |
| Figure 12. Velocity profile for Z axis direction (along main gallery) – cross-section 60 m | 26 |
| Figure 13. Realise of 25 m ³ pure CH ₄ – time: 45 s after realise, geometry with cross-bars..... | 26 |
| Figure 14. Visualisation of CH ₄ continuous realise, realise source – 2" pipe | 26 |
| Figure 15. Distribution of CH ₄ concentration including calibration equations. Variable "ft" - mass fraction of CH ₄ in ambient air. Simplified sidewalk geometry 400 m. Cross-section along the Z axis..... | 28 |
| Figure 16. Case study diagram..... | 28 |
| Figure 17. Initial condition for distribution of CH ₄ concentration along the Z axis of the gallery. Summary of the cases analysed..... | 29 |
| Figure 18. Overall device..... | 31 |
| Figure 19. 150 mm steel pipe | 32 |
| Figure 20. Pressure signals measured in the transparent 250 mm tube near the ignition source, at 5.5 m and at 15.5 m from ignition source..... | 33 |
| Figure 21. Pictures of flame propagation when the transparent tube is captured on film closely (5 ms between two pictures) | 33 |
| Figure 22. Comparison with experimental and estimated flame velocity | 37 |
| Figure 23. Experimental and modelling pressure for 11,6%H ₂ /air mixture in 15 m long cloud in INERIS tunel | 37 |
| Figure 24. Methane concentration distribution during experiment Ex-03..... | 39 |
| Figure 25. Changes of gases concentration and temperature during experiment Ex-03..... | 39 |
| Figure 26. Changes of pressure and flame zone location during experiment Ex-03..... | 40 |
| Figure 27. Explosion development registered by one of cameras | 40 |
| Figure 28. Partially burnt insulation of an electrical wires..... | 40 |
| Figure 29. Changes of methane concentrations at 100 m distance from blind end of the gallery measured close to its ceiling and over the floor..... | 41 |
| Figure 30. Zone of methane combustion in upper part of the gallery | 42 |
| Figure 31. Facility extension | 42 |
| Figure 32. Measurement sections in the gallery | 43 |
| Figure 33. Explosive test of 24,45 m ³ air-methane mixture (Test 1)..... | 46 |
| Figure 34. Explosive test of 24,45 m ³ air-methane mixture (Test 2)..... | 46 |
| Figure 35. Explosive test of 48,3 m ³ air-methane mixture (Test 3) | 46 |
| Figure 36. Damage to facilities an chain barriers | 47 |
| Figure 37. Estimated overpressure signal – Type A trial | 48 |

| | |
|---|----|
| Figure 38. Estimated overpressure signal – Type B trial | 48 |
| Figure 39. Results of sensor response time testing | 51 |
| Figure 40. Diagram of fast air pressure monitoring system | 52 |
| Figure 41. Block diagram of surface station SP/DTSS | 53 |
| Figure 42. Cassette of a surface station SP/DTSS | 53 |
| Figure 43. Receiver module OCGA | 53 |
| Figure 44. Block diagram of NSGP transmitter..... | 54 |
| Figure 45. View of the NSGP transmitter | 55 |
| Figure 46. Layout of the pressure sensors in the excavation 414/1/H..... | 56 |
| Figure 47. Changes in pressure in the tested excavation during a normal operation of the ventilation system..... | 57 |
| Figure 48. Changes in pressure in the excavation induced by a blast wave on 17.08.2016..... | 57 |
| Figure 49. Changes in pressure in the excavation induced by a blast wave on 19.08.2016..... | 57 |
| Figure 50. Changes in pressure in the excavation induced by a blast wave on 24.08.2016..... | 58 |
| Figure 51. Changes in pressure in the excavation induced by a blast wave on 26.08.2016..... | 58 |
| Figure 52. Block diagram of system software | 59 |
| Figure 53. CisK6 Module – integration. decoding and archiving the measurements | 59 |
| Figure 54. A window of the program Cisnienie..... | 60 |
| Figure 55. Program Cisnienie – estimation of the current values of pressure | 60 |
| Figure 56. A window of the program Lokalizacja..... | 61 |
| Figure 57. Flowchart of the algorithm of data analysis..... | 62 |
| Figure 58. Flowchart of a location algorithm..... | 63 |
| Figure 59. A window of the program Lokalizacja – measuring data and configuration of workings. | 64 |
| Figure 60. A window of the program Lokalizacja – determination of the place of the potential methane explosion | 65 |
| Figure 61. A window of the program Lokalizacja – message showing a potential place of methane explosion | 65 |
| Figure 62. Layout of pressure sensors during experiments..... | 66 |
| Figure 63. Location of transmitters in the working face area No 4a | 66 |
| Figure 64. Changes in absolute pressure caused by detonation of fuse..... | 67 |
| Figure 65. Changes in absolute pressure caused by attempt at initiation of methane explosion | 67 |
| Figure 66. Changes in absolute pressure caused by attempt at initiation of methane explosion | 67 |
| Figure 67. Changes in absolute pressure caused by methane explosion | 68 |
| Figure 68. Changes in absolute pressure caused by methane explosion..... | 68 |
| Figure 69. Changes in absolute pressure caused by methane explosion..... | 68 |
| Figure 70. Changes in absolute pressure caused by methane explosion..... | 69 |
| Figure 71. Changes in pressure caused by operation of the air dam installed in the raise No. 5 | 69 |
| Figure 72. Changes in pressure caused by operation of a shearer and a power support | 70 |
| Figure 73. Changes in pressure caused by a change of atmospheric pressure | 70 |
| Figure 74. Analysed course of changes in pressure recorded in the face area caused by opening the air dam | 71 |
| Figure 75. Visual summary of measuring results for a normal state and an emergency state during opening the air dam in the raise 5..... | 71 |
| Figure 76. Analysed course of changes in pressure recorded in the face area caused by operation of a shearer and a power support | 72 |

| | |
|--|----|
| Figure 77. Visual summary of measuring results for a normal state and an emergency state during operation of a shearer and a power support | 72 |
| Figure 78. Analysed course of changes in pressure recorded in the face area caused by a change of atmospheric pressure | 73 |
| Figure 79. Visual summary of measuring results for a normal state and an emergency state during a change in atmospheric pressure | 73 |
| Figure 80. Example of location of absolute pressure sensors (PB) and differential pressure sensors (PR) for "U" ventilation system..... | 75 |
| Figure 81. Example of location of absolute pressure sensors (PB) and differential pressure sensors (PR) for "Y" ventilation system | 75 |
| Figure 82. Example of location of absolute pressure sensors (PB) and differential pressure sensors (PR) for "Z" ventilation system..... | 75 |
| Figure 83. Example of location of absolute pressure sensors (PB) and differential pressure sensors (PR) for "H" ventilation system..... | 75 |

List of tables

| | |
|---|----|
| Table 1. Time evolution of the flame front wrinkling..... | 16 |
| Table 2. Summary of results of flame propagation velocity calculations - analysed cases..... | 29 |
| Table 3. Summary of large scale tests..... | 38 |
| Table 4. The amounts of methane for 5 tests | 44 |
| Table 5. Small scale tests..... | 45 |
| Table 6. Average values of parameters measured at different locations..... | 45 |
| Table 7. Full galery tests | 45 |
| Table 8. Maximum values registered by the sensors | 46 |
| Table 9. Technical data of the surface station SP/DTSS | 54 |
| Table 10. Technical data of the transmitter NSGP | 55 |
| Table 11. Velocity of a blast wave and response times of the sensors | 58 |
| Table 12. Results of calculations for the data recorded on 20.12.2016 | 71 |
| Table 13. Results of calculations for the data recorded on 6.12.2016 | 72 |
| Table 14. Results of calculations for the data recorded on 12.12.2016 | 73 |
| Table 15. Results of calculations of the initiation place of methane explosion | 74 |
| Table 16. List of methane ignitions occurred in the years 2003-2013 caused by spontaneous fire in the mines in Poland | 76 |

2 FINAL SUMMARY

WP 1 – Project coordination

WP Leader: **GIG** Partners: **AITEMIN, INERIS, EMAG, FSB, PGG**

The general management of technical works was conducted during the whole Project. In all, five coordination meetings and one internal meeting of the simulation group were organized. The project website was created and updated. No important problems have been found relating to this work package.

Having written to our former Ukrainian partner (DTEK) inviting them to make use of the results of the project (publications, the possibility of using the system developed within the project and other uses) we have yet to receive any response from them.

However all the partners are still willing to share the results and benefits of the project with DTEK, with particular reference to the monitoring pressure system in Ukrainian mines.

As AITEMIN could no longer participated in EXPRO project starting from 16.11.2016 GIG replaced AITEMIN on the position of Project Coordinator. Despite of the change management of technical work was conducted as planned, including coordination meetings and exchange of experimental and numerical results. To facilitate the exchange a common disk space was made available for all participants.

WP2 – Development and calibration of explosion numerical models

WP Leader: **GIG** Partners: **AITEMIN, INERIS, EMAG, FSB, PGG**

The developed and verified numerical models can be used to determine the pattern of explosion propagation and to determine the propagation speed of the flame. The used calculation methods allow the analysis of cases described by 3D geometry. They also allow for any detail of the geometric description of the analysed case. Nevertheless, attention should be paid to the close dependence of the size of the analysed domain and the detail of the geometric description with the hardware resources and the time necessary to obtain solutions. The applied models take into account the inhomogeneity of the gas mixture, which increases the possibilities of practical use of numerical tools.

In particularly large computational domains, problems with flame propagation have been reported. The explanation of this solver features requires further work.

The developed solver can be used to:

- Perform post-factum event analysis, case scenario analysis;
- Analyse events in underground gallery, excavations, tunnels etc.;
- Analyse possible flame propagation scenarios in various industry sectors where there is a risk of explosion: plants;
- For educational application - to better understand the phenomenon.

Experiments in 400 m underground gallery were conducted. Flame propagation and its range, pressure development, as well as gas concentration changes were recorded. Those data were used as a reference to numerical models and pressure monitoring system.

Test with transparent and steel tubes were performed addressing question about influence of wall roughness, changes in cross section and bends on flame propagation. Pressure changes, flame position and flow velocity were measured. Tests in transparent tubes with varying cross section and T-shape bifurcation as well as test at real scale in 80 m long underground gallery were also carried out.

To carry out the methane explosion trials at FSB the existing test gallery in Mina Sarita was used. Several different types of explosion trials was carried out: preliminary tests with a small amount of gas, tests in which the explosive mixture was confined into balloons and tests in which a bounded by a plug length of the entire section of the gallery was flooded by explosive mixture. The standard scenario in which tests were carried out simulate explosions progress in a cul de sac where there are some machines working: a roadheader, an air duct, etc. It is also equipped with a booster fan.

Collected experimental data were shared among participants and used for analysis and verification of Air Pressure Monit System and numerical simulations.

WP3 – Development of fast air pressure monitoring system

WP Leader: **EMAG** Partners: **GIG, PGG**

The objective of WP3 was to develop a fast data acquisition system that is capable to record transient changes in the air pressure at the mine areas with high explosion risk. This system should help identify the precise location of the ignition point after an explosion has occurred, what is a fundamental data for determining the causes of the explosion during the post-incident investigation phase.

The systems to be developed must be able to register fast changes in the absolute and differential pressure at several points, and to store them in a safe way, so that data can be analysed after the accident, even if the measuring systems are destroyed by the explosion (a kind of "black box" function).

In the first instance it was carried out the analysis of commercially available measuring devices designed for measurements of absolute and differential pressure used in the underground mining in Poland and Europe. On the basis of the acquired information about the available devices it was decided to modify the existing solutions related to pressure measuring (a sensor of type THP-2) and to apply for transmission and data archiving the equipment used for assessment of rock bump hazard and used in systems for control of changes in rock mass stress made by geotomography methods. These systems are characterised by very quick digital transmission of analogue signals available from pressure sensors installed in the underground mines. The works undertaken within the framework of the WP3 consisted in development of a sensor pressure which would work with a surface station of the system; the data transmission and recording with frequency up to 500 Hz should be available. In the following part of the WP3 it was developed software for the system consisting of four modules operating with each other. The pressure sensors (NSGP transmitters) were certified in accordance with ATEX. The lab tests and the industrial trials were made (in EM "Barbara" and in Coal Mine "Ruda – Ruch Halemba"). Data from the tests allowed the development of rules and guideline for detection of the tolerable and non-tolerable levels of pressure changes.

During the course of the WP3 it was developed a sensor called NSGP transmitter. The sensor performs the functions of measurements of absolute pressure in the range of 800 ÷ 1300 hPa with accuracy of $\pm 30\text{Pa}$ and data transmission frequency of 500Hz. The sensor has appropriate ATEX certificates which allowed us to carry out its functional trials in the underground mine. The system software was developed; it allowed data communication, data processing and measuring data archiving as well as locating initial places of a possible explosion based on recorded pressure measurements. A complete measuring system and functioning of algorithms designed for location of explosion site were tested during experiments carried out in the EM "Barbara".

The only problem within the framework of the WP3 was obtaining the ATEX certificate. Elaboration of technical documentation for approval purposes of the NSGP sensor was associated with making many changes related to requirements of intrinsic safety standards. For this reason the Task T3.1 was delayed for about 3 quarters. This delay had no negative impact on the implementation of the project. The lack of the ATEX certificate delayed only the trials in the mine for about 1 quarter.

As a result of the works within the WP3 there have been developed the modified pressure sensors which met the given requirements. There has been developed a measuring system consisting of surface devices (a central station of the SP/DTSS system) and underground equipment (NSGP sensors). The system software was developed which allowed data communication, data processing and measuring data archiving, as well as locating initial places of a possible explosion based on the recorded pressure measurements. A complete measuring system was tested during experiments of explosions carried out in the EM "Barbara" and under conditions of normal work in a mine. Results from the tests allowed the development of rules and guideline for detection of the tolerable and non-tolerable levels of pressure changes.

WP4 – Explosion mitigation systems

WP Leader: **GIG** Partners: **AITEMIN, INERIS**

This Work Package was cancelled. Only the review of European experiences in the use of triggered barriers was prepared. The conclusion of the review are as follows.

Developing a triggered barrier system capable to stop methane explosions at an early stage has been a common objective in most coal mining countries across Europe. There has been a significant number of research projects on this field, as well as many validation experiments in controlled conditions. The concept of all the systems developed so far has been very similar, although there are differences in the specific design and the technologies involved.

The results obtained in the different series of experimental tests carried out in the last two decades have been good in general terms, although it has not been possible to assure a 100 % of the reliability in the operation and efficiency of the barriers. The capacity of the triggered

barriers to stop an explosion strongly depends on the explosion parameters and the gallery dimensions, and therefore it is not possible to find a general solution for all situations. Each specific explosion scenario requires an individual analysis.

All this, together with the high price of this type of equipment, and other practical constraints, such as their large size, and the difficulties to install, move and maintain the units underground, have probably prevented the general deployment of the triggered barriers at European level.

The practical experiences on the efficiency of triggered barriers to stop an explosion in real conditions is therefore very limited, and, according to the review made, is mainly concentrated in Ukraine. The experience in this country proves that the reliability of the triggered barriers is not as good as it should be.

WP5 – Integration and dissemination

WP Leader: **GIG** Partners: **AITEMIN, INERIS, EMAG, FSB, PGG**

The Final Report that integrates contributions from all participants has been prepared. The Report was stored in the common disk space of the Project.

Several publications have been prepared and published. Some other have been accepted for the next International Symposium on Hazard, Prevention and Mitigation of Industrial Explosions (ISPMIE) Conference that will be held in August this year, in Kansas City, USA.

Results of project were also presented during meeting organized for directors of the mines and for staffs of the mines responsible for safety.

3 SCIENTIFIC AND TECHNICAL DESCRIPTION OF THE RESULTS

3.1 OBJECTIVES OF THE PROJECT

The main aim of the EXPRO project was to develop tools and means that can help to adopt measures for mitigating the damages of the methane explosions in the mine infrastructure and in particular in critical equipment. A first condition to achieve this objective was to be able to predict the distribution of the potential mechanical and thermal effects of a methane explosion in a specific situation, with enough degree of accuracy and a high spatial resolution. Secondly, it was required to develop means that can help to identify the causes originating an explosion after it has occurred, and in particular the ignition point, in order to adopt the adequate preventive measures in the future, and thirdly, to search methods to mitigate the effects of the explosions over the mine infrastructure and to prevent the propagation of the explosion to other areas of the mine.

The explosion effects depend on a number of circumstances and conditions, such as the volume and concentration of the methane-air mixture, the 3-D geometry of the area of the mine where the explosion is produced, and the specific location of the ignition point. The influence of the obstacles existing in the area (mining equipment, ducts, etc.) is also important, as they will modify the propagation of air pressure waves, and could in some cases cause pre-compression effects in certain zones, increasing the dynamic effects of the explosion. A detailed knowledge of the explosion process and the specific influence of each one of the different parameters involved is therefore a basic requirement for the adoption of preventive measures.

In order to achieve these goals, the project included research works in three different and complementary areas:

- Getting a better understanding of the mechanical and thermal effects caused by the methane explosions, and a detailed 3-D distribution of such effects, by developing numerical models of explosions in different mine geometries and conditions, which will be validated with real scale explosion tests. This will enable to determine the optimal position for critical equipment in different mine designs, and will also help to investigate the explosion causes and the location of the ignition point by analysing the effects of the explosions after they occur.
- Development of an innovative air pressure monitoring system specially designed to record data that can help in the investigations after the occurrence of an explosion, and in particular for the determination of the ignition point.
- Testing and validating mitigation systems which are being used today in mines outside the EU, in order to check if they are capable to reduce the effects of the explosions and prevent the formation of secondary explosions.

3.2 COMPARISON OF INITIALLY PLANNED ACTIVITIES AND WORK ACCOMPLISHED

WP 1 – Project coordination

Even though there were significant changes (DETEK, AITEMIN resignation), all activities in this WP has been performed and completed according to the introduced amendments to the initial plan (modifications of Technical Annexes).

WP 2 – Development and calibration of explosion numerical models

All work in this Workpackage (Task) has been performed and completed according to the plan thanks to extension of the Project duration.

WP 3 – Development of fast air pressure monitoring system

The only problem within the framework of the WP3 was obtaining the ATEX certificate. Elaboration of technical documentation for approval purposes of the NSGP sensor was associated with making many changes related to requirements of intrinsic safety standards. For this reason the Task T3.1 was delayed for about 3 quarters. This delay had no negative impact on the implementation of the project. The lack of the ATEX certificate delayed only the trials in the mine for about 1 quarter.

WP4 – Explosion mitigation systems

As DETEK was not able to participate in the Project is was agreed by European Commission to cancel further activities in WP4 after finishing Task 4.1 *Review of experience*. The Task was concluded with Deliverable D11 *Report on the review of European experiences in the use of triggered barriers*.

WP5 – Integration and dissemination

All work in this Workpackage (Task) has been performed and completed according to the plan.

3.3 DESCRIPTION OF ACTIVITIES AND DISCUSSION

3.3.1 WP2 – Development and calibration of explosion numerical models

WP Leader: **GIG**

Partners: **AITEMIN, INERIS, EMAG, FSB, PGG**

Task 2.1 – Definition of explosion scenarios

GIG scenarios

Several accidents that took place in Polish coal mines have been analysed. Out of them two accidents has been chosen considering the possibility of their experimental simulation in the underground workings of Experimental Mine Barbara.

The first scenario represents general conditions of the methane explosion in the mine KWK Wujek-Slask. An abrupt release of a large methane volume was released into the underground experimental entry.

The second scenario represents general conditions of the methane explosion in the mine KWK Halemba. A slow, continuous release of methane at the closed end of the 400 m experimental entry resulted in a formation of methane/air mixture with a distribution of the methane concentration varying along the entry's length. The ventilation conditions were kept constant: the air speed was between 0.2 m/s and 0.3 m/s.

FSB scenarios

Spanish explosion scenarios are based in the specific conditions of steep seam mining, using sub level caving method.

There are some parameters that have relevant influence in the development of a methane explosion, apart from the exploitation method itself, as for instance the geometry of the explosion zone, the ventilation regime, the existence of obstacles, the gas volume, the distance from the ventilation tube to the exploitation front, etc.

The different explosion scenarios which can take place in real conditions have been studied, and also how to reproduce them in the explosions test gallery that the Santa Barbara Foundation has at La Ribera de Folgoso, León (Spain).

Four different explosion hypotheses were considered, according to the applied exploitation method, features of the layer, geometry of the gallery, equipment inside the gallery, ventilation conditions, volume of methane and ignition point:

Hypothesis 1- Manual advance heading

This first hypothesis is that of a dynamic gas and coal outburst that implies an sudden increase of methane concentration in the coal advance front, and ignition is produced by a mechanical spark. The manual equipment includes drilling hammer, pneumatic drill, monorail, electrical panzer, compressed air pipes and ventilation.

Hypothesis 2 - Advance heading with roadheader

The second hypothesis is related with the advance heading with roadheader when using the sub level caving method, and includes the characteristics of the coal layer, the geometry of the gallery, the equipment existing inside the gallery, the ventilation conditions, the expected volume of methane and the most probable ignition point.

This scenario considers a methane outburst where the ignition is caused by an electric spark. The equipment inside the gallery includes a roadheader, a pneumatic drill, and a monorail, several compressed air pipes and ventilation ducts, etc.

Hypothesis 3 - Caving face (methane)

This third hypothesis is a Rockburst that causes a massive methane release, the ignition is caused by an electric spark and the work equipment includes: drilling hammer, pneumatic drill, metallic shoring, electrical chain conveyor, compressed air pipes and ventilation ducts, etc.

Hypothesis 4 - Caving face (explosive)

This fourth hypothesis, is that of a situation in which blasting shots are performed to the coal seam, and the ignition is caused by the explosive itself. The work equipment includes: drilling hammer, pneumatic drill, monorail, electrical chain conveyor, compressed air pipes and ventilation ducts, etc.

After a detailed analysis, it has been finally decided to reproduce hypothesis number 2 with the characteristics previously defined.

Task 2.2- Development of numerical models

The work completed at INERIS

Physical modelling

A priori study: which phenomena should be accounted for by the model?

A flame propagating in a tube undergoes numerous phenomena that could interact between each other (see Figure below):

- When the flame moves, it pushes fresh gases in front of the flame front. The created flow can produce turbulence,
- The flame, when propagating, emits a pressure wave that can be reflected in the tube,
- The flame when interacting with turbulence can be accelerated (or decelerate and quench if turbulence is very intense) and produce turbulence at quicker rate, because of the acceleration,
- The pressure wave can destabilize the turbulent flame leading to a flame front acceleration or deceleration, the coupling being potentially influenced with the flame front / turbulence interaction,
- If the tube walls are non-adiabatic, the burned gases can be cooled, leading to hot gases contraction and a slower flame. Acoustics is influenced as well as sound speed in burned gases, linked to temperature, is changed.

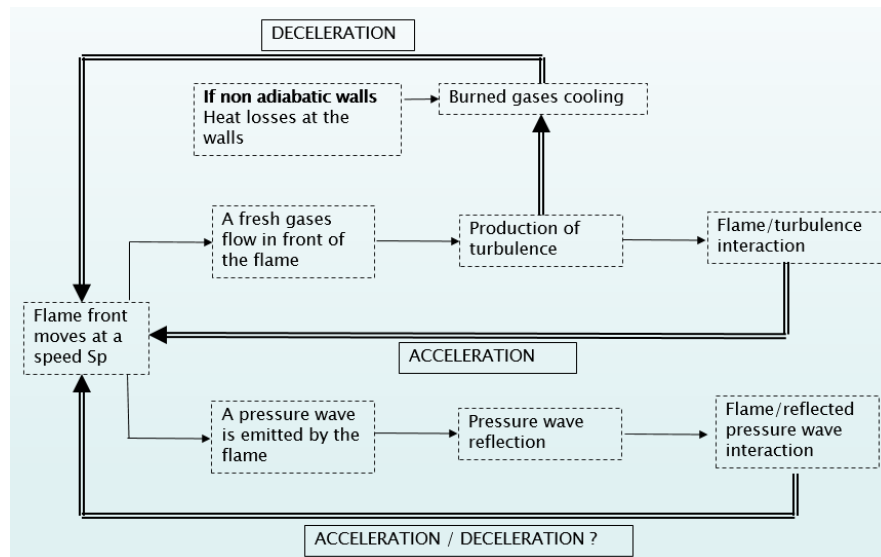


Figure 1. Some key phenomena of the flame propagation in a tube

These observations *imply* at least:

- the solved equations should be compressible,
- the acoustic time should be solved.

Furthermore, the *developed* model should be suitable for real cases ie explosions in mines.

In these situations, the flammable mixture is most likely non-homogenous before ignition. As the flame speed depends on the local fuel/air equivalence ratio, such clouds could lead to a non-spherical flame due to a spatial distribution of flame speed. This deformation at the scale of the whole flame increases its average speed and leads to a higher pressure in the burned gases.

Thus, heterogeneity effects have to be accounted for in the numerical model of the flame.

Mine explosions are also characterized by their potentially large scale. The flammable cloud length being limited by the galleries walls, it can be hundreds of meters long. Even if the cloud dimensions remain about ten meters, acoustics can play a role on the flame dynamics and all potentially reflecting walls should be theoretically modelled.

This need of a large scale modelling impose a global model formalism that could be used at small scale for validating purposes and large scale as well.

Model

Numerical Tool

The software used for the computations was OpenFoam 3.0.0.

When writing the report, the up-to-date version of OpenFoam was OpenFoam 5.0 (released in July 2017).

At the beginning of the project, OpenFoam 2.3.0 was chosen by all modellers. Nevertheless, the computing machine used by INERIS evolved after a maintenance and the numerical architecture was optimized for OpenFoam 3.0.0 and maybe later versions. That is why OpenFoam 3.0.0 was finally retained.

The computations were run in parallel on several cores of the CEA supercomputer. The computations times were about 10 hours for 1s of physical time with 256 2.4 GHz Intel Xeon cores

Turbulence modelling

It did not appear realistic to solve numerically the Navier-Stokes transport equations and extra equations related to combustion for mine explosions. Such a computation wouldn't be carried quickly enough (i.e. in several days) or may be impossible to perform due to memory overloading on the computing machines.

In small and medium scale combustion cases, Large-Eddy Simulation (LES) was the formalism chosen to model turbulent flows, especially these related with unsteady and geometry dependent effects such as flame instabilities.

In practice, designing the proper mesh requires a trial-and-error process with a computation for a first mesh.

URANS modelling emerged as a simpler solution to perform computations in a proper way and this formalism was preferred for the computations of the project.

Many RANS turbulence models were available in OpenFoam 3.0.0 such as: k-epsilon, k- ω , k- ω SST, Spalart-Allmaras.

The chosen model were adapted to wall bounded flows.

Equations set

A new solver was developed based on the reactingFoam solver. In reactingFoam, transport equations are solved for: pressure, momentum, energy and the partial densities for chosen chemical species.

The source terms of the chemical species mass fractions were obtained from an Arrhenius law.

INERIS modified this solver, adding a transport equation for a progress variable. This quantity evolves monotonously across the flame front, equals 0 in the fresh gases and 1 in the burned gases. This quantity is commonly used in premixed combustion modelling for tracking the flame front position.

INERIS also changed the way the time step was computed. It was basically computed with a CFL condition from the convective field. INERIS added the sound speed to the local flow velocity for performing the computation, thus limiting the time step more than it was.

Turbulent wrinkling factor study

In OpenFoam, the turbulent wrinkling factor Ξ is estimated through a transport equation or an algebraic closure.

The behaviour of the transport equation can be hardly a priori studied. Nevertheless, the algebraic closure can be a priori investigated.

Specialist literatures provide measurements of turbulent flame speeds for methane/air flames at several pressures (from 1 to 10 bar).

The algebraic closure of XiFoam writes:

$$\Xi = 1 + \left(1 + 2\Xi_{shape}(0.5 - b) \right) \Xi_{coeff} \sqrt{\frac{u'}{S_l} R_\eta}$$

The value Ξ_{coeff} is tuned to recover the experimental values. This work is performed for pressures: 1,2,3,5 and 10 bar. Other correlations were tested: the Gülder correlation and the Bray correlation (used in the FLACS code).

The following choices were made for the constant in the XiFoam algebraic closure.

It appears that a change of Ξ_{coeff} with pressure should be accounted for to keep a physical behavior of the OpenFoam correlation.

The Gülders and Bray correlation overestimated the experimental wrinkling factor from 1 to 3 bar. But these overestimations decay when pressure increases, and the proper order of magnitude is recovered for 5 and 10 bar.

To conclude, theoretically, the flame speed should not exceed the proposed closure for the equilibrium flame wrinkling factor.

Wall treatment

In OpenFoam, the available model for the walls were:

- nutLowReWallFunction: assumes the center of the closest cell to the wall is located within the viscous sub-layer. The turbulent viscosity is then set to 0.
- nutkWallFunction: assumes the first cell is in the logarithmic sub-layer. y^+ is built from the turbulent energy at the wall.
- nutUWallFunction: also assumes a location of the first cell in the logarithmic sub-layer. y^+ is built from the velocity field at the wall.
- nutUSpaldingWallFunction: is an extension of the previous model, valid also for the viscous sub-layer.

In the tube the velocity of the fresh gases in front of the flame changes with time, as the flame is first laminar and, roughly, keeps on accelerating with time. It might be possible that at different instants a cell closest to the wall is in the viscous sub-layer and later in the logarithmic sub-layer.

Wall laws are also available in OpenFoam for rough walls: nutkRoughWallFunction and nutURoughWallFunction.

The difference between these boundary layers and the “smooth” ones is the logarithmic value relies on a value E^* instead of E where $E^*=E/\text{f(roughness)}$ where roughness is the absolute roughness in mm.

Comparison with experiments

250 mm inner diameter tubes

PMMA Tube

The Figure 2. shows the x-t diagrams obtained from the processing of the high-speed camera movie for the plastic tube and from the OpenFoam computation. Note the numerical diagram refers to the position of the $c=0.5$ point, where c is the progress variable, on the tube axis. If the position was the leading edge of the flame, the numerical diagram would be slightly different.

The OpenFoam results are related to the fine mesh for the 250 mm tube.

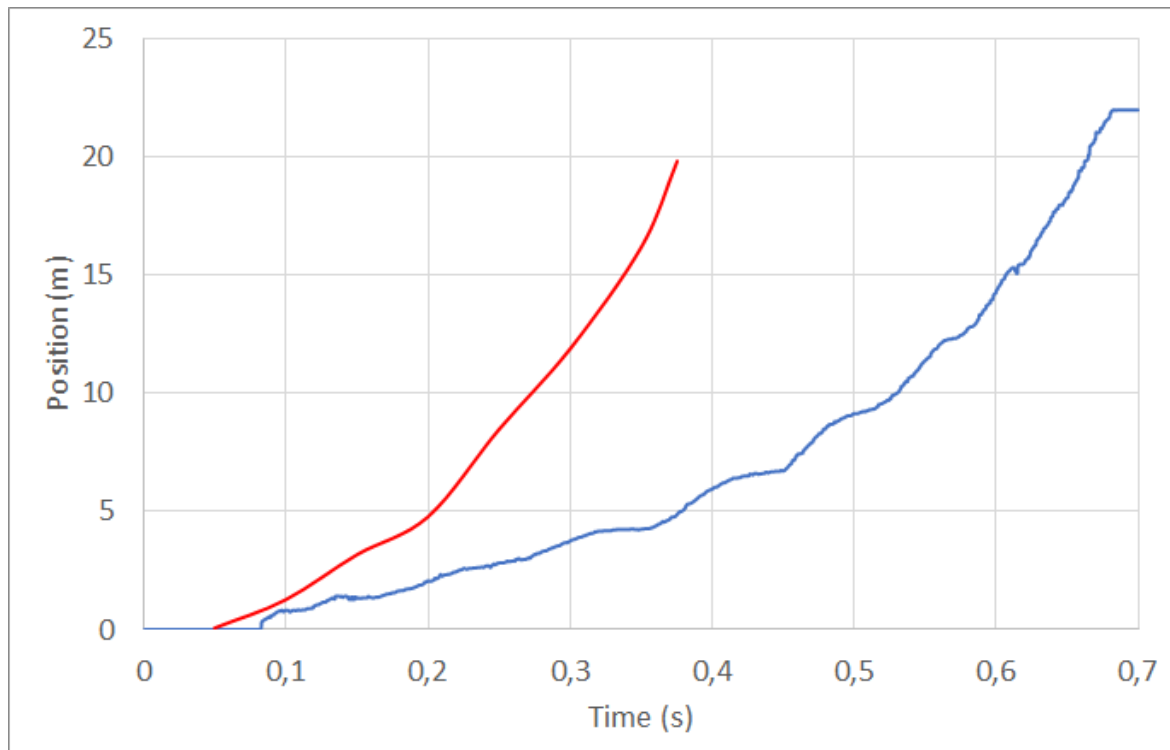


Figure 2. Comparison with experiments

Blue: experimental flame trajectory, red: computed trajectory for adiabatic walls.

It appears the flame predicted by OpenFoam propagates way quicker than the measured one, from the start to the end of the propagation.

On the numerical curve, 3 characteristic time intervals appear. For each interval the flame speed is globally constant, even if slight oscillations appear:

- 0-200 ms, average flame speed ~ 25 m/s
- 200-350 ms, average flame speed ~ 65 m/s
- 350-400 ms, average flame speed ~ 140 m/s.

From the first to the third time-interval, the flame is continuously accelerating, the flame speed being doubled from a time interval to another.

It can be seen in the flame shape changes during the propagation. The flame is first spherical then elongated, tulip-shaped and finally elongated again until it reaches the tube open end. Nevertheless, numerically, the flame shape evolution is not the only quantity explaining the flame speed evolution. Indeed, the global fresh gases consumption speed is related to both: the flame surface and the mean wrinkling factor on the flame surface.

The table below details the flame wrinkling with time on certain parts of the flame front and the flame surface evolution for each time interval.

Table 1. Time evolution of the flame front wrinkling.

*half distance between the tube axis and the wall

| Time (ms) | Wrinkling factor on the axis (-) | Wrinkling factor on the sides (-)* | Flame surface evolution between (t) and (t-100 ms) (-) |
|-----------|----------------------------------|------------------------------------|--|
| 150 | 1 | 1.5 | Decrease |
| 200 | 1 | 2.5 | Increase |
| 250 | 1.5 | 4 | Decrease |
| 300 | 3 | 4 | Increase |
| 350 | 4.5 | 5 | Increase |

The mean flame wrinkling increases with time and it increases quicker between flame center and the walls than on the axis. Turbulence is the most intense close to the walls because the zero velocity on walls promotes shear stress.

As the flame propagates, it accelerates, boosting the shear stress at the walls leading to a continuously increased turbulence production and continuously accelerated flame.

Several assumptions could explain why the predicted flame is too quick when compared with experiments as:

- The boundary condition for pressure is not properly set: the atmosphere should be modelled, enabling to account for a better description of pressure wave/tube outlet interaction,
- The turbulence is produced at a higher rate than it should be,
- The flame/interaction leads to an overestimated flame speed as in the current model, the flame instantaneously changes its speed depending on the local turbulence. This weakness is related to the choice of an algebraic closure for the wrinkling factor computation.

The computation was first performed with the reference mesh but in this case, $y+$ values in the range 300-800, from 100 ms until the end of flame propagation were obtained. They are greater than the upper value of the theoretical validity range of the wall laws.

The computation was then carried out with the fine mesh for which $y+$ values remain below 200 from $t=0$ ms to $t=350$ ms, ie the main part of the flame propagation.

In order to study the impact of turbulence modelling on the result, another computation is performed with no turbulence model (i.e. no turbulent viscosity in the transport equations, no wall law and no wrinkling of the flame linked to turbulence). This computation was performed with the coarse mesh, as, for numerical reasons, the computation crashed with the reference mesh.

The previous x-t diagram is completed with the "laminar" flame and is shown below.

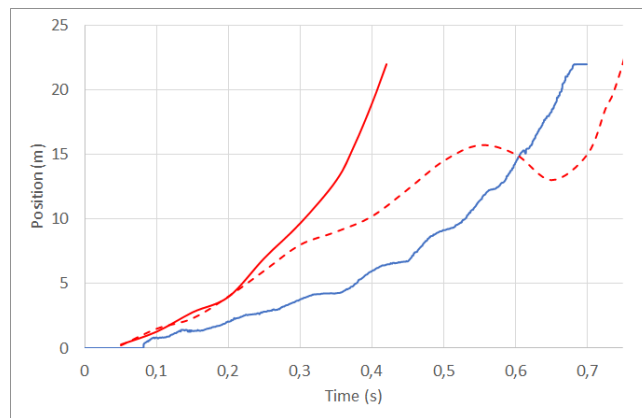


Figure 3. Comparison with experiments

Blue: experimental flame trajectory, red: computed trajectory for adiabatic walls.

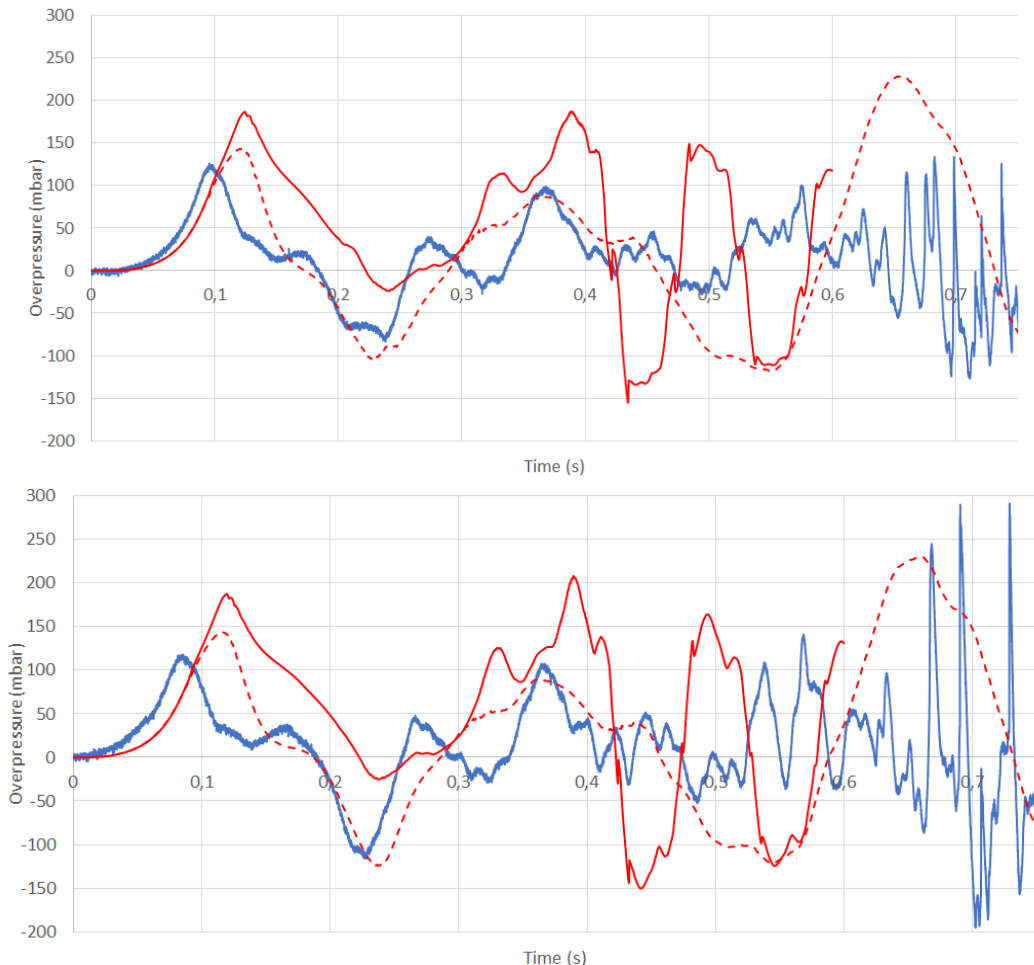
From 0 to 200 ms, the laminar and turbulent flames have the same propagating speed, meaning this phase is purely laminar. This phase is nevertheless quicker than the measured one.

From 200 to 550 ms, the laminar flame is quicker than the experimental one but the flame speed order of magnitude is recovered, the average speed on this time interval being 25 m/s for the measured flame and 35 m/s for the real one.

From 550 ms until the end of flame propagation, the laminar flame slows down, goes backward and then accelerates again whereas the measured flame keeps on accelerating on this time interval.

The real flame behaviour is more approached by the laminar flame model than by the turbulent one but the final acceleration (550 ms until the end) is not fully recovered by the laminar model. Nevertheless, even for the laminar flame, the velocity until 550 ms is too high.

The pressure signals measured at 0 m, 5.5 m and 15.5 m from ignition point are shown below for the turbulent and laminar flames. They are compared to the numerical pressure signals computed at 4 m, 6 m and 16 m from ignition point.



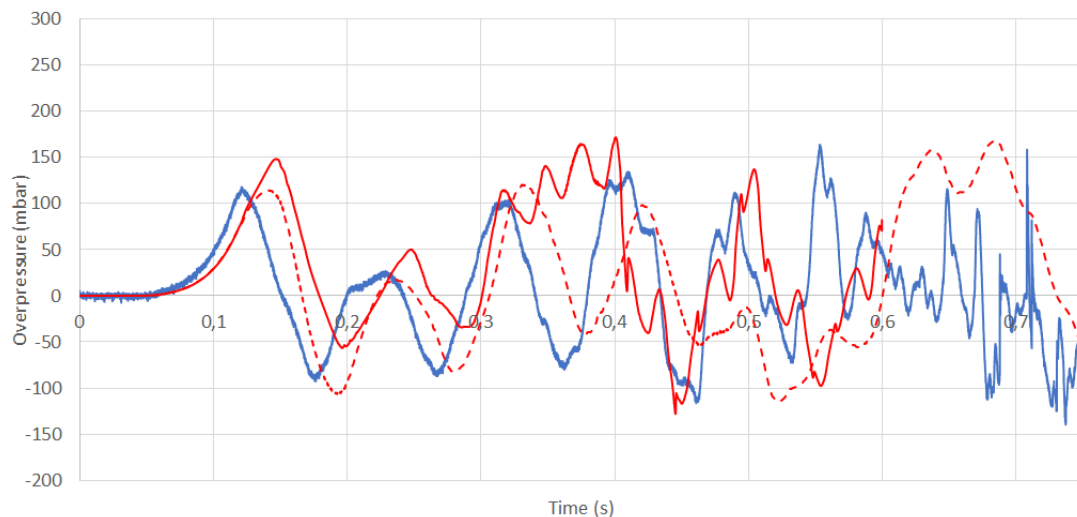


Figure 4. Comparison with experiments

Pressure signals close to the ignition point (top), 5,5 m from ignition point (middle), 15,5 m from ignition point (bottom). Blue: experiment, Red line: modelled turbulent flame and red dotted line: modelled laminar flame.

The laminar flame agrees quite well with the envelope of the experimental pressure signal in terms of peak overpressure and periods from 0 to 400 ms roughly even if some short periods are not fully recovered.

The experimental flame seems to be almost laminar from 0 to 250 ms.

The turbulent flame recovers good orders of magnitude for the overpressure peaks but there are delays between modelled and experimental characteristic periods of the pressure signal.

According to the modelling results:

- the first 250 ms of flame propagation seem to correspond to a purely laminar flame.
- From 250 ms until the end of flame propagation, the propagation is likely driven by acoustics / flame interaction with increasing turbulence effect when the flame approaches the tube open end.

Metal Tube

OpenFoam computations were also performed for the metal tube. The Figure below shows a comparison between the computed x-t diagram for the metal tube and measured flame positions for 4 instants.

The OpenFoam results are related to the fine mesh for the 250 mm tube.

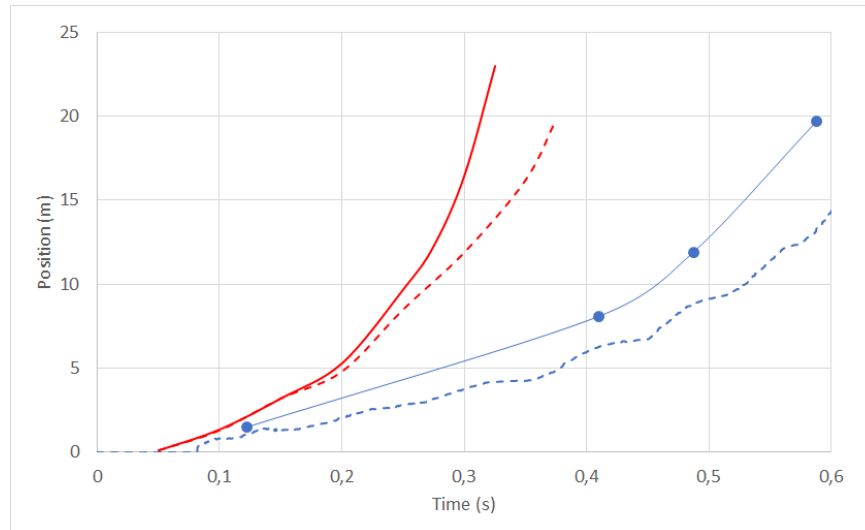


Figure 5. Comparison with experiments

Blue dots: 4 measurements of flame position for the metal tube. Blue dotted-line: measured flame position for the plastic tube. Red line: diagram for the modelled metal tube. Red-dotted line: diagram for the modelled plastic tuve (with turbulence).

Again, the numerical flame is too quick compared to the real one. It is about 2 times quicker.

Also plotted are the numerical and measured x-t diagrams for the plastic tube. It appears the numerical diagrams are very close for the metal and the plastic tube, whereas the gap is slightly larger between the measured x-t diagrams for both tubes.

The pressure signals measured at 0 m, 5.4 m and 15.8 m from ignition point were compared to the numerical pressure signals computed at 4 m, 6 m and 16 m from ignition point.

The experimental trend is well captured by the model for the first 300 ms. The periods of pressure oscillations are very close to the experiment. Nevertheless, the pressure is overestimated as the flame is too quick.

The difference for the first pressure peak may be notably explained by the assumption of adiabatic walls. Nevertheless, accounting for more realistic heat losses in a new computation could lead to an underprediction of the first pressure rise slope.

Note that the chosen characteristic value for the roughness could be challenged as it was taken from the literature but not measured in the test tubes. Another roughness value could lead to other acceleration mechanisms.

The y^+ values remain below 200 from the beginning of the computation until 300 ms meaning the wall law was theoretically used within its validity range during this time interval.

Note: It was observed (not shown) the flame could artificially accelerate if the y^+ criterion was not respected, due to a too coarse mesh.

150 mm inner diameter tubes

OpenFoam computations were also performed for 150 mm inner diameters tubes for both materials.

PMMA Tube

In this case, the y^+ values reached a maximum value of 170, lower than the upper valid value for applying the wall law.

For both models, the flame speed appears globally quite steady even if some moderate oscillations can be observed. Note that some oscillations correspond to a flame that moves back towards the ignition point.

The average flame speed is about 30 m/s for the turbulent flame and 35 m/s for the laminar one. Note that surprisingly, the laminar flame burns the whole mixture quicker than the turbulent flame. It seems the coupling between acoustics and the turbulent flame can lead to a flame that is, in average, slower than a purely laminar flame coupled with acoustics.

In the 250 mm tube, the difference between the 2 models is much more important as the turbulent flame is going twice faster than the laminar one. For this tube, the coupling between acoustics and turbulent flame is different.

From both situations, it seems the coupling between a turbulent flame and the acoustics depends on the tube diameter.

The pressure signals measured at 0 m, 5.4 m and 15.5 m from ignition point are shown below. They are compared to the numerical pressure signals computed at 4 m, 6 m and 16 m from ignition point.

The peak overpressures and the envelope of the pressure signals are quite well recovered by the laminar modelling.

The signal is well modelling with the turbulent flame from 0 to 150 ms. After this time, whereas the peak overpressures orders of magnitude are well approximated, the numerical signal is in opposition of phase with the experimental one.

Metal Tube

The computation was performed with the very fine mesh, enabling to keep y^+ values below 200 from the beginning of the computation until the time $t=230$ ms.

The Figure below shows a comparison between the computed x-t diagrams for the metal tube and measured flame positions for 4 instants. The flame propagation in the metal tube was computed for adiabatic walls.

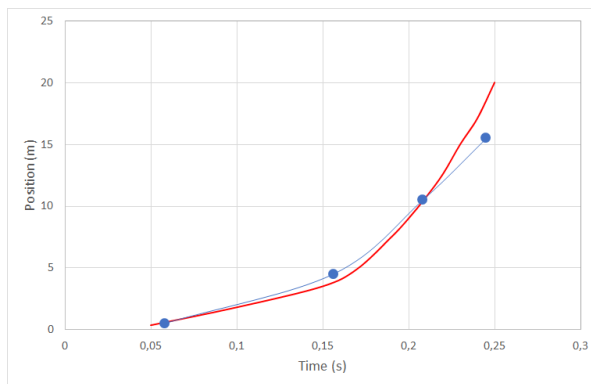


Figure 6. Comparison with experiments

Blue dots: 4 measurements of flame position for the metal tube. Red line: diagram for the metal tube modelled with adiabatic walls.

The x-t diagram of the numerical flame is quite close to the experimental one. The experimental and numerical flame speed follow the same evolution from 0 to 200 ms. After 200 ms, the numerical flame accelerates stronger than the real flame. The experimental and numerical pressure signals are very close from 0 to 200 ms, which is coherent with the numerical agreement for the flame position history.

The strong flame acceleration generates a pressure peak which is more than twice higher than the experimental one (Figures below).

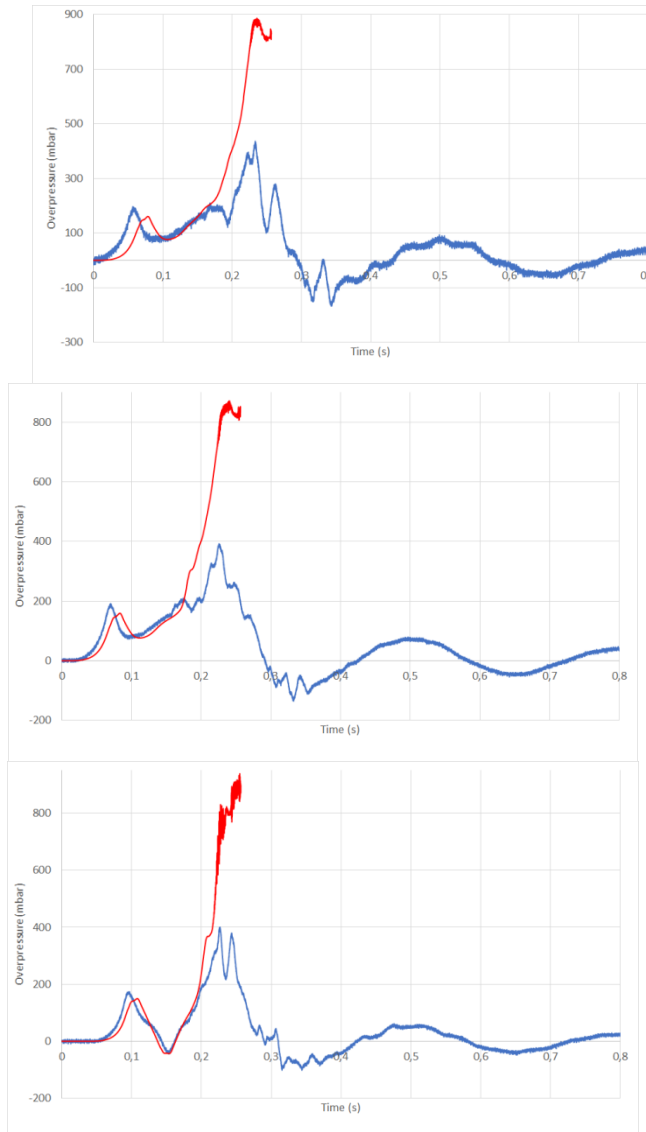


Figure 7. Comparison with experiments

Pressure signals close to the ignition point (top), 5.5 m from ignition point (middle), 15.5 m from ignition point (bottom). Blue: experiment, Red: modelling.

Conclusions

- The flame modelled accounting for the turbulent effect on the flame is too fast when compared with the experiment for the PMMA tubes. A much better agreement is obtained when neglecting the turbulence effect. It seems the turbulence model produce too much turbulence and/or at an overestimated rate.
- The flames modelled in the metal tubes were quite close to the experiment for the main propagation part. For both metal tubes, the flame acceleration at the end of its propagation is overestimated leading to very high overpressures when compared with the experiment. The effect of wall roughness on flame dynamics was clearly highlighted.
- All key physical features were at least qualitatively included in the tube modelling and major trends were recovered: impact of acoustics, impact of wall roughness, impact of tube diameter, overpressure orders of magnitudes, characteristic periods of the pressure signals
- More accuracy could be gained with a better modelling strategy for turbulence production. Other approaches such as LES could be regarded in detail as well as DES, which is supposed to offer a good trade-off between accuracy and cost between RANS and LES.
- An extra work to be performed is checking if the proposed tube modelling could be in practice re-used for modelling explosions in mines. The potential limiting factor would be the required cells number for modelling large scale explosions.

The work completed at GIG

Numerical model study – implementation on small, medium and large scale

Models and methods description

Gas mixture explosion simulation is made with the OpenFOAM software. Gas mixture explosion (methane-air) solver has been made using reaction flame propagation model b-Xi. Premixed combustion is based on reaction regress variable b ("regress" because $b=1$ for fresh gas mixture and $b=0$ for fully burned mixture). Transport equation is solved for b . Turbulent flame speed (St) is calculated using Weller combustion model for calculation Ξ ($St=Su*\Xi$).

Additionally, the following models have been used:

- Laminar flame speed model: Gülder,
- Turbulent model: k-epsilon.

Gas mixture and reaction product physical parameters as a function of temperature have been described with use of:

- JANAF table for:
 - heat capacity,
 - enthalpy,
 - entropy.
- Sutherland formula for viscosity calculation.

Preliminary models tests have been performed for homogenous mixture.

Numerical simulation for 20 dm³ and 5 m³ chambers

Numerical simulation of gas mixture explosion have been performed.

Gas mixture composition: quiescent mixture 9.8% CH₄ + air.

Initial conditions:

- Temperature: 25°C
- Pressure: 990 kPa

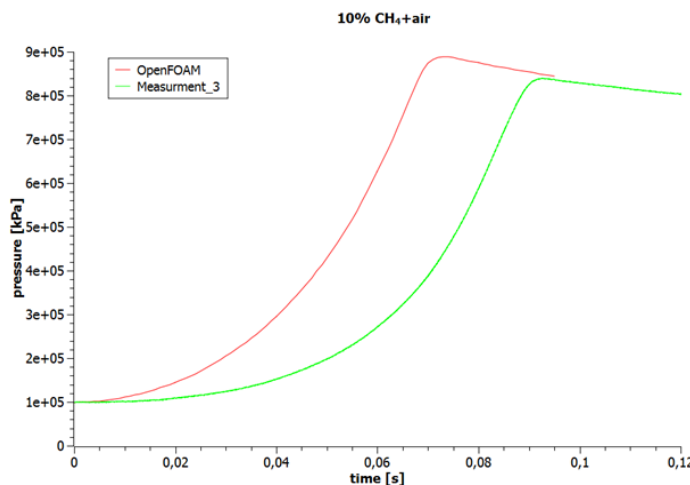


Figure 8. Pressure-time history, 20 dm³ sphere, XiCoef=0.5; XiShape=1.0; u' coeff. 0,9

Result obtained for 20 dm³ sphere (Figure 8) shows that a certain adjustment of b-Xi model is necessary. Additionally heat losses to the walls for post-combustion phase (part of chart after maximum pressure point) seems to be more intensive than the measured. Calculated wall heat transfer is strongly dependent on turbulence model. For the purposes of the presented case the k-epsilon model has been used.

Pressure-time history for 5 m³ chamber (Figure 9) (lab tests made in EXPRO Project in EMB) simulation also confirm above conclusions.

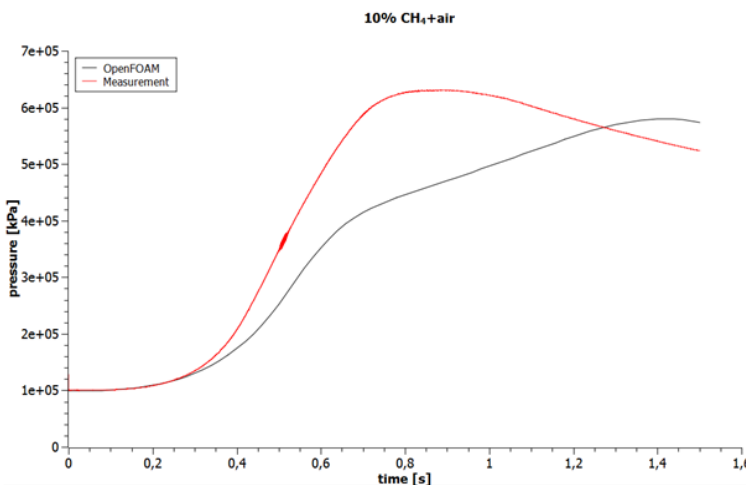


Figure 9. Pressure-time history, 5 m³ chamber, EMB test condition

Preliminary flame propagation parameters adjustment

Following parameters of Weller combustion model (b-Xi) have been adjusted: XiCoef, XiShapeCoef, uPrimeCoef.

Adjustment have been performed with a simple geometry (20 dm³ sphere) and homogenous, quiescent 10 % CH₄+air mixture. The series of numerical calculations has been performed. That case has been chosen due to minor influence of wall heat transfer.

Development of solver for non-homogeneous mixture

At the beginning of the project and for adjustment purposes, the calculations made were based on the assumption of a homogeneous distribution of methane concentrations. This is a purely theoretical situation, since in real conditions a methane-air mixture with a homogeneous concentration distribution would be rather unrealistic to achieve.

The developed solver (based on reaction flame propagation model b-Xi) was modified by introducing an non-homogeneous premixed gas mixture. The following changes were made:

- the variable ft transfer equation responsible for storing the methane concentration distribution is resolved, and the updated ft variable keeps the concentration distribution up to date,
- Gulder laminar burning velocity model was replaced by the SCOPE model.

Model SCOPE introduces laminar burning velocity S_L as a function of: ft (gas mass fraction), p (pressure) and T (temperature).

SCOPE model adjustment has been performed using data from following publications:

- Laminar Burning Velocities and Markstein Numbers of Hydrocarbons/Air Flames, L.K. Tseng, M.A. Ismail, G.M. Faeth, Combustion and Flame 95: 410-426, 1993.

Implemented SCOPE model is described by following polynomials:

$$S_L = a_0(1 + a_1x + K + \dots + a_6x^6) \left(\frac{p}{p_{ref}}\right)^{p_{exp}} \left(\frac{T}{T_{ref}}\right)^{t_{exp}}$$

The following values of the explosion limits were assumed for methane-air mixture:

LEL (Lower Explosion Limit): ~5 % (volume concentration) ($\phi=0.522$)

UEL (Upper Explosion Limit): ~15% (volume concentration) ($\phi=1.58$)

where: ϕ – equivalence ratio

Two polynomials are defined describing full explosion range (from 5 % to 15 % CH₄ in air).

SCOPE characteristics have been presented on Figure10.

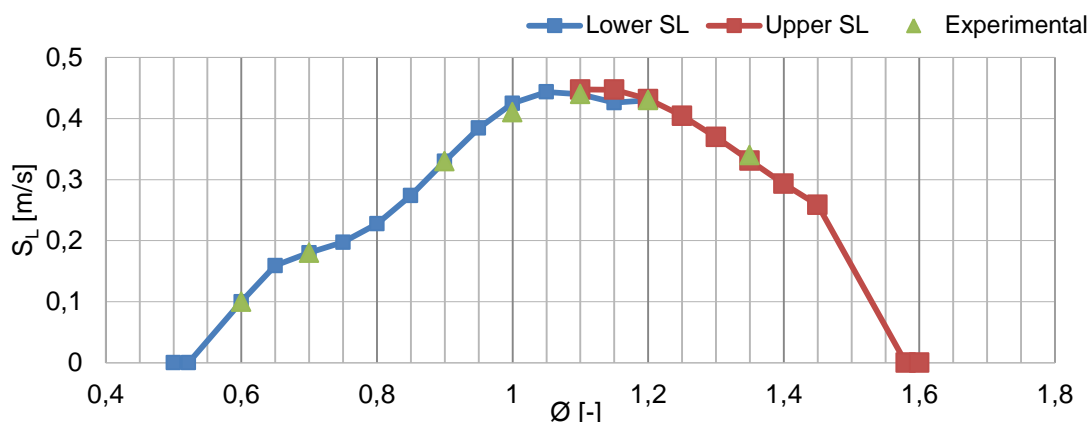


Figure 10. Laminar burning velocity SL as a function of equivalence ratio Φ - SCOPE model

The SCOPE model has been verified by the following tests:

- Test 1 – chamber 5 m³; Gulder model vs. SCOPE model. Homogenous gas mixture. Lab test data are present.
- Test 2 -chamber 5 m³; SCOPE model. Non-homogeneous gas mixture. (Lab test data are not present).
- Test 3 - chamber 5 m³; SCOPE model. Homogenous gas mixture. Alternative location of ignition source.

Test 1

This test was performed for a 5 m³ chamber geometry. The purpose of the test was to verify the operation of the solver with the implemented SCOPE model. Verification was made by comparing the explosive pressure profile with the Gulder model used for homogeneous mixtures. The comparison was made for homogeneous methane-air mixer (10% CH₄ + air). The boundary conditions and the initial conditions for both are defined in the same way.

Comparison of pressure-time histories for tested models has been presented in Figure 11

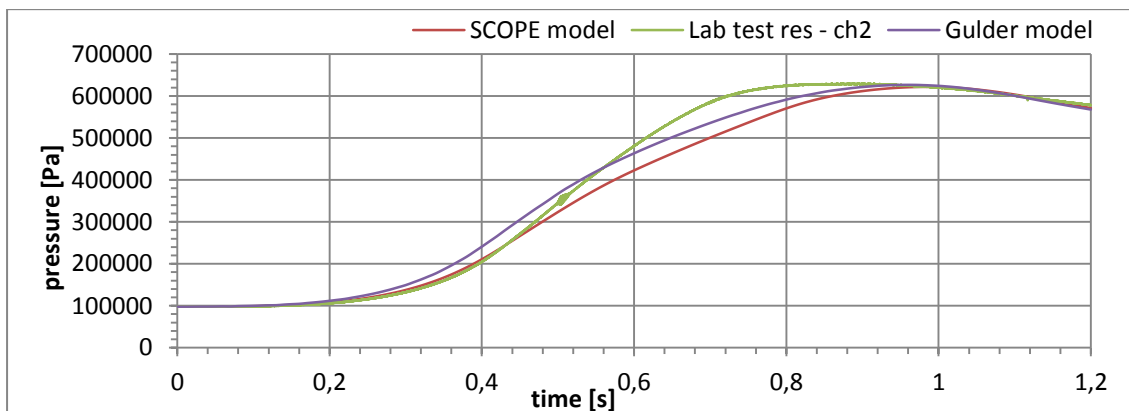


Figure 11. Pressure-time history – comparison of laminar burning velocities models for homogeneous (Gulder model) and non-homogeneous (SCOPE model) cases

During numerical testing, the influence of the equation solving method on the determination of the Ξ parameter was also under consideration. Coefficient Ξ is responsible for determination of turbulent burning velocity according to the following relations:

$$S_t = S_L * \Xi i$$

and further for determination of reaction regress variable (b).

Following methods are available for determination of flame wrinkling factor Ξ :

- algebraic equation
- equilibrium transport equations.

The manner of flame propagation in large geometry (also 5 m^3 chamber) depending on used solution method has been also tested. Solver instabilities encountered during the calculations for large volumes prove the need of the tests. These instabilities were not identified previously in calculation results for small domains like 20 dm^3 sphere.

Calculation results for "Test 1", "Test 2", "Test 3" and "Test 4" were obtained using algebraic equation method.

The results of Test 1 analysis show a high degree of consistency in the results obtained using the SCOPE and Gulder models. However, the obtained explosive pressure waveforms show satisfactory (but incomplete) aggregation with laboratory results.

Discrepancy between the numerical data and laboratory results is primarily dictated by intensive heat exchange with the vessel walls. The pressure-time history shows an apparent refraction (decrease of dp/dt) at about 0.55 s after ignition. This is the time when the flame front reaches the chamber wall. This demonstrates the high sensitivity of the obtained results to the definition of boundary conditions for heat exchange with the walls.

Slight differences in the course of explosions for the Gulden and SCOPE models are due to the following factors:

- a) Different definitions of the models' parameters result in discrepancy of achieved final results. Applied SCOPE model reflects very accurately changes of the S_L values resulting from the temperature and pressure changes with regard to the obtained results using Gulder model. Difference of obtained results for tested models is almost constant and reaches about 0.02 m/s. Better adjustment of both models convergence needs improvement of SCOPE model's polynomial parameters Figure 8. Occurrence of non-physical peaks was explained later in this report.
- b) Despite of higher values of S_L obtained for the model SCOPE, achieved speed of explosion pressure growth is smaller than in case of Gulder model. It is resulting from obtaining slightly smaller values of coefficient Ξ and consequently turbulent burning velocity S_t .
- c) Physical parameters definition. For SCOPE model because of its usage (non-homogeneous mixtures) parameters are defined as typical mixture (ideal). Used material definitions are related to each single component (fuel, oxidizer). But for Gulder model parameters are defined for complete mixture. One set of data for complete mixture and one set of data for burnt products. That completely different approaches give very similar results but some minor differences may happened.

Test 2

This test was performed in order to verify stability of solver in the conditions of in-homogeneous mixture. Subject example is must recognized as a theoretical-one as there was no lab tests, which could verify if the obtained results are in accordance with realistic development of flame face and pressure of the explosion.

Test was performed using geometry of the 5 m^3 chamber, the same as in test 1.

Initial and boarder conditions were defined similar like in test 1 with the exception for the initial CH_4 concentration distribution. Initial concentration was defined as gradient from 6% to 12% in the space taking 50% of tank's height. Remaining space was filled with air.

In the place of ignition the mixture (according to previously performed tests) CH_4 concentration was about 6 % of CH_4 in the air.

According to S_L values determined using k-epsilon model there are visible three peaks (for the times: 500 ms, 1200 ms and 1500 ms) where values are much higher (over 2 m/s) than reasonable value level. That values are the effect of numerical instabilities occurred close or on boundary layer (chamber wall). That instabilities produce extremely unreasonable values but their importance for the final results are rather minor.

Results of S_L values determined using SST model have physical values (maximum about 0.5 m/s).

Performed test prove, that solver is stable and the achieved solutions are very likely. Flame propagates through all fresh mixture in assumed flammable limits. Mixing process is also visible. Achieved values ranges (except for very local instabilities in the boundary layers) are also very likely. Likely means, that the values are in reasonable ranges in physical meaning but there is no possibility to confirm the values at that moment.

However the occurrence of local instabilities have not significant influence for final results but can cause convergence problems during the solutions for full scale 400 m gallery. So the aim for determination of factors caused instabilities are important for future, full scale calculations. The possible reasons, which are under consideration are: mesh definition on boundary layer, turbulence model coefficients values, which are strictly effected on calculated heat loses and wrinkling factor (χ_i) value.

Usage of SST model provide less heat loses than k-epsilon. Interrelations between heat loses and pressure-time history are very high. Influence of heat loses on pressure is easy to notice at 0.9 s for k-epsilon waveform.

Test 3

Due to the fact that developed models would be used for large scale calculations, where not all initial and boundary conditions can be precisely determined, testing for alternative ignition point location has been performed. Results obtained for alternative location of ignition source can be compared with the results obtained for SCOPE model in Test 1 and laboratory test data.

That case demonstrate the influence of shifting the ignition point for about 0.5 m. Locations of ignition points have been presented on as "ign1" and "ign2". All calculations in Test 3 have been performed using SCOPE model, SST turbulence model and homogenous 10% CH₄ methane-air mixture. There are not significant differences in pressure-time history and other parameters caused by ignition point location changing.

Test 4

Because of strong influence of wall heat loses on pressure-time history for explosion in chamber 5 m³ one more test has been performed – an adiabatic case

Adiabatic case provides very good confirmation for laboratory data in dp/dt value. It proves good setting of model b-Xi coefficients value.

It can be noticed, that calculated pressure-time waveform starts rising up earlier, than laboratory data. It is caused by definition of ignition source – correlation ignition volume, number of cells where ignition occurred and ignition strength. These parameters have to be set optimally but has to deliver enough energy to let reaction propagate completely (variable b has to have value close to 0 in burned products).

Determination of methane-air concentration in full scale domain (400 m gallery)

That part of development is meant for preparing tools and methods in order to estimate gas mixture initial composition in full scale geometry (400 m gallery). Using the same solver for estimation of CH₄ gas mixture composition (as initial condition) and for explosion progress has no sense. Mainly because of time consuming methods used to calculate reaction progress. Due to that facts simpler solver has been used for gas mixture estimation.

Following simplifications have been applied:

- adiabatic domain – no heat transfer to domain walls,
- isothermal gases – gases temperature have been set only for estimation transport parameters,
- ideal gas mixture – transport parameters have been estimated as for ideal mixture.

These assumptions let to perform gas distribution calculations in reasonable time. Calculation for full scale geometry is very time-consuming because of mesh dimension and time to analyse. Typical time to analyse is about 600 s. Mesh dimensions for full scale geometry have from 3 to 12 million cells. So simplifications in solver had to be done.

Many test for release scenarios have been performed. Ventilation conditions for each numerical calculations (for 400 m gallery) have been set according to measurement results. Air velocity has been measured in 3 cross sections marked as B, C and D. Up to 12 (for C and D) and 15 (for B) measurements points have been used to determine air velocity profile in each cross section. Average air velocity has been set for 0.2 m/s.

Release of pure CH₄ from balloon

That case represents scenario with sudden realise of large amount of pure methane. Applied geometry does not include details (cross bars) to reduce number of mesh cells.

Realise of 50 m³ of CH₄ has been modelled as cuboid fully filler gallery cross-section below the bars (1.68 m x 1.68 m x 17 m).

Applied geometry simplifications reduce the turbulence at higher part of gallery and decrease the mixing process. Obtained results show tendency to disturb of velocity profile. Figure 12 presents the velocity profile for 60 m cross-section where maximum velocity along Z axis (along main gallery) reach over 0.6 m/s. That value is over 3 times above average velocity. Large cloud of CH₄ (just after balloon destruction) has strong tendency to go up. It is additional volume force, which in result disturb quite uniform velocity profile. That behaviour can also be observed in full scale tests results. Time for maximum peak values are also marked. Calculated local speed determined from methane propagation times are: 1.18 [m/s] (between 40 and 60 sensor) and about 0.87 [m/s] (between 60 and 80 sensor). That velocity profile is stronger at the beginning of mixing process when large amount of high concentration methane is present.

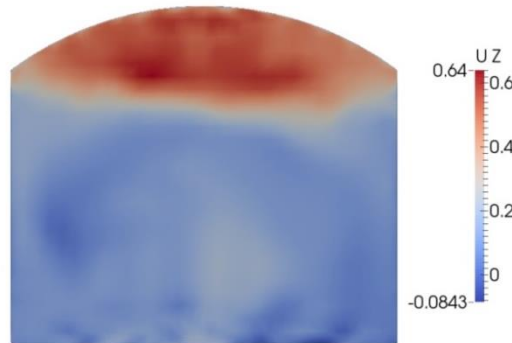


Figure 12. Velocity profile for Z axis direction (along main gallery) – cross-section 60 m

To check the tendency for mixing caused by cross-bars the following test has been performed. Cross-bars have been modelled in the first 35 m of gallery and realise of 25 m³ of CH₄ has been applied.

Figure 13 presents a visualisation of CH₄ distribution along gallery. Presence of cross-bars cause better mixing process but there is still strong tendency to stratify.

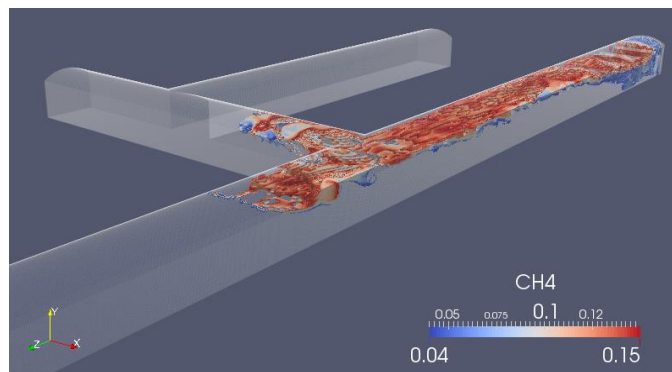


Figure 13. Realise of 25 m³ pure CH₄ – time: 45 s after realise, geometry with cross-bars

The second type of methane realise is continuous jet. Figure 14 presents CH₄ distribution for following conditions: air inlet: 1.3 m³/s (average 0.2 m/s in gallery cross-section), CH₄ inlet: 0.1 m³/s. Source of CH₄ was 2" pipe. Jet realise is able to mix gases more efficient than balloon method. Mixing efficiency strongly depends on source shape and initial turbulence applied by that source

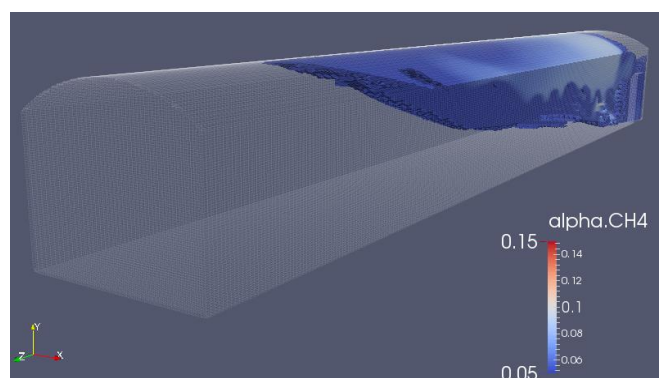


Figure 14. Visualisation of CH₄ continuous realise, realise source – 2" pipe

All above cases present strong gases tendency to stratify. Uniform mixture is hard to obtain in such large domain. That tendency has been proved also in full scale experiments.

Ultimate approach for methane-air mixture setup.

Numerical calculations of methane dispersion in the large scale gallery were performed. The boundary conditions and initial calculations were defined based on the configuration of large scale real-time studies (Task 2.3). Calculations were carried out for the abrupt outflow of large amounts of methane (balloon) and continuous release of methane (nozzle).

Numerical calculations of the explosion were performed on a full scale for 400 m gallery geometry. The model implemented in the project described the non-homogeneous distribution of gas mixture (SCOPE), which is a fundamental issue in view of the propagation of explosion. Due to the configuration design scheme for the calculation, it is irrelevant whether a continuous methane (nozzle) outflow scenario or abrupt release (balloon) was considered. The key factor is the obtained methane concentration distribution, which in numerical experiments has been determined using an independent solver (independent from the solver analysing the explosion).

The described procedure diagram and scope of work results from a series of calculations and tests carried out during the project implementation.

Determination of initial conditions of methane concentration distribution in the area of 400 m gallery was carried out in the following steps:

- a) preliminary determination of the distribution of CH₄ concentrations in the gallery area (numeric calculations – solver 'noEReactingFoam', detailed geometry),
- b) determination of calibration factors based on numerical experiment data (point (a) and laboratory experiment data (e. g. Ex-05),
- c) scaling of the CH₄ concentration distribution to the distribution of experiment concentrations on a full scale.

Preliminary determination of CH₄ concentration distribution in the gallery area was carried out using full geometry of the gallery. The full geometry reflects the constructional details of the gallery - transverse beams placed at a height of approximately 1.9 to 2.1 m above the floor. The application of detailed geometry at the stage of initial determination of concentration distribution allows to reflect the structure of flow velocity, local turbulence values and CH₄ concentration distribution disturbances caused by transverse beams.

To determine the concentration distribution, noEReactingFoam solver was used (modified standard ReactingFoam solver - without energy equation). Calculations were made for 1.5 s in order to determine the initial speed distribution without taking into account the turbulence model (as laminar flow) in the analysed geometry. Subsequently, the turbulence model (SST) was activated for the predefined distribution rate. Calculations were continued until completion of the transverse corridor (cross-cut) - about 60 seconds.

The velocity and concentration in gas detection points have been monitored. Calculations were carried out to the velocity steady state. For such defined velocity distribution and turbulence, the CH₄ concentration distribution was corrected again to the values obtained during the tests (linear analysis). The CH₄ concentration distribution prepared in such a way was used as initial conditions for XiFoam solver.

Linear equations were used as calibration equations for the distribution of CH₄ concentrations. Scaling was carried out in two directions:

- along the 400 m axis of the gallery (axis from the model's coordinate system) – absolute scaling,
- in the vertical direction of the gallery (Y-axis of the model coordinate system) – relative scaling.

The determination of the calibration equations was based on the CH₄ concentration values recorded by the measurement system before the ignition of the gaseous mixture (full scale experiments, Task 2.3).

The calibration equation along the Z axis is based on the indications of 5 sensors located along the gallery at a height of about 2 m above the floor. The calibration equation along the Y-axis is based on the indications of 2 sensors located successively at the following heights: 2 m and 1.4 m. The sensors are located at 100 m of the gallery.

Examples of calibration equations to reflect the initial conditions of an Ex-05 experiment are given in the form:

- for horizontal distribution along the axis Z: $cZ_{CH_4} = -0.0003 \cdot z + 0.0956$
- for vertical distribution along the axis Y: $cY_{CH_4} = -0.8149 \cdot y - 0.6299$

The determined calibration parameters of the linear equations apply only to the case under consideration and refer directly to the initial results of the concentration distribution of CH₄.

The distribution of CH₄ concentrations obtained by this procedure was used as the starting point for numerical calculations of explosion propagation.

As initial conditions for velocity distribution and turbulence, the values obtained during the initial determination of CH₄ distribution using a detailed 400 m gallery geometry were used. An example of CH₄ concentration distribution, including calibration equations and simplified gallery geometry, is shown in Figure 15. Colour map shows the variable "ft" - mass fraction of CH₄ in ambient air.

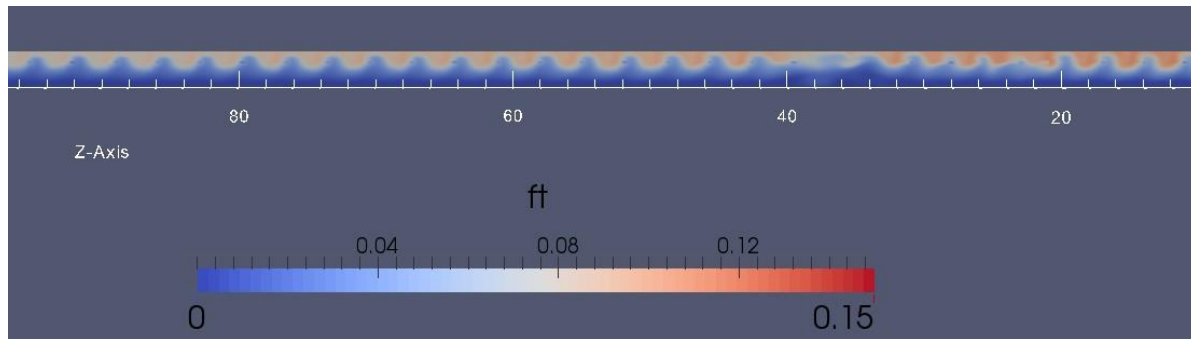


Figure 15. Distribution of CH₄ concentration including calibration equations. Variable "ft" - mass fraction of CH₄ in ambient air. Simplified sidewalk geometry 400 m. Cross-section along the Z axis

For flame propagation calculations, a simplified sidewalk geometry, excluding transverse beams, was used. The solution is resulting from a series of full scale gallery calculations and the difficulty of large geometries.

A series of flame propagation calculations were performed on a 400 m long gallery. The target strategy for the analysis of solutions was to perform calculations according to the scheme presented in Figure 16. The baseline solution used was the data from experiment Ex-05 (Task 2.3). The resulting CH₄ concentration distribution has been modified by applying the following coefficients: 0.7 to 1.4, thus creating a four case group of solutions. Value of variable "ft" was subject to modification - mass fraction of CH₄ in atmospheric air.

The mixture ignition, for each case, was done on 81.5 m from the closed end of the gallery. During full scale tests, in the examined case, the ignition of the mixture occurred 80 m from the closed end of the gallery.

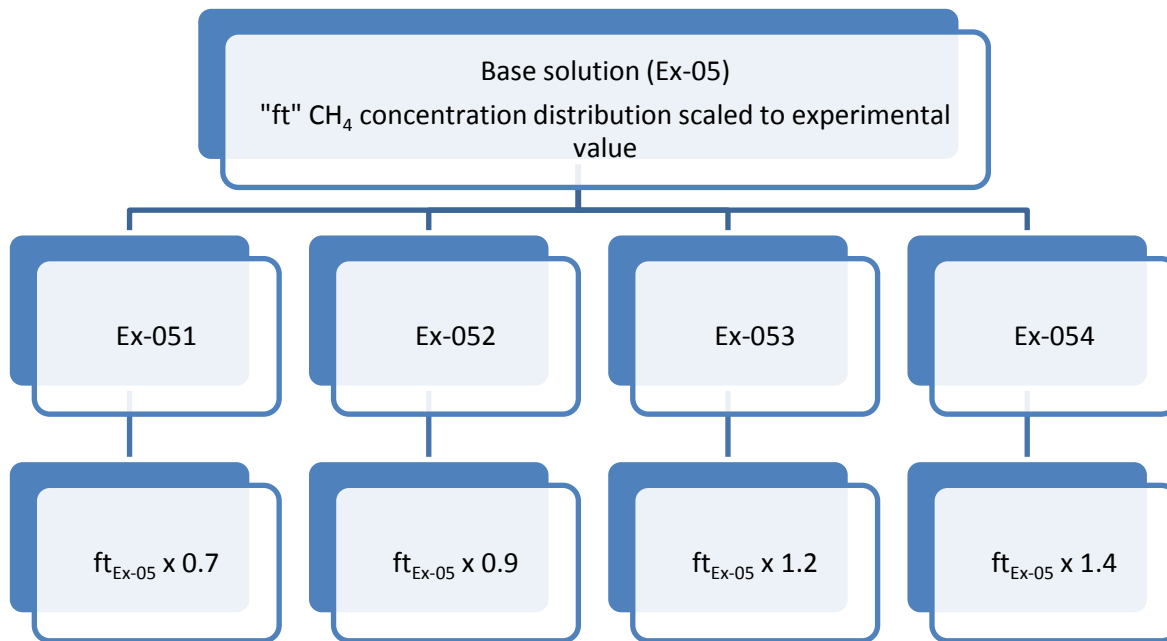


Figure 16. Case study diagram

Figure 17 shows the CH₄ concentration values at calculation domain points corresponding to the measurement points during large scale experiments. The statement includes values for the analysed cases based on Ex-05 experiment. The analysed cases were marked as: Ex-051, Ex-052, Ex-053, Ex-054.

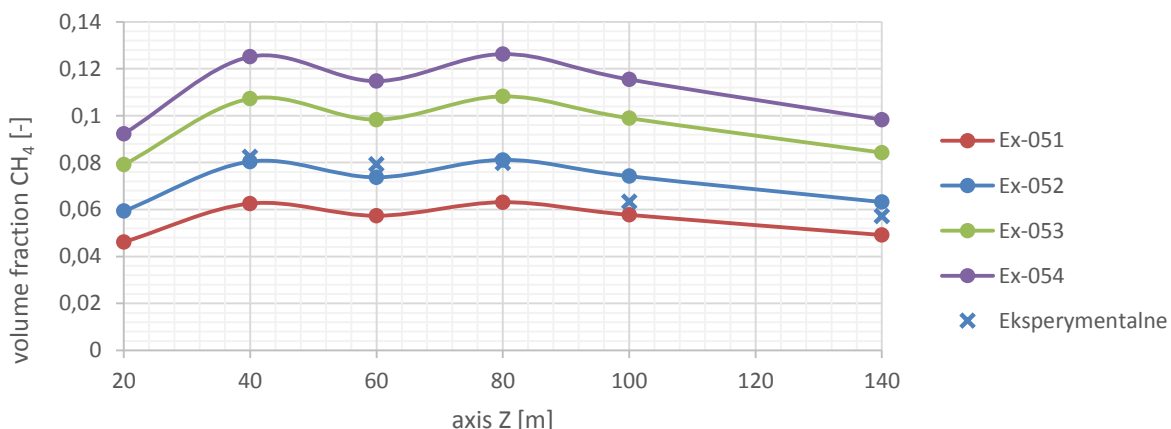


Figure 17. Initial condition for distribution of CH₄ concentration along the Z axis of the gallery.
Summary of the cases analysed

For the presented configuration of the initial conditions, a series of calculations have been performed using the solver.

Full scale calculations - results

It is extremely difficult to determine the distribution of CH₄ that accurately reflects the experiment on a large scale. Especially for measuring purposes during the experiment. Therefore, an analysis scheme based on the development of a number of configurations was adopted. The results obtained in this way allows better evaluation of computational solver performance.

As a result of the previous work on stability of obtained solutions, large scale calculations were performed for adiabatic domain.

Table 2 shows the flame propagation velocities obtained for the analysed configurations. The flame propagation velocities obtained are coincident in order of magnitude with the full scale test results (Task 2.3). The adopted method of analysis illustrates the significant influence of CH₄ concentration distribution on the course of flame propagation in the gallery in terms of the flame velocity pattern. For configuration solutions with low CH₄ concentrations - Ex-051 and Ex-052, an increase in the flame propagation velocity is visible at the following measurement points (concentration distribution CH₄ – Figure 17). For the configurations Ex-053 and Ex-054, the initial flame propagation acceleration (higher velocities in the initial flame propagation phase) is slowed down.

The reason for such a course of reaction is to generation of the mixture in the initial phase of explosion. The cases Ex-053 and Ex-054 at the point of ignition "contain" a mixture with a similar concentration to stoichiometric mixture or richer. As a consequence of the reaction initiation and flame propagation, an additional volume of reactive mixture is generated by mixing with the air from the lower part of the gallery. This pattern of the explosion initial phase is not possible for poor mixtures (at concentrations below stoichiometric). The effects of mixing the substance as a result of the initiated explosion cause further reduction of concentration and thus decrease in the parameters responsible for the velocity of flame propagation.

Table 2. Summary of results of flame propagation velocity calculations - analysed cases

| Distance from the closed end of the gallery [m] | CFD C ₀ Ex-051 | CFD C ₀ Ex-052 | CFD C ₀ Ex-053 | CFD C ₀ Ex-054 |
|---|---------------------------|---------------------------|---------------------------|---------------------------|
| [m] | [m/s] | [m/s] | [m/s] | [m/s] |
| 40 | - | - | - | - |
| 60 | 12,8 | - | - | - |
| 80 | | | | |
| 100 | 27,9 | 20,2 | 76,2 | 67,4 |
| 140 | 59,3 | 29,72 | 24,2 | 36,4 |

In each of the analysed configurations there were problems with propagation of flame in the opposite direction to the air current flow direction. Only in the case of Ex-051 the propagation of the flame towards the closed end of the gallery was recorded, which resulted in recording the reaction on 60 m gallery. In other cases, the propagating flame did not reach a level of 60 m (21.5 m from the ignition source).

Possible causes of flame propagation difficulties have been identified for the entire length of the gallery:

- Problems with convergence of equations solutions due to unfavourable relations of parameters: propagation velocity (reaction rate) - mesh resolution. This reduces the quality of the parameters solution associated with the flame propagation velocity and, as a result, may disturb the determined turbulent combustion velocity values. In the analysed configurations local occurrence of not physical values of parameter Ξ_i were observed. As a result, lowering the turbulent combustion rate below the local mixture flow velocity may result in blockage of flame propagation.
- The use of a simplified geometric model, with the result that there are no sources of turbulence in the flame propagation area. Lack of turbulence factors influences the turbulent combustion rate.

In the analysed configurations there was no significant increase in pressure during flame propagation. Only insignificant pressure fluctuations of 5 kPa at experimental values of 50 kPa. The resulting pressure values are directly affected by the reaction in the gallery. The pressure obtained results from the fact that part of the calculation domain volume was not included in the reaction (no flame propagation below 60 m).

Conclusions

During the stage of calculations many problems have been discovered. High sensitivity of solver to the resolution of the computing mesh was recognized. Tendency for the solutions (when applying adaptation time step – according to max. value of Courant Number) to irrational decreasing time step (increase of Courant Number value). Behaviour has impact on the results of calculations. It can be observed when flame face is passing the zones of computing mesh crossings. The crossing zones can be described as the zones between the mesh with high and small resolution (despite of defining the transition zone). Change of the time step "inflexible" results in stabilisation of the solution. The works on solution control algorithm using numbers of PIMPLE outer loops are being conducted. Introduction of time adaptation step based on the criteria of certain number of external loops required to obtain assumed convergence level may allow for effective conducting of the calculations in big scale.

It was proved, that the obtained results are different when different turbulence models: k-epsilon and SST are applied. Using SST model provides more stable solutions for the boundary layer. It reduces arising irrational values (peaks) of both: laminar combustion speed S_L and wrinkling factor Ξ_i . More stable solutions are of highest importance for the full scale calculations (full scale 400 m gallery).

Applied description of ignition source can be problematic when defining ignition energy, which can be observed in too fast development of flame face in early stage of explosion. It has minor effect however when analysing big scale geometries (small impact of initial stage of explosion on its final pressure development).

Conducted calculations of air-methane mixture propagation confirm and imagine phenomenon observed during lab tests.

The effect of big volume of methane displacement (release from the balloon) was recognized. Impact of big volume of released methane on the flow profile, which is developed in the experimental gallery can be clearly observed by increased flow speed in higher part of the gallery. Achieved speeds are higher than 1 m/s and can be clearly observed in the initial stage of release.

Besides, it was also observed translocated, local decrease of methane concentration. It results from methane diffusion in the cross gallery.

Obtained results of methane concentration profiles in the cross sections of experimental gallery were confirmed. Tendency to develop in-homogenous mixtures was confirmed.

For the calculations in full scale (400 m gallery) the solver with following parameters was applied:

- Parameters applied to establish Ξ_i and determining variable b
 - $\Xi_i\text{Coef} = 0.15$
 - $\Xi_i\text{ShapeCoef} = 1.5$
 - $u'\text{Coef} = 1.5$
- Method of determining Ξ_i : algebraic at early stage (up to 0.5 s after ignition) then transport approach
- Laminar burning velocity: SCOPE model
- Turbulence model: SST
- Wall Heat transfer: adiabatic

As a result of the performed works, a computational solver (with above settings) has been implemented which enables the analysis of the methane-air mixture explosion phenomenon. The operation of the solver was verified in conditions of homogenous and non-homogeneous mixtures, in relation to small (20 dm³), medium (5 m³) and large (400 m gallery) scale experimental tests.

The results of the calculations, in particular the flame propagation velocities, obtained for a non-homogeneous methane-air mixture on a large scale (the most complex case) conform to the experimental data (order of magnitude). However, using a solver to analyse large scale phenomena poses a number of problems related to the definition of the mesh and achieving a compromise between its density and the possibility of obtaining solutions. One of the possible solutions to the problem is the use of a mesh adaptation scheme or PDR approach.

Task 2.3 – Real scale tests

One of the purposes of the EXPRO project is to provide some physical knowledge about gas flame propagation in long ducts like mine galleries, with investigation of flame acceleration mechanisms and effects of geometrical changes:

- Influence of duct roughness,
- Change of cross section, bends, T-shape bifurcation,
- At small scale with advanced metrology (pressure sensor, flame probes, high speed video in transparent pipes),

and to check physical rules for extrapolation by a few additional tests complementary to large scale tests performed in WP2.

Experimental set-up

Overall device

The experimental device was composed by 24 m long pipe filled with a flammable mixture (Figure 18). The flammable mixture was prepared in a 2 m³ spherical vessel by partial pressure and was injected in the tube. The initial pressure in the 2 m cube vessel was around 5 bar. The filling of the tube was made with 2 bar of mixture, which represent 4 m³ of mixture.

Tubes are made of transparent PMMA or steel (Figure 19). Two diameters were tested: 150 and 250 mm. The tube was closed on the side of the gas injection and ignition source. The other extremity was covering by a plastic sheet drilled with the small hole to avoid a pressure rise-up of the tube during gas injection.

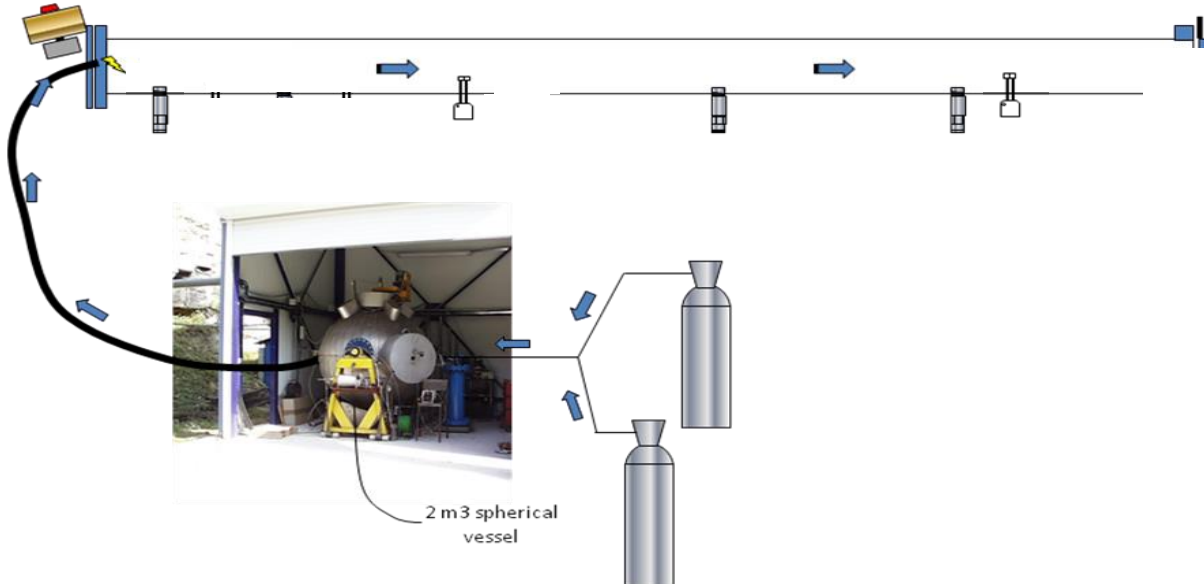


Figure 18. Overall device

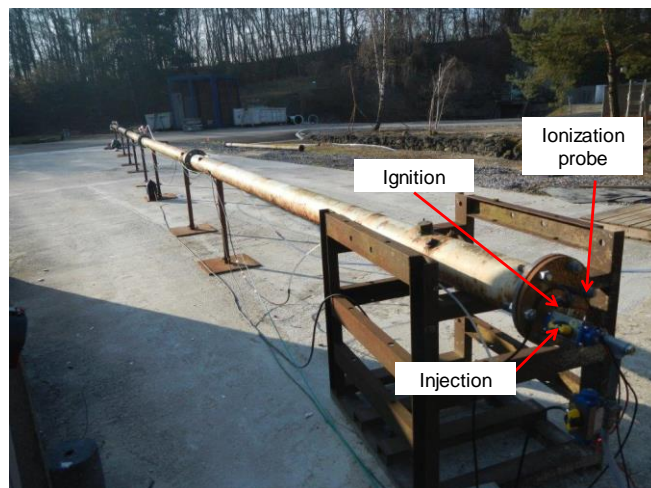


Figure 19. 150 mm steel pipe

Instrumentation

The instrumentation was composed by:

- Three pressure sensors:
 - Near the ignition, at 5.5 m and at 15.5 m,
- For flame detection in steel pipes:
 - Flame probes: photovoltaic cells which catch the light produced by the flame (at 0.5, 4.5, 10.5 and 15.5 m from ignition source),
 - Ionization probes in the first meter (4.5, 45 and 90 cm from ignition source).
- For flame detection in transparent pipes:
 - Photron fast video camera,
- Two Pitot probes to measure flow velocity.

The flammable mixture was ignited by an electrical spark (100 mJ) located at the center of the closed end of the tube.

Flammable mixtures

Five flammable mixtures were studied for the 150 mm steel straight pipe:

- 10 % methane in air,
- 8.4 % methane in air,
- 15,5 % hydrogen in air,
- 17,5 % hydrogen in air,
- 21 % hydrogen in air.

Eleven flammable mixtures were studied in the 250 mm transparent straight pipe:

- 6,5 % methane in air,
- 8 % methane in air,
- 10 % methane in air,
- 11,7 % hydrogen in air (same reactivity of 6,5 % CH₄/air mixture),
- 13,2 % hydrogen in air (same reactivity of 8 % CH₄/air mixture),
- 14,7 % hydrogen in air (same reactivity of 10 % CH₄/air mixture),
- 16 % hydrogen in air,
- 18 % hydrogen in air,
- 20 % hydrogen in air,
- 22 % hydrogen in air.

Two flammable mixtures were studied in the 250 mm steel straight pipe:

- 10 % methane in air,
- 20 % hydrogen in air.

The objective was to study the influence of reactivity of flammable mixtures on flame propagation.

Results and conclusions

- a typical test: stoichiometric methane air mixture in transparent 250 mm tube
- parametrical studies the comparison between the different situations:
 - Influence of pipe material,
 - Influence of diameter of pipes,
 - Influence of ignition source.

Typical test: stoichiometric methane-air mixture in transparent 250 mm tube

Figure 20 presents the pressure signals measured in the transparent 250 mm tube near the ignition source, at 5.5 m and at 15.5 m from ignition source. Figure 21 presents pictures of flame propagation when the transparent tube is captured on film closely. Some details of flame surface can be distinguished.

A first pressure rise-up in the tube until 120 mbar at 75 ms. This first pressure peak represents the first flame stretching due the hydrodynamic instability. Then the flame stops and the pressure decreases due to its extinction on the walls. Afterwards, the flame is submitted to strong accelerations, decelerations and stops due to the interactions with the acoustic waves in the tube. Indeed, the typical acoustic frequency of the tube can be estimated with the formula $f = c/2L$ where c is the sound velocity estimated around 500 m/s in stoichiometric methane air mixture, L is the length of the tube. The frequency is 10 Hz and the frequency of velocity oscillation is around 11 Hz. These interactions are also visible when compare the flame velocity and flow velocity measured by pitot probes in the middle of a section of tube at 10 and 18 m. It is noticed a good superposition of flame velocity and flow velocity oscillations.

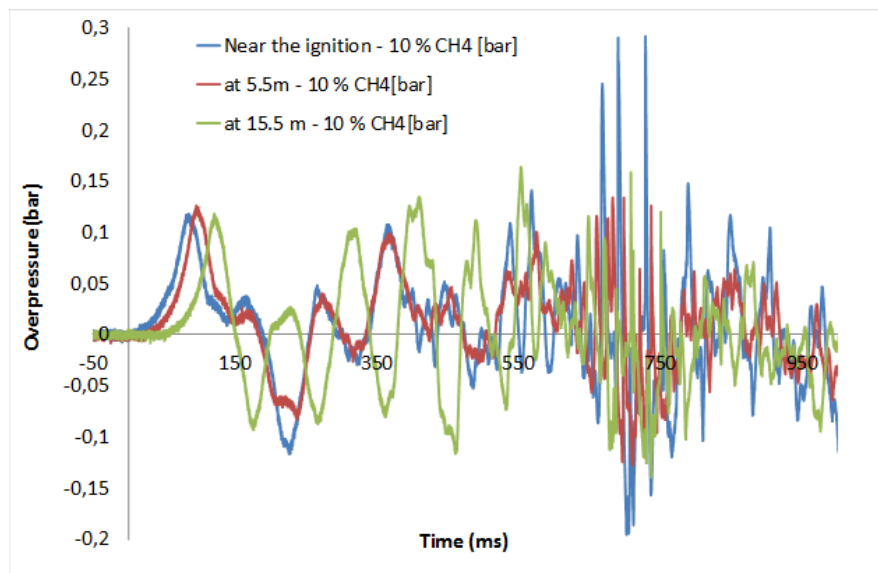


Figure 20. Pressure signals measured in the transparent 250 mm tube near the ignition source, at 5.5 m and at 15.5 m from ignition source

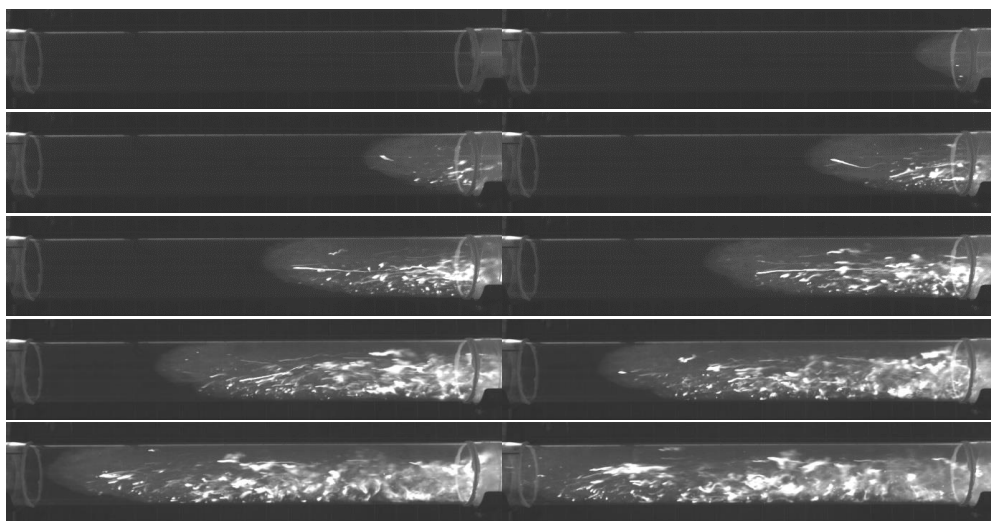


Figure 21. Pictures of flame propagation when the transparent tube is captured on film closely (5 ms between two pictures)

It was noticed that the flame velocity suffers from strong oscillations with a frequency which increase as far as the flame progresses in the pipe. Despite these oscillations it seems that the flame progresses with a mean velocity which increase. Thus, the flame seems to have a uniformly accelerated movement. The value of this acceleration is around 200 m/s².

Focusing on flow field near the edge of tube, it is noticed velocity oscillations around 2 m/s. Comparing the raw signals delivered by the probe before the ignition and during the flame propagation, it is noticed that the two signals have the same order of magnitude in frequencies and fluctuations. Thus, these oscillations are just noise and no turbulence.

Influence of pipe material

The influence of pipe material was studied by comparing the pressure signals in 250 mm plastic transparent tube and 250 mm steel tube for stoichiometric methane-air mixture.

It was noticed that the order of magnitude of pressure is conserved in the two tests. The global dynamic was conserved in term of frequencies of oscillation for example. But, the amplitude of oscillations was different. The amplitude in the plastic pipe is twice the amplitude in the steel pipe at 15 m. Up to know there was no clear explanation to these differences. Pressure losses measurements were made in both pipes and show that roughness is quite similar. This observation could be linked to the stiffness of material. Observing the velocity in plastic and steel pipes in the middle of a section and near the edge at 10 m from ignition source, it was noticed that the maximum velocity gradient (middle-edge) in plastic pipe (around 15 m/s) is higher than the maximum velocity (middle-edge) gradient in steel pipe (around 10 m/s).

For more reactive mixture (20 % hydrogen / air mixture), the beginning of pressure signals was similar in the two pipes, which shows a similar appearance of hydrodynamic instabilities. But, a strong acceleration occurs in steel pipes until a velocity near to 1000 m/s when the flame was around 11 m from ignition source.

The influence of pipe material was more significant for smaller diameter. It was noticed the first pressure development is similar for the both pipes. But, after the first pressure peak, an overpressure rise-up occurs with a maximum around 450 mbar for the steel pipe whereas in plastic pipe, there was no pressure increase.

An explanation of this phenomenon could find observing the flow velocity measured by the pitot probes in the middle and at the edge of the pipe for steel pipe.

Comparing the flow field behaviour in the 150 mm and 250 mm "rough" steel pipes, it was noticed that the flow near the edge is more disturbed in the small pipe. These fluctuations are not linked to an electrical disturbance. This fact could underline the influence of the turbulence of boundary layer in small diameter pipe than bigger one.

Influence of tube diameter

The impact of the tube diameter was experimentally studied as tests with 24 m long steel tube and diameters of 150 and 250 mm were performed as well for stoichiometric methane/air mixture. Comparing the pressure signals, it was noticed a significant difference.

Analysing the first peak corresponding to the flame elongation due to the hydrodynamic instabilities, the overpressure in the 150 mm tube (around 190 mbar) is twice the overpressure in the 250 mm tube (around 100 mbar).

Influence of ignition source

INERIS studied the influence of ignition source in 150 mm steel tube for stoichiometric methane/air mixture. There were tested:

- a pyrotechnical match:
 - Energy = 60 J,
 - Creation of several hot particles after ignition,
 - Removable protective cap,
 - Tests are performed with and without protective cap.
- an electrical spark:
 - Energy = 100 mJ,
 - Ignition in one point.

Comparing the pressure signals, it was noticed the maximum overpressure is obtained for the ignition with the pyrotechnical match covered by its cap. Indeed, the hot particles created by the ignition of match were directed in the same direction by the cap. Thus, the location of several ignition points in the same direction was more efficient than dispersed several ignition points (pyrotechnical match without cap) or one single ignition point (electrical spark). However, the electrical spark had been favoured by explosion.

Influence of bend on flame propagation

Tests with short bend in 250 mm transparent tube had been performed for stoichiometric methane air mixture and 20 % hydrogen-air mixture. The length of the bend was around 1 m and the bend radius was around 0.7 m. The bend was located at 17 m from the ignition source. Four pressure sensors were installed on the edge of the plastic transparent pipe near the ignition, at 5,5 m, at 15,5 m and at 19 m.

It was noticed the order of magnitude of overpressure is very similar for the straight pipe and the bend. The first flame development was the same which shows that the concentration of flammable mixture was the same in the both case. The pressure signals for straight pipes had strong oscillations linked to the acoustic whereas the pressure signals for curved pipe were smoother. The pressure on curved pipe seemed to be the average pressure in straight pipe. The bend modified completely the acoustic of the pipe reducing considerably the oscillations.

Influence of soft reduction on flame propagation

Tests with soft reduction between 250 mm and 150 mm transparent tubes had been performed for stoichiometric methane air mixture. The length of the soft reduction was around 1 m. It was located at 17 m from the ignition source. Five pressure sensors are installed on the edge of the plastic transparent pipe near the ignition, at 5,5 m, at 15,5 m, 17,4 m after the reduction and at 22 m at the end of the pipe.

It was noticed the order of magnitude of overpressure is very similar for the straight pipe and the pipe with soft reduction. The first flame development was similar in the both case until 30 ms. The pressure signals in both configurations presented strong oscillations with the same frequencies.

Influence of sharp reduction on flame propagation

Tests with sharp reduction between 250 mm and 150 mm transparent tubes had been performed for stoichiometric methane air mixture. The length of the sharp reduction was around 0,3 m. It was located at 15,8 m from the ignition source. Five pressure sensors were installed on the edge of the plastic transparent pipe near the ignition, at 5,5 m, at 15,5 m, 16,4 m after the reduction and at 21 m at the end of the pipe.

It was noticed the pressure developments are very similar for the sharp and the soft reduction configuration. The pressure oscillations had the same frequency. The only noticeable different is the magnitude of overpressure is slight higher around 20 mbar, which represent an increase of flame velocity around 5 to 10 m/s.

Influence of T-shape bifurcation

Tests with T-shape bifurcation with 250 mm transparent tubes had been performed for stoichiometric methane air mixture.

A first configuration of tests was performed with the ignition source located near the closed extremity where gas was injected. The two other extremities were opened. The T-shape bifurcation was located at 18 m for the gas injection. The length of straight pipe between T-Shape bifurcation and the end of tube was 7 m. The length of the small part perpendicular to the main tube axis was 4 m. Four pressure sensors are installed on the edge of the plastic transparent pipe at 5,5 m, at 15,5 m, at 19 m in the axis of the pipe and at 1,75 m in the short section.

It was notice the first pressure peak is identical for straight pipe and pipes with T-shape bifurcation. The flame propagation begins to the same way for both configurations. After, that it was noticed strong differences on flame development and pressures. The magnitude and the frequencies of pressure oscillations were completely different. The magnitude and frequency were lower than straight pipe configuration.

A second configuration of tests was performed with the ignition source located at the extremity of the 4 m long short part. This extremity was closed when the stoichiometric methane-air mixture was ignited. The location of gas injection did not change. A pneumatic valve was on the flange to allow the short part filling. The other extremity was opened. The position of T-shape bifurcation and pressure sensors were the same as the previous configuration.

It was noticed that Pshort, P-19m and P 15,5 m have the same evolution (magnitude and oscillations). Until 400 ms, the maximum overpressure is under 80 mbar. After 400 ms, the flame enters in the long pipe. The overpressures rised up around 400 mbar for Pshort, P-19m and P 15,5 m, and keep on rising-up in the 18 m closed part of the pipe. The overpressure reached 500 mbar at 5.5 m from the closed end. The overpressure measured at the closed end was around 1,3 bar, which could be a reflected pressure. This level was sufficient to destroy the last 2m long part of the plastic pipe.

Phenomenological model

This part presents the physic implemented in the phenomenological tool. The principle case is the flame propagation in 24 m long straight pipe opened in one end and closed to the other side near the ignition source. The diameter is 250 mm. The flammable mixture is a stoichiometric methane-air mixture.

As presented above, the flame propagation and flame trajectory suffer from strong acoustic oscillation after a first flame development and a first overpressure peak.

Estimation of acoustic frequency according to the flame position in the pipe

It's possible to estimate the resonance frequencies of constant section pipe although it contains gases of different nature. It was proposed an approximative version of associate acoustic theories. The tube with length L, closed at one end and open at the other, contains burnt gases until the x_f position. The acoustic waves propagate with the ab velocity. In the other part of the tube, it contains unburned gases where acoustic waves propagates the au velocity. The period of acoustic oscillation is given by :

$$T = \frac{2 \cdot x_f}{a_b} + \frac{2 \cdot (L - x_f)}{a_u}$$

The frequency is given by the formula :

$$f = \frac{a_b \cdot a_u}{2 \cdot [(L - x_f) \cdot a_b + x_f \cdot a_u]}$$

The formula permits to estimate the oscillation frequency with a good agreement for the first part of the pipe.

Estimation of overpressure

It is quite classical to suppose the flame propagates as a piston. From the start of its propagation, the flame sends a pressure wave. It propagates behind the flame and reflects at the opposite extremity. After, the pressure wave interacts with the flame.

It's possible to represent that by a simple equation, this expression is valid until the reflected pressure wave comes back and interact with the pressure wave and for moderate overpressures.

$$\Delta p(t) = \rho \cdot c \cdot U(t)$$

where Δp is the pressure in the burnt gases, ρ is the density of the mixture, c is the sound velocity and U represent the flow velocity induced by the piston effect behind the flame.

Estimation of first overpressure peak

An analysis of ignition phase in explosion in pipes shows that the first pressure peak P_1 is linked to the first flame elongation due to the hydrodynamic instabilities. This elongation last from the spark to the instant when the flame reaches the pipe edges. The magnitude of the overpressure seems to be directly depend to the expansion velocity of the burnt gases represented by the parameter $E.Su$ (E = expansion ratio, Su = laminar burning velocity). This correlation seems to be independent from the diameter of the pipe.

Thanks to the previous equation and knowing the value of the first peak, it's possible to know the value of flame velocity during this first phase. Moreover precisely analysing the beginning of the trajectory, allows noticing that the pressure rise-up and the flame velocity can be cut in three difference phases:

- 1- The flame develops with a slow velocity, which corresponds to the expansion velocity,
- 2- The flame accelerates, the pressure rise-up to reach P_1 ,
- 3- The flame stops, the pressure decreases and this time corresponds to the acoustic time of pipe defined by $2*L/c$.

Flame acceleration

After the first peak, the later phases of flame development shows a self-accelerated motion of flame despite the oscillation. The analysis of the EXPRO data and the past experimental INERIS data, show that the value of acceleration is not dependant from the geometry of pipe although a vibratory behaviour could be overlapped. A reasonable correlation between the expansion velocity of the burnt gases represented by the parameter $E.Su$ and the value of flame acceleration can be found. The analysis of past INERIS data doesn't show an influence of pipe diameter, but the recent EXPRO data seem underline the influence of small diameter on flame acceleration. However, it's difficult to quantify experimentally this influence. However, the correlation seems to be consistent with the EXPRO test for larger diameter.

The self-accelerated motion can estimate by the following equation:

$$V_f = a_F \cdot t$$

Where V_f is the flame velocity, a_F is the flame acceleration and t is the time.

Complete estimation of flame velocity

It's possible to construct the evolution of flame velocity during its propagation assembling all the bricks previously presented.

The second phase is the coupling of the self-accelerated motion of flame whose value of acceleration is defined by $E.Su$ and the acoustic oscillations of pipe by multiplying the average velocity with the sinus of frequencies. The value of acceleration for stoichiometric methane/air mixture is 130 m/s^2 .

Figure 22 presents a comparison with experimental and estimated flame velocity.

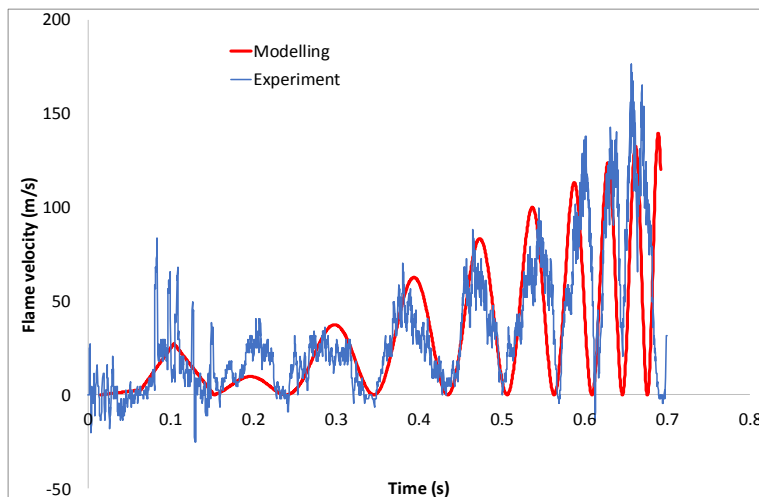


Figure 22. Comparison with experimental and estimated flame velocity

Application to large scale tests

For larger structures like tunnel or mine where the acoustic is less significant due to the length and the dimension of tunnel, the model is applicable.

It was applied it on INERIS explosion tests in a 140 m long tunnel filled with 15 m long hydrogen air cloud at the closed end of the gallery ignited by a pyrotechnical match. Two concentrations of flammable clouds are modelled:

- 11,6 % of H₂ in air,
- 14,1 % of H₂ in air (Figure 23).

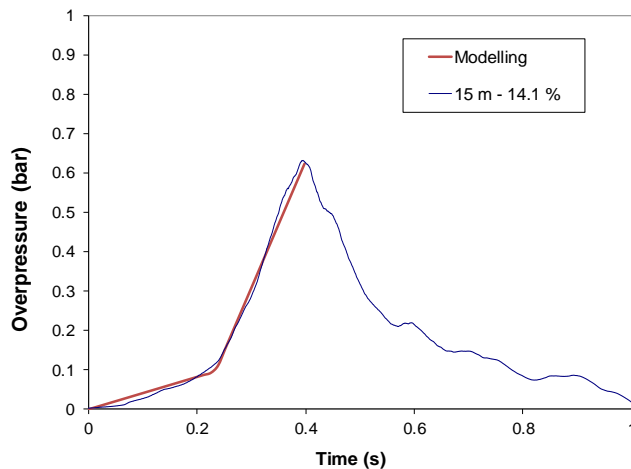


Figure 23. Experimental and modelling pressure for 11,6%H₂/air mixture in 15 m long cloud in INERIS tunel

Large scale tests at GIG

The experiments that consisted in introducing methane into the mining working and then initiating its explosion were performed in the 400 m gallery at the level 46 m of Experimental Mine „Barbara” in Mikolow. Cross-section of this gallery is 7.5 m². In all tests, stream of blowing ventilation, during methane distribution in the gallery varied from 0.2 m/s to 0.3 m/s.

The goal of the experiments was:

- identification of methane distribution in coal mine atmosphere for different methane release methods and low ventilation stream velocities,
- recording of the explosion parameters: pressure and flame speed,
- visual recording of individual stages of methane ignition and its explosion,
- correlation of the explosion parameters with the effects of explosion and its destructive impact on critical elements of working infrastructure,
- collection of data required for calibration and validation of computer models of methane explosion in the mining workings.

Methane with concentration of 100 % v/v was introduced in the blind end of the gallery (point 0) in two ways:

- directly from the set of tanks, through gas installation and 2" diameter pipe, into the space of gallery. Initially pipe outlet was totally opened, and in the following tests it was locked with the wellhead improving effectiveness of methane dispersion,
- using special sleeve with its diameter of about 1.9 m made from PVC wrap filled with methane. The sleeve was teared apart using several sections of blasting fuse NITROCORD 8. Detonation was initiated with the detonators ERGODET 0.45A N, safe in the presence of methane. Remote initialisation was enabled by specially designed blasting line connecting detonators with the ground surface.

The former method simulated slow methane occurrence in the working. The later method provided rapid release of big methane volume at initial stage of the gallery, avoiding however ignition of methane with the explosive tearing apart above mentioned sleeve. One running meter of the sleeve can hold about 2.8 m³ of methane (100 % v/v).

In order to monitor atmosphere parameters during the tests, Integrated Safety System SMP-NT/S made by EMAG-serwis was applied. It consisted of controller's desk, supply and transmission panels, installed in the control room on the ground surface, and the sensors installed in the underground test working. The sensors were placed along the working, usually close to the ceiling, in different configurations, which were described later in another chapters of this report. Set of sensors consisted of :

- absorptive sensors in the methane infrared radiation DCHIR operating in the range from 0 to 100 % v/v CH₄ (3 pcs.),
- catalytic methane sensors MM-4 (0 to 5 % v/v CH₄) + thermo-conducto-metric (5 to 100 % v/v CH₄) (3 pcs.),
- absorptive sensor in the carbon dioxide infrared radiation DCD (0 to 5 % v/v CO₂),
- electro-chemical sensor of carbon monoxide DCO-H (0 to 10 000 ppm CO),
- electro-chemical sensor of carbon monoxide MCO (0 to 1000 ppm CO), connected with system via middle switchboard MCCD,
- electro-chemical sensor of oxygen MO₂, connected with system via middle switchboard MCCD,
- temperature and moisture sensors CT and MH connected with system via middle switchboard MCCD.

Measuring stations equipped with pressure and flame radiation measuring systems are located in the cheek of the 400 m experimental gallery, in the short parallel gallery and in the connecting them inset. Pressure measurements are done by piezo-resistance pressure sensors (model: Kistler 4045 A10) together with adjusted amplifiers. Intensity of flame radiation is done by photo detectors with integrated amplifier (Thorlabs, model: PDA20H EC). Photo detectors were separated from the gallery space using sapphire lens, which increases view angle of the sensor protecting it at the same time from high temperature impact and dust. In each of measuring stations electrical (voltage) signals from flame and pressure sensors are converted into frequency optical signals and transmitted via optical fibres to underground control station, where the reverse conversion into electrical frequency is taking place and finally its transmission to the surface data acquisition system. Pressure and flame radiation intensity changes in the time function were recorded using platform NI PXIE-1073, equipped with three cards 6363 X. Registration of the signals always started with the impulse initiating explosion.

Visual registration of the experiments was made. Subject to tests' assumptions, video recording took place in two, three or four locations.

In total, 9 tests were performed. Table 3 summarises the results.

Table 3. Summary of large scale tests

| Test | Methane release | Ignition location | p_{max} bar g | u_{max} m·s⁻¹ | Flame range |
|-------------|---------------------------|--------------------------|-----------------------------------|--|--------------------|
| Ex01 | Sleeve ~14 m ³ | | | | |
| Ex02 | Sleeve 25 m ³ | several | | | No ignition |
| Ex03 | Sleeve 50 m ³ | 80 m | unmeasurable | 4 | 60 – 100 m |
| Ex04 | 2" pipe 50 m ³ | 100 m | unmeasurable | 5 | 60 – 100 m |
| Ex05 | 2" pipe/nozzle | 60 m | 0.64 | 79 | 20 – 200 m |
| Ex06 | 2" pipe/nozzle | 40 m | 0.57 | 143 | 20 – 200 m |
| Ex07 | 2" pipe/nozzle | Cross-cut | 2.25 | 500 | 20 – 200 m |
| Ex08 | Sleeve 60 m ³ | Cross-cut | 0.48 | 57 | 20 – 160 m |
| Ex09 | Sleeve 60 m ³ | Cross-cut | 0.16 | 29 | 30 – 120 m |

Figures 24, 25, 26, 27 and 28 and photos present typical results obtained in each test. Changes of methane concentration in the function of time and distance from point 0 of the gallery are shown in Figure 24.

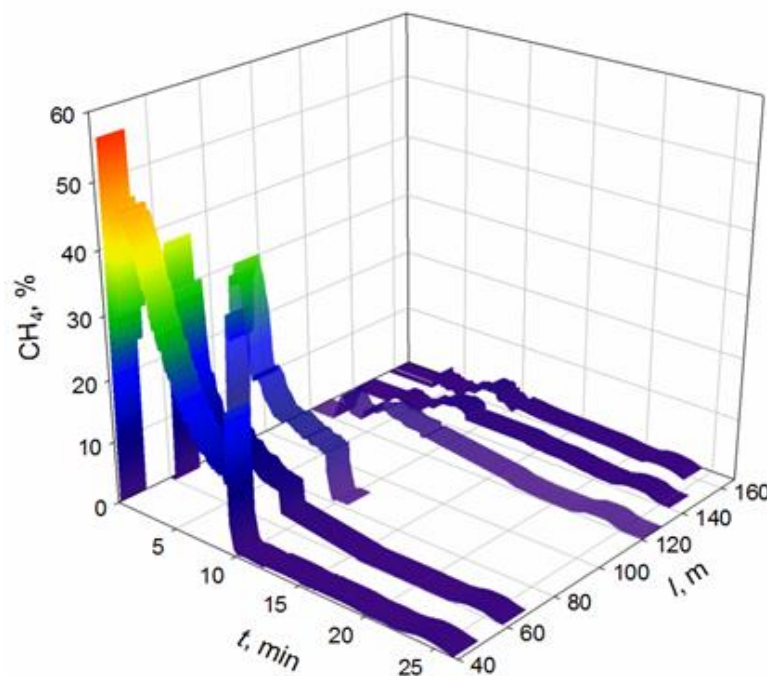


Figure 24. Methane concentration distribution during experiment Ex-03

Figure 25 shows the readings of remaining gas and temperature sensors, considering their location in the main roadway.

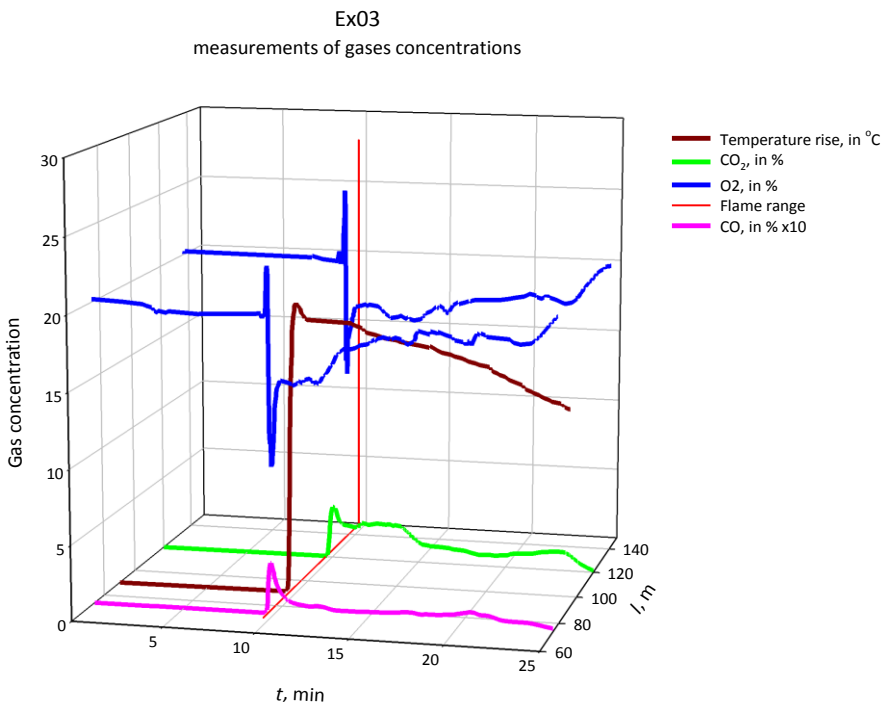


Figure 25. Changes of gases concentration and temperature during experiment Ex-03

Changes of pressure caused by methane combustion and speed of moving the combustion zone shown the graphs in Figure 26.

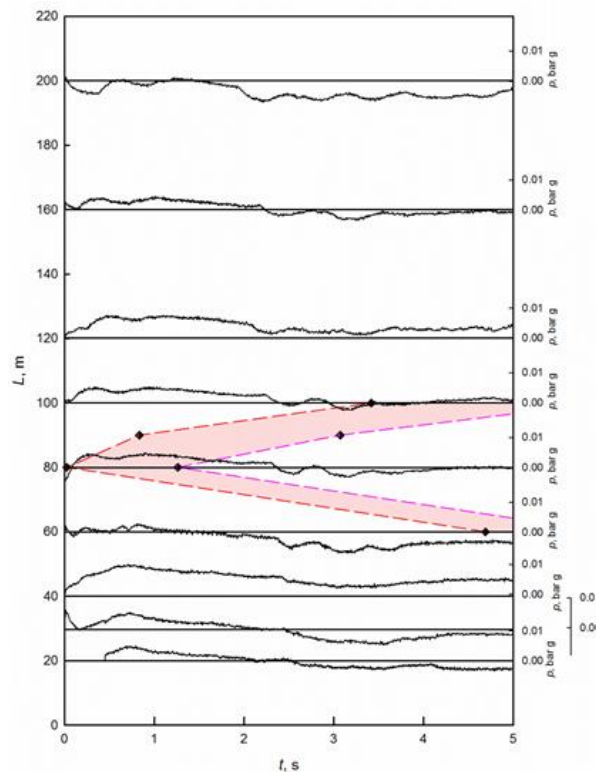


Figure 26. Changes of pressure and flame zone location during experiment Ex-03

In the gallery spaces close to the ceiling methane concentrations higher from upper explosion limit were observed. Methane combustion was observed there. The explosion developed below those accumulations (Figure below).

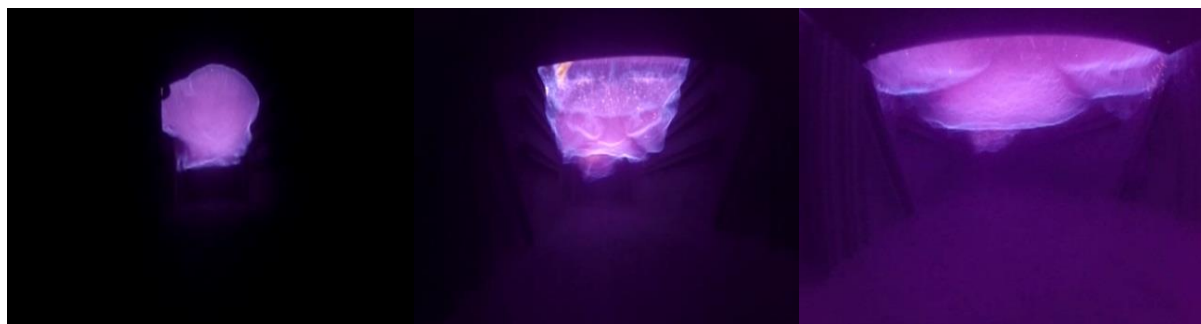


Figure 27. Explosion development registered by one of cameras

Mechanical damages of the sensors after each experiment were inspected. The Figure below present partially burnt insulation of an electrical wires.



Figure 28. Partially burnt insulation of an electrical wires

Conclusions

Conducted experiments proved, that keeping metrological functionality of the system and first of all its elements, installed in underground workings, needs assurance of :

- fixing durability of the sensors in their place of installation,
- fixing of the wire connecting sensor with permanent installation both to the ceiling and to the cheek of the working to eliminate free hang of the wire,
- using explosion proof casing „d” (fire proof cover) of detective elements of the sensor,
- installation of the sensors in appropriate way, to minimize possibility of their movement due to explosion pressure wave i.e. installation should be arranged in a way assuring smallest possible exposure of sensor’s cover area towards impact of explosion (pressure wave), if it does not affect its measurement functionality.

Readings of the sensors directly after the explosion are under impact of increased pressure and temperature, that is why they are less credible. In the conducted experiments they got back their metrological efficiency after several, few dozen minutes from the disturbance.

The most susceptible for temporary pressure and temperature changes are the sensors equipped with electrochemical and absorptive detecting elements in infrared band.

Conducted experiments proved, that releasing big volumes of methane into mining working results in its diffusion mainly close to the working’s ceiling. There are large gradients of gas concentration across workings’ cross section. It refers both cases, i.e. sudden outflows (experiments with PVC sleeve), as well as constant methane outflow into the working. Situation is changing when obstacles exist in the stream of the gas outflow. The obstacles may increase significantly turbulence resulting in better methane mixing with mine atmosphere. In case of slow methane release it mixes better within working’s volume as the process of concentration increase is much slower. Even though, however the distribution of methane concentration is non-homogenous. Plot in Figure 29 demonstrate this phenomenon. It shows changes of methane concentration close to the gallery’s ceiling and at the height of 0.2 m over the floor in experiment Ex-05, when methane was introduced by use of the pipe fitted with the nozzle that changed turbulence in the gas stream significantly and splitting it into several smaller streams.

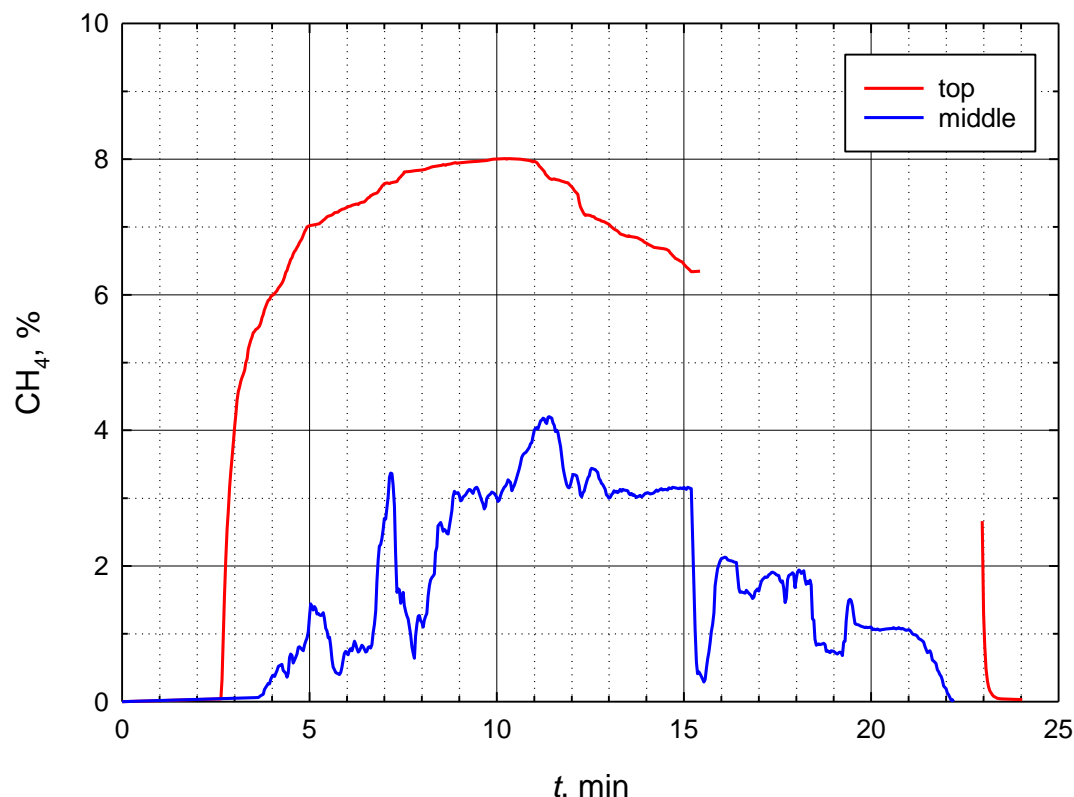


Figure 29. Changes of methane concentrations at 100 m distance from blind end of the gallery measured close to its ceiling and over the floor

In the cases, when methane concentration across working’s cross-section was highly non homogenous speeds of the flame front were very small, mostly not exceeding several m/s. This observation confirms miners’ evidence, who survived after methane explosions in Polish coal mines. They claimed, that after seeing „the explosion” they managed to shelter against it. The combustion zone was moving along the gallery in its upper part, as shown in Figure 30.

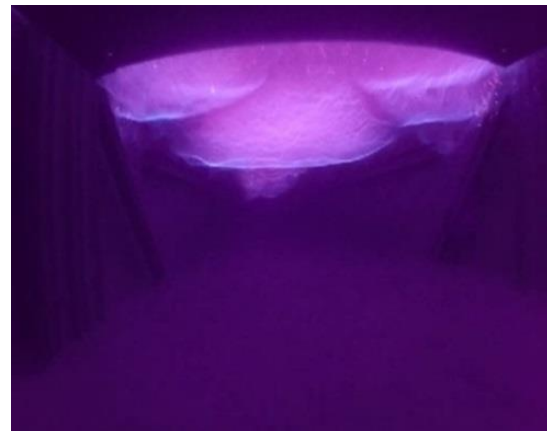


Figure 30. Zone of methane combustion in upper part of the gallery

AITEMIN & FSB real scale tests

To carry out the methane explosion trials, it was used the previously existing test gallery in Mina Sarita. This gallery is placed in rock, and before EXPRO project was about 110 m length, of which the last 12 were a “cul de sac”, as it has a ventilation shaft of 75°, at 100 m from the beginning which communicates with the main upward incline gallery connecting floors 0 and 7, connecting with it up to the floor 2.

For carrying out the trials, it was necessary a “cul de sac” gallery of at least 25 m, so FSB proceeded to continue the existing gallery. In this last zone built, a ceiling was built, to simulate a main ventilation, if it was required in the tests.

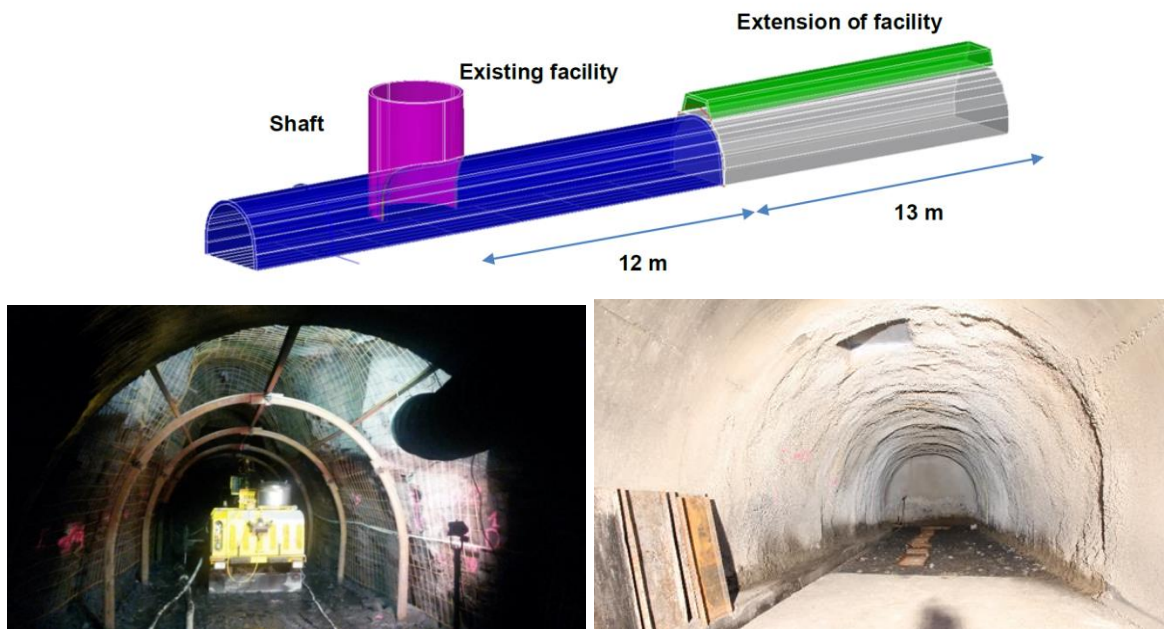


Figure 31. Facility extension

A new shelter, has been built for the EXPRO project. This shelter is closed and shielded by a gate of two 10 mm steel doors. The support have been made with bolts, metal wire mesh and minimum thickness of 10 cm of shotcrete (Figure 31).

Equipment and installations

The systems that were acquired and implemented for the trials are as follows:

- Injection system for explosive mixture (methane + air).
- Nitrogen purge of pipelines system.
- Compressed air purge of “cul de sac” and shelter system.
- Power supply system (power and lighting).
- Environmental control system (intrinsically safe).
- Starting detonation system.
- Control and general monitoring: data acquisition and imaging system.

In addition to existing ones, as the gallery main ventilation.

Injection of explosive methane – air mixture system

To carry out the tests, methane bottles train was located inside the new shelter, in the test gallery. The maximum expected consumption has been defined depending on the type of test. The gas storage was limited to the minimum amount required for a single test, and the remainder of bottles outside until use.

The gas supply system had a purge system, so that once the necessary amount of methane would be supplied to the receptacle, all the gas system could be cleaned, preventing the explosion from spreading to the bottle store. To prevent the gas return, there was a non-return valves that stopped the exhaust to the pipe.

Control system

To gather all the information needed to perform calculations of pressure transmission throughout the test gallery and ventilation behaviour in the mine, a number of measuring stations was installed along the test gallery (Figure 32). The main parameters to be controlled were the pressure, wave speed, flame presence and air temperature. The instrumentation used had to be sufficiently reliable and able to withstand severe environmental conditions that occurred in the test gallery.

Moreover, it was necessary to add to previous instrumentation, one that allowed to make a proper and safe control of the electromechanical elements used in the test, and to provide the necessary signals for generating safety actions to protect equipment and people at the facility.

The control system installed therefore collected all the information generated by the operating instrumentation, control and safety, providing adequate real-time representation of all parameters, and performed processing and storing information for later use.

The control device comprising three subsystems:

- Data Acquisition System
- Image Capture System
- Control system and general monitoring.

The data acquisition system took samples of pressure, temperature and flame speed in different sections of the gallery during test execution.

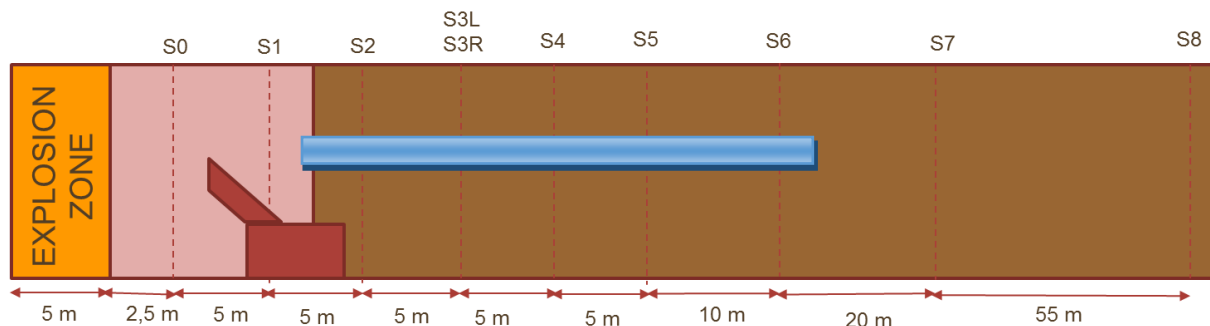


Figure 32. Measurement sections in the gallery

The data acquisition system was located in the test gallery shelter, and is able to send to external PCs full duration of the test with the above premises for further processing (200 samples/second for 48 sensors).

The Image Capture System was also located in the test gallery shelter. This System comprised a camera connected to a system of rapid imaging, specifically KODAK SR-500 system 500 fps. It also integrated a SONY 8mm recording system. The camera was placed in the test gallery, protected by steel armour. The other elements remain within the shelter. The start of the recording system was triggered by the overall control system.

The overall control system allowed communication via Ethernet that came from the shelter outside the test gallery.

Types of tests

Several different types of explosion trials was carried out: preliminary tests with a small amount of gas, tests in which the explosive mixture was confined into balloons and tests in which a bounded or a plug length of the entire section of the gallery was flooded by explosive mixture.

The standard scenario in which tests was carried out simulate explosions progress in a "cul de sac" where there are some machines working: a roadheader, an air duct, etc. It is also equipped with a booster fan.

As explosive it was used gaseous methane, supplied by a bottle of compressed gas, located in the test gallery shelter. Through monitoring sensors, necessary contribution of methane is determined to achieve an explosive mixture with a concentration between 5 and 15% CH₄. Using the CCTV video camera, preparation operations and filling the bags of methane was recorded.

Roadheader Structure

For the trials, a simulator of roadheader has been built. It is made of 4 mm steel, and to have real strength and weight conditions, inside it, there were water containers with sand filling the remaining spaces.

Three different types of tests were carried out: preliminary trials, whose objective were the start-up of the entire facility, small scale trials, where latex balloons were used as explosive gas containers, being easy to get the explosive mixture, controlling the injected flow rates of air and methane, and complete gallery trials, where an important length of the gallery were overflow.

Preliminary trials

A total of 5 preliminary trials were carried with small amount of explosive mixture between 200 and 600 litres (Table 4).

Explosion tests were carried using balloons (less than 1 m diameter), which is a volume of explosive mixture of about 300 litres per balloon. Nevertheless, volumes over 200 litres on the balloon caused breakage thereof. For this reason, trials were carried out using 1, 2 or 3 balloons to avoid exceeding 200 litres each one.

The explosive mixture was air-methane, with a concentration of 10% CH₄. Before the injection of methane, the air was injected in the balloon; later, after purging the pipe with nitrogen, methane was injected.

A total of 5 trials were carried out, without secondary ventilation in the "cul de sac" and without using the roadheader structure.

The amounts of methane for these tests were:

Table 4. The amounts of methane for 5 tests

| EXPLOSIVE MIXTURE | | | | | |
|-----------------------|-----|-----|-------|--------|---------|
| Test number | 1 | 2 | 3 | 4 | 5 |
| Air litres | 180 | 180 | 270 | 360 | 540 |
| Methane litres | 20 | 20 | 40 | 45 | 65 |
| Total litres | 200 | 200 | 310 | 405 | 605 |
| Methane concentration | 10% | 10% | 12,9% | 11,11% | 10,74 % |

According to the results:

- a) This trial generated a deflagration reaction.
- b) Photocell was unable to register the flame propagation. This type of sensors was replaced by Ultraviolet flame detectors
- c) Temperature propagation reached Section 4 (35 meters from the ignition point).

In order to determine the influence of the balloon explosion and the ignition systems, additional tests were carried out using only air into the balloons (3 balloons and 600 litres of air) and identical setup. The results show no variation in the pressure values

According to these results, there was no influence of the balloon or the ignition systems in the pressures indicated by sensors.

Small scale trials

Once the preliminary tests were finalized, the definitive instrumentation was installed in 10 measurement sections.

9 measurement sections were installed on the right side of the gallery and 1 measurement section was installed in the left side in order to check the symmetry of the phenomenon. To protect the sensors of the blasting phenomena, these sensors were installed inside concrete pillars attached to the walls of the mine.

In addition, the data acquisition and control system was adapted to the new set of sensors, and the software was reprogrammed according to the new requirements.

Some tests were carried out installing a roadheader simulator in the "cul de sac", and some test were carried out using secondary ventilation.

According to the planning, a total of 10 trials were performed with the following configurations (Table 5)

Table 5. Small scale tests

| Test | Roadheader | Secondary Ventilation | Number of tests |
|--|------------|-----------------------|-----------------|
| Small scale (8 m ³ balloon) | NO | NO | 2 |
| Small scale (8 m ³ balloon) | NO | YES | 2 |
| Small scale (8 m ³ balloon) | YES | NO | 3 |
| Small scale (8 m ³ balloon) | YES | YES | 3 |

Small scale explosion tests were carried out using plastic balloons manufactured using greenhouse plastic heat-sealed.

The explosive mixture was 8000 litres air-methane, with a concentration of 10% CH₄. Before the injection of methane, the air was injected in the balloon; later, after purging the pipe with nitrogen, methane was injected.

The following Table 6 presented an example of the average values of parameters measured at the selected locations.

Table 6. Average values of parameters measured at different locations

| Static Pressure (Average of max) (bar) | S0 | S1 | S2 | S3 R | S3 L | S4 | S5 | S6 | S7 | S8 |
|--|--------|--------|--------|--------|--------|--------|--------|--------|--------|--------|
| Roadheder: No Ventilation: No | 0.9730 | 0.9720 | 0.9668 | 0.9611 | 0.9572 | 0.9619 | 0.9587 | 0.9568 | 0.9484 | 0.9556 |
| Roadheder: No Ventilation: Yes | 1.0177 | 1.0138 | 1.0029 | 0.9907 | 0.9816 | 0.9944 | 0.9894 | 0.9890 | 0.9917 | 0.9978 |
| Roadheder: Yes Ventilation: No | 1.0010 | 0.9734 | 0.9701 | 0.9646 | 0.9568 | 0.9653 | 0.9618 | 0.9606 | 0.9625 | 0.9658 |
| Roadheder: Yes Ventilation: Yes | 0.9901 | 0.9692 | 0.9639 | 0.9586 | 0.9529 | 0.9592 | 0.9555 | 0.9532 | 0.9561 | 0.9607 |

Full gallery tests

Full gallery blasting tests were carried using a plastic sheet to seal the final part of the gallery.

To determine the exact volume in the gallery and the point to install the plastic sheet, a 3D survey of the final part of the gallery was made.

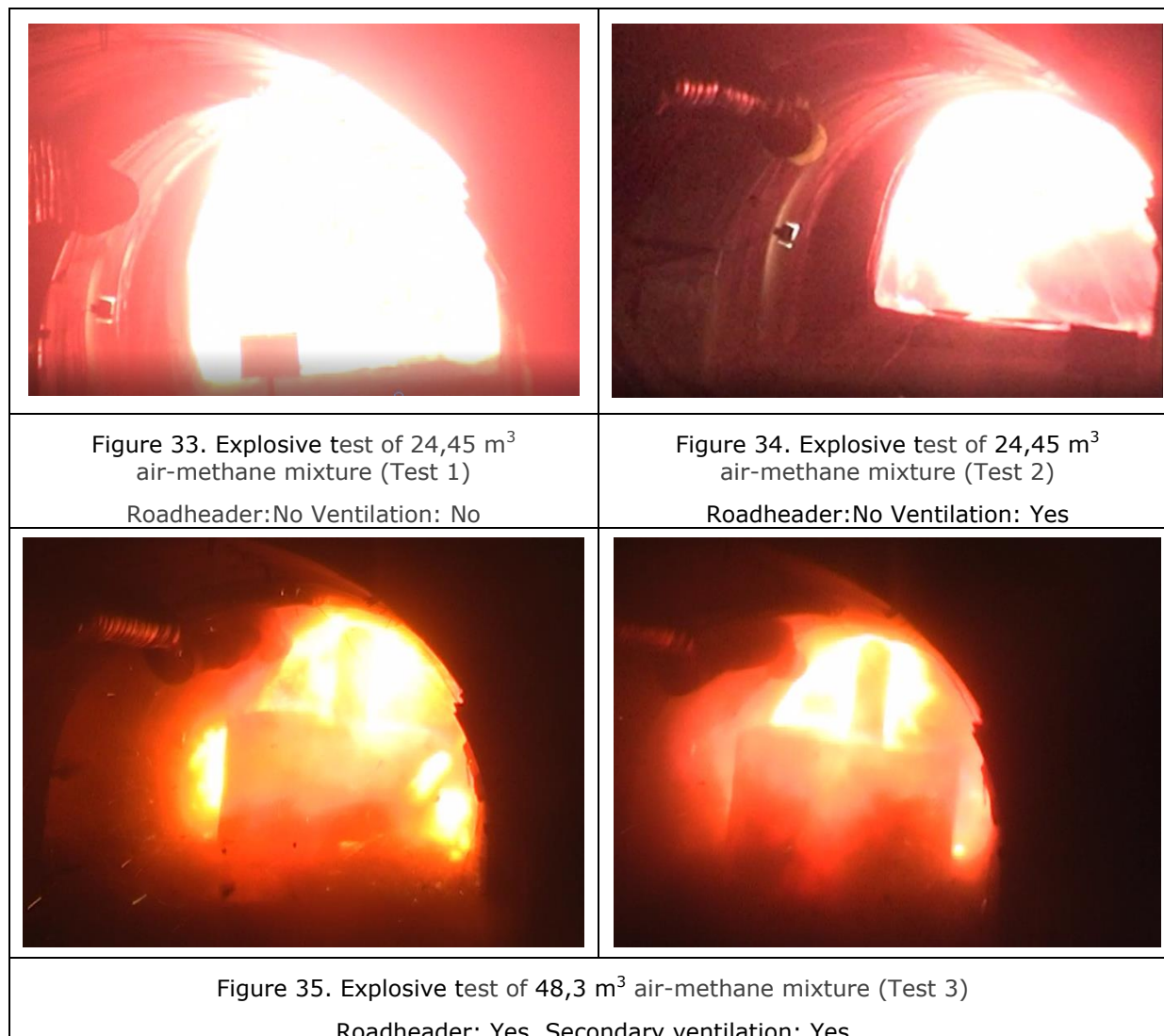
In tests 1-6, the explosive mixture of 24450 litres air-methane, with a concentration of 10% CH₄ was used. Methane was injected directly in the "cul de sac" using the air accumulated for the mixture(example photos on Figures 33, 34).

In 4 tests, the explosive mixture of 48300 litres air-methane, with a concentration of 10% CH₄ was used. Methane was injected directly in the "cul de sac" using the air accumulated for the mixture (example photo on Figure 35).

The tests condition were as follows (Table 7)

Table 7. Full galery tests

| Test | Roadheader | Secondary Ventilation | Number of tests |
|----------------------------------|------------|-----------------------|-----------------|
| Full section 22.5 m ³ | NO | NO | 1 |
| Full section 22.5 m ³ | NO | YES | 1 |
| Full section 22.5 m ³ | YES | NO | 2 |
| Full section 22.5 m ³ | YES | YES | 2 |
| Full section 45 m ³ | YES | NO | 2 |
| Full section 45 m ³ | YES | YES | 2 |



The following Table present an example maximum values registered by the sensors in one of the tests.

Table 8. Maximum values registered by the sensors

| Test 1 | S0 | S1 | S2 | S3 R | S3 L | S4 | S5 | S6 | S7 | S8 |
|-------------------------------|--------|--------|--------|--------|--------|--------|--------|--------|--------|--------|
| Static Pressure (bar) | 1.0575 | 1.0477 | 1.0329 | 1.0190 | 1.006 | 1.0283 | 1.0194 | 1.0269 | 1.0288 | 1.0414 |
| Dynamic pressure (bar) | 0.1461 | 0.1436 | 0.1270 | 0.1177 | 0.123 | 0.1123 | 0.0874 | 0.1050 | 0.1074 | 0.1153 |
| Top temperature (°C) | 325.32 | 263.27 | 217.53 | 156.99 | 156.99 | 111.86 | 79.14 | 37.41 | 15.30 | 13.65 |
| Side temperature (°C) | 312.03 | 256.50 | 198.07 | 112.45 | 112.45 | 107.50 | 29.81 | 29.62 | 14.08 | 14.19 |
| Flame detector | 1 | 1 | 0 | 0 | 0 | 0 | 0 | 0 | 0 | 0 |

Results

- 25 explosion tests were carried out using different amounts of mixture air-methane 10% and combining the presence of roadheader and secondary ventilation (5 preliminary trials, 10 small scale tests with 8000 litres and 10 full gallery tests with 24450 litres and 48300 litres). Some of tests caused damages in the gallery (Figure 36).
- The preliminary tests were used to validate the injection and initiation systems, as well as the types of sensors to be used in the tests and their disposition.
- The small scale tests and full gallery tests have allowed to obtain a large amount of data of pressures and temperatures, which help to understand the behaviour of the explosive phenomenon, as well as the influence of the roadheader and secondary ventilation in its propagation.

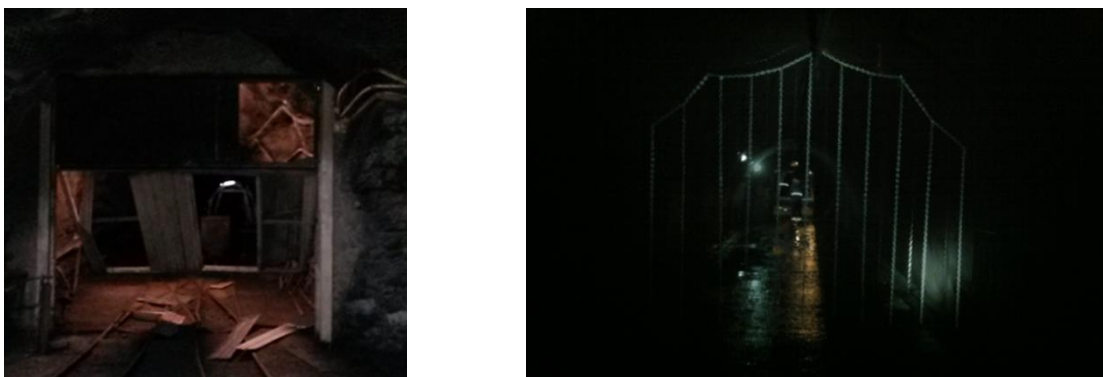


Figure 36. Damage to facilities an chain barriers

Conclusions

Preliminary trials (200-600 litres explosive mixture air-CH₄):

- This trial generated a deflagration reaction.
- Photocell was unable to register the flame propagation. This type of sensors was replaced by Ultraviolet flame detectors in posterior trials.
- Temperature propagation reached Section 4 (35 meters from the ignition point).

Small scale trials (200-600 litres explosive mixture air-CH₄):

- The propagation of the flame reached only the first section (2,5 metres from the explosion area), being independent of the type of test.
- The static and dynamic pressures decrease very slightly in the first sections, while in the last sections they are maintained and even increased. This may be due to the coupling of wave fronts.
- There are dispersions of results between similar trials, which indicates that there are many parameters that intervene in the evolution of the phenomenon and are difficult to control.
- By installing the roadheader the static and dynamic pressures decrease faster in the first sections, returning to the normal pace behind the roadheader.

Full gallery trials (24450 and 48300 litres explosive mixture air-CH₄):

- The presence of the roadheader causes a mitigation in the propagation of the explosion, so much for the pressures as the temperatures, being more remarkable the decrease of the pressures.
- Secondary ventilation increases the effects of the explosion in terms of pressure (static and dynamic), but decreases the temperatures.
- The increase of the methane amounts up to 48 m³ does not cause an increase in the pressures but in the temperatures. This is because despite having more amounts of methane the mixture is more imperfect, which causes the phenomenon to be slower (deflagration and not detonation).

Task 2.4. – Exchange of results

Comparison of FSB tests results with INERIS model

The phenomenological model of INERIS is applicable when the flammable cloud is ignited at the closed end of a tunnel. Among the large-scale tests performed by the EXPRO partners, only the FSB tests correspond to this situation.

The model is applied on full gallery trials using the same acceleration factor (110 m/s²) as the INERIS small scale tests:

- Type A (24.5 m³): This test was carried out by filling the last 2.5 m of the gallery (22 m³) with 2.200 litres of methane (10% methane), without roadheader and secondary ventilation.
- Type B (47.8 m³): This test was carried out by filling the last 5 m of the gallery (45 m³) with 4.500 litres of methane (10% methane), with roadheader and secondary ventilation.

For type A trials, the final flame position is around 10 m. The measured flame velocity is around 80 m/s. The average overpressure measured in different positions in burnt gases is around 160 mbar.

The Figure 37 presents the estimated overpressure for the Type A trial. The maximum overpressure is around 190 mbar. The maximum flame extension is around 10 m, the same of magnitude of the test. The maximum flame velocity is around 50 m/s. The model gives a good order of magnitude of final flame position, overestimates the overpressure and underestimates the flame velocity.

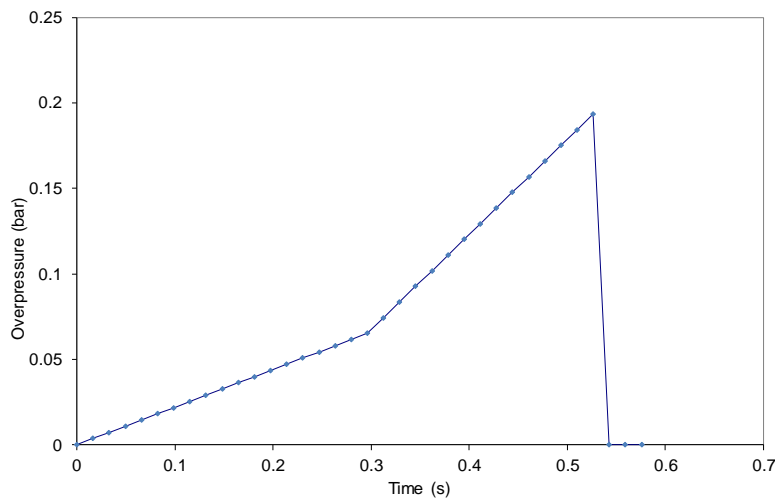


Figure 37. Estimated overpressure signal – Type A trial

For type B trials, the final flame position is around 22 m. The measured flame velocity is around 90 m/s. The average overpressure measured in different positions in burnt gases is around 70 mbar.

The model is not able to account for the presence of the roadheader. The Figure 38 presents the estimated overpressure for the Type B trial. The maximum overpressure is around 280 mbar. The maximum flame extension is around 20 m, the same of magnitude of the test. The maximum flame velocity is around 70 m/s. This estimation conducts to the same previous conclusions. The model gives a good order of magnitude of final flame position, overestimates the overpressure and underestimates the flame velocity.

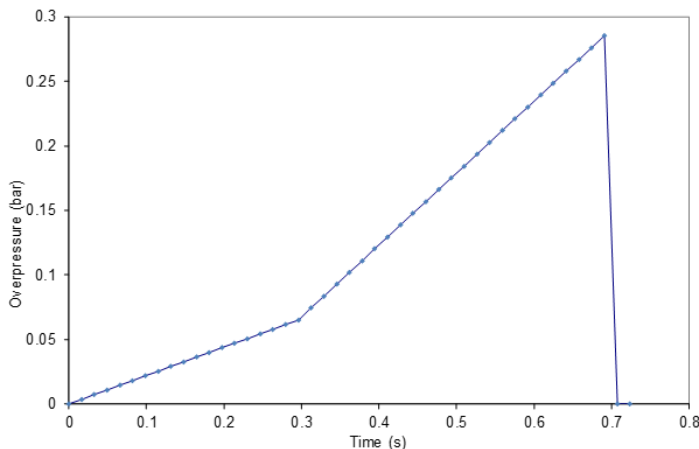


Figure 38. Estimated overpressure signal – Type B trial

The model seems to give the good order of magnitude on final flame positions and is conservative regarding the explosion overpressure.

3.3.2 WP3 – Development of fast air pressure monitoring system

WP Leader: **EMAG**

Partners: **GIG**, **PGG**

Task 3.1 – Modification of devices

The objective of WP3 was development of fast air pressure monitoring system which would be able to record fast changes in the air pressure in the mine areas with high explosion risk. The main task, in addition to the accurate measurement of air pressure, is the opportunity to identify the precise location of the ignition point after an explosion has occurred. Information about ignition point is a fundamental data for determining the causes of the explosion during the post-incident investigation phase.

At the beginning of the work there were defined the assumptions and main parameters that the system should comply. In the Task 3.1 it was also carried out an analysis of existing solutions for pressure monitoring equipment in the mines and opportunities to use them in the EXPRO project.

Assumptions and parameters of fast air pressure monitoring system

Analysis of the literature about behaviour of explosions has shown that the levels of pressure during explosion could be very high (up to 10MPa) and a speed of blast wave could be up to about 2000 m/s. Even though a measurement of very high pressure is possible, the system for fast data pressure measurement (designed in EXPRO project) equipped with high pressure sensors can't be useful for precise air pressure measurements which are normally performed in the mines. The reason is a too low accuracy at a level of atmospheric pressure. Therefore, we can use typical precise air absolute pressure sensors for developing the system. The basic requirement for these sensors is response time which must be minimum 10Hz. In this way we can precisely watch and analyse pressure in normal operation of the ventilation system and precisely locate the ignition point after an explosion has occurred.

A system designed and developed for fast air pressure measurement should fulfil the following conditions:

- a) measure changes of absolute air pressure in range up to 1300hPa;
- b) frequency of pressure measurement should be minimum 10Hz;
- c) protect the sensor element against high pressure blast wave;
- d) record data independently in underground sensor and in computer at the surface;
- e) have a battery backup in underground sensor;
- f) have a precise time synchronization between sensor and computer;
- g) transmit data using existing mine telemetric network up to about 9 kilometres;
- h) software which will be able to precisely locate the ignition point on the basis of time of pressure changes (peaks) and location of sensors in controlled mine area.

Meeting the above specified requirements allows to develop a system which will be able to register fast changes in the absolute pressure at the several points and store them in safe way independently in the sensor located underground and computer system at the surface. That solution provides an opportunity to analyse data after the accident even if the measuring devices will be destroyed by explosion (black-box), and provide analysis of air pressure in normal conditions of mine ventilation system.

Review of existing solutions for pressure monitoring equipment and system for fast data analysing

Below there have been shown devices most commonly used to measure absolute air pressure in the Polish mines. Also there has been presented a system for data visualization and processing related to seismic events in hard coal mines that have been taken into account in order to be applied in the EXPRO project.

Absolute air pressure meter µBAR (IMG PAN)

A hand-held air pressure meter of type µBAR is designed for measurements of absolute air pressure mainly in the excavations of deep mines. The measuring accuracy of the meter is very high. The pressure meter applies a sensor made by Setra Company (USA) of type SETRA 470. The µBAR meter may be used for current measurements made by ventilation service in mines as well as for research measuring experiments. Due to very high time stability of the SETRA 470 sensor, the results of measurements can be a basis for determination of aerodynamic potentials and making snapshots of mining ventilation systems.

For ventilation analysis purposes there are used portable air pressure measuring devices in selected points of a mine. Works of post-accident commissions in mines have shown that air pressure monitoring and recording for analysis purposes are very important for evaluation of hazards.

Characteristic of the air parameter meter THP-2

A construction of the stationary version of the THP-2 is based on a miniature high accuracy pressure transducer and a semiconductor temperature and humidity detector with digital output which are mounted together with an electronic circuit and a local display in a robust casing. Software of the THP-2 meter allows a multi-point correction of the processing characteristic and an operation with a surface central station within a methane-fire monitoring system.

Analogue signals from a pressure transducer and digital signals from temperature and relative humidity detector are introduced to the input of the microprocessor. The measuring results are processed and then introduced via microprocessor to a local display and by means of a C/A converter to the analogue outputs.

The measuring values are also available for an auxiliary micro-controller (single integrated circuit) which makes a communication protocol with a monitoring system card via a modem. The modem is connected to a supply-transmission line via a power unit. Push-buttons and service sockets are also connected to the microprocessor.

The air physical parameter meter THP-2 is characterized by very good qualitative and quantitative metrological parameters.

Technical parameters:

- Outputs of measuring signals – by means of a modem transmission in V23 standard, on a supply line to a system of linear telemetric outstations.
- Power supply – by means of a current source 40 mA DC of the supply-transmission module with a voltage of 56V.
- Max. line resistance – 600 Ω.
- Overall dimensions – 160 x 120 x 77 mm.
- Mass – about 1.5 kg.
- Protection degree (IP rating) – IP 54.
- Certification type (protection symbol) –  I M1 Ex ia I.
- Measuring range:
 - absolute pressure – 800÷1300 hPa.
 - temperature – 0÷50°C.
 - humidity – 0÷100%.
- Conditions of operation:
 - temperature – 0÷50°C.
 - relative humidity – 0÷100% without condensation.
- Accuracy:
 - absolute pressure in the range of 800÷1300 hPa – ±0.3 hPa.
 - neutral zone – 800÷805 hPa.
 - temperature in the range of 0÷40°C – ±0.5°C.
 - additional error in the range of up to 50°C ± 0.2°C.
 - relative humidity in the range of 10÷90% ± 2%.
 - additional error in the ranges of 0÷10% and 90 ÷ 100% – ±1.5%.

The THP-2 meter may be used in the underground mines in methane hazardous areas of category "a". "b" and "c" and in zones qualified as Z2 and Z1 of methane explosion hazard.

Temperature, humidity and atmospheric air pressure sensor DPT

A stationary temperature, humidity and atmospheric air pressure sensor DPT has metrological characteristics similar to the THP-2 sensor, because there has been used also the same SETRA detector, model 278 for pressure measurements. The electronic circuit has been made according to the series of types of DXX sensors made by EMAG-SERWIS.

System of visualization and processing of data on seismic events in hard coal mines ARAMIS M/E.

The system is used to locate rock bursts in a mine, to determine the energy of bursts and to assess rock burst hazards. Depending on the extent of the mine, the system is based on seismometers or optionally on low frequency geophones. The system uses intrinsically safe data transmission, centrally supplied from the surface, which enables to transmit 1-, 2- or 3-axial velocity movements (X. Y. Z). The sampling of signals is performed by means of 24-bit Sigma Delta converters, providing high dynamics of conversion and recording.

The seismic system ARAMIS M/E includes:

- Application server to determine the location and energy of the shock and software to assess the risk of rock burst.
- Archive (recording) server.
- Digital signal transmission system DTSS.
- Transmission surface station SP / DTSS including:
 - OCGA digital receivers.
 - transmission control module ST / DTSS GPS satellite clock.
 - switching power supply module and the safety transformer.
- Surface station cooperates with underground transmitting stations SN/DTSS.

Conception of fast air pressure monitoring system

During the works on the conception of fast air pressure system two main problems occurred: to find out a precise and fast pressure transducer with pneumatic protection against destruction by high-pressure blast wave and to find out very fast transmission system for transmit and record data from pressure transducer.

After investigation of existing devices which are capable to measure fast changes of air pressure we have decided to modify THP-2 sensor which is based on a miniature high accuracy pressure transducer (SETRA Type 278). The tests performed in a laboratory showed that this pressure transducer has sufficient response time and can be used for fast pressure measuring (Figure 39). The testing consisted in bringing high-pressure pulse (about 8 MPa) to transducer and record the response signal. In this case pressure transducer was protected against destruction by special protection pressure controller.

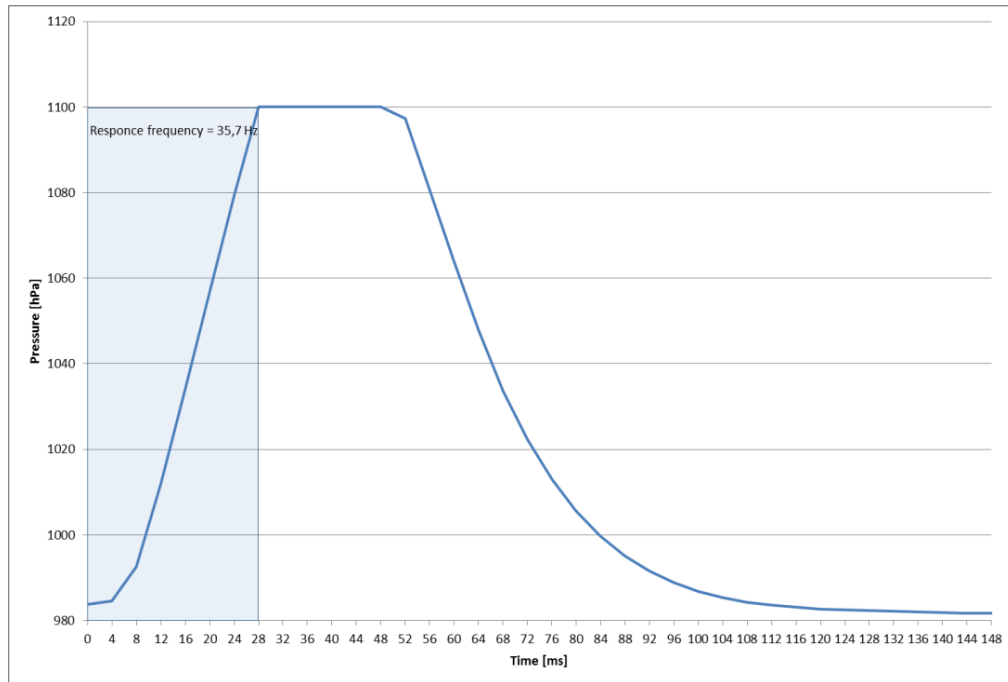


Figure 39. Results of sensor response time testing

The test was repeated twenty times and the results always were about 35Hz and this is a satisfactory result.

The developed fast pressure sensor based on a miniature high accuracy pressure transducer (SETRA Type 278) were equipped with battery back-up and internal memory buffer for storage data in case of damage of power supply/transmission infrastructure. For transmission data from pressure sensors located underground it was used a modified seismic transmission system ARAMIS M/E. This system allows to power supply and transmission data from sensors with frequency up to 150Hz. The modification was applied to the transmitters NSGA, battery back-up and memory buffer together with modified THP-2 sensor. All data recorded in sensors and on the surface database were sync by GPS clock.

The system support up to six fast pressure sensors and provides a power supply and data transmission using existing mine telemetric network up to about 9 kilometres. The data received from sensors is stored and analysed by software package which was developed in the Task 3.3.

Description and technical data of developed fast air pressure monitoring system

There were done the works on modifying the existing pressure sensor of the type THP-2 developed by ITI EMAG for purposes assumed in the project. It has been used a detector of type Setra 278 for pressure measuring. A measuring frequency of the sensor has been determined during laboratory tests. The results have shown that a response of the sensor to sudden changes in pressure in the whole measuring range is about 37.5 Hz; this is almost four times better as assumed (10 Hz). The electronic circuit of the sensor has been adjusted to operation with a measuring system providing for data processing and archiving with a frequency of 500 Hz. The detection element used in the sensor has been selected in such a way that it has been possible to make simultaneously the analysis of pressure measuring results under normal conditions of operation of a ventilation system of a mine (with measuring accuracy of $\pm 30\text{Pa}$) and the possibility of determination of location of a possible explosion (after its occurring). The sensor has been fitted with an internal memory; there have been stored the measuring data even if the transmission/supply line has been broken. The developed sensor operates with the surface station SP/DTSS. This station provides for supply, transmission and archiving of data from NSGP sensors to the surface.

The developed pressure sensor NSGP has been assessed in accordance with requirements of the Directive 94/9/WE (ATEX) and received an appropriate certificate.

A fundamental function of the system designed for measurement of fast changes in pressure should be ability to locate a place of initiation of a possible explosion in a given area of a mine. The information on a place of initiation of explosion could be got thanks to recording fast changes in pressure induced by a shock wave of explosion. and thanks to exact information about location lay-out (distances) of sensors in the area. The main problem of the works on the system was development of a technical solution enabling us to send very quickly the measuring data from precise pressure sensors located underground to the surface. The solution of this problem has been a method of a suitable conversion of an analogue measuring signal from a pressure sensor into a digital signal. A theory of measurements shows that the most advantageous method consists in amplification of a signal very close to its arising (a sensor) and then transmission of the amplified signal of high amplitude. In case of a big range of changes in signals (high dynamics) it may occur that the maximum amplitude of the signal can be limited as a result of so called saturation which can cause a loss of information. Due to use of analogue-to-digital conversion of an appropriate resolution close to a source of signal initiation, it is possible to eliminate this event of saturation. The above mentioned phenomena of signal distortion occur at recording the fast-changeable courses in mines, characterized by a high dynamics of signal changes. A range of dynamics which should characterize the measuring equipment for recording the fast changes in pressure and detection of initiation of a possible explosion should have a value of about 90 [dB], which corresponds to 14 bit conversion at least. Taking into consideration the above mentioned problems related to design of the measuring-transmission lines of the system for measurement of fast changes in pressure, there has been implemented a 16-bit conversion.

A structure of a system for recording the fast changes in pressure has been shown in Figure 40.

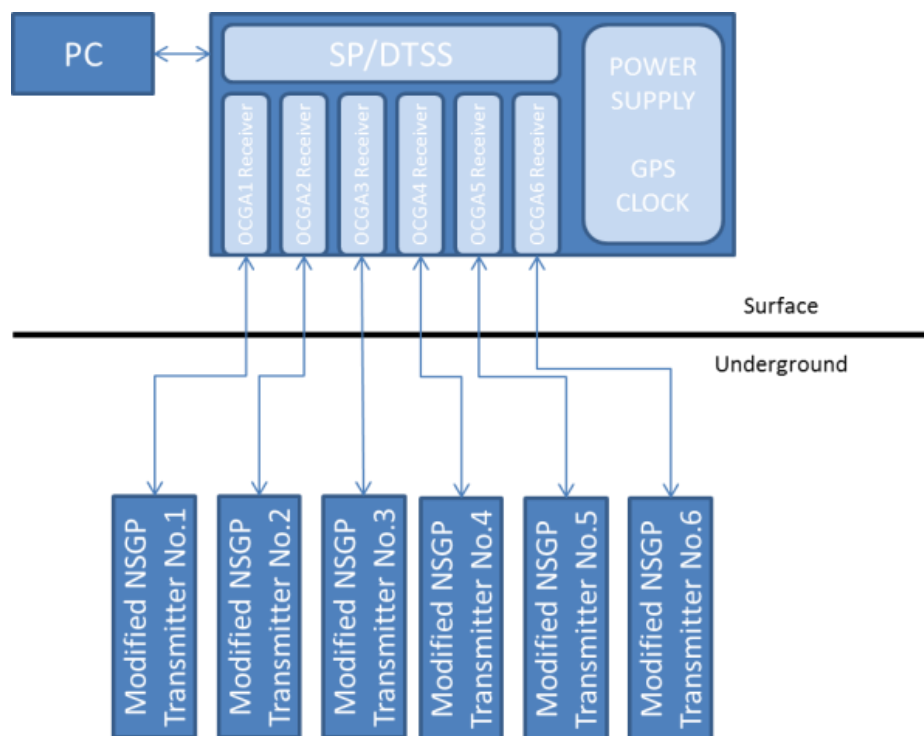


Figure 40. Diagram of fast air pressure monitoring system

The system contains the following devices:

- A surface station SP/DTSS fitted with receivers of data transmission type OCGA (6 pcs.). Originally it has been used in rock bump hazard risk systems and in rock mass stress control systems based on geotomography methods. The system is characterized by very fast digital transmission of analogue signals got from pressure sensors installed in the underground of mines. The data may be transmitted with frequency of 500 Hz at a distance up to 9 km by means of telecommunication mining cables. The received data are archived and analysed by PC. Because the station does not operate in an explosion hazardous area. therefore only its output circuits are intrinsically safe. A construction of the station meets requirements of the harmonized standards: PN-EN 60079-0:2009, PN-EN 60079-11:2012, PN-EN 50303:2004.
- Transmitters NSGP (senders of pressure measuring signals – 6 pieces). The NSGP transmitters are included in a digital transmission system DTSS and serve for data collecting from pressure sensors (SETRA Type 278), analogue-digital conversion and data transmission to a surface station SP/DTSS. The NSGP transmitter is intrinsically safe of group I and M1 category and meets requirements of the harmonized standards: PN-EN 60079-0:2013, PN-EN 60079-11:2012.

Description of a surface station SP/DTSS

A surface station SP/DTSS is designed for reception, processing and time synchronizing of measuring data from NSPG transmitters connected (by telecommunication lines) to the surface station. A block diagram of the surface station is presented in Figure 41 and its technical data in Table 9.

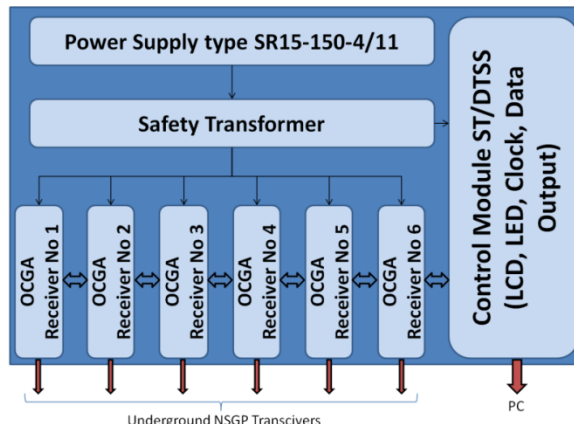


Figure 41. Block diagram of surface station SP/DTSS

The SP/DTSS surface station is installed in the surface in a mine control room. Every OCGA receiver is connected with one of NSPG transmitters by means of a two-wire telecommunication cable. The surface station is mounted in a cassette casing CARDPAC II type 3/4U which has been shown in Figure 42. The surface station may operate 16 measuring lines simultaneously; however there have been used only 6 measuring lines (OCGA receivers) in the project. Aside from the receivers, the cassette of the surface station contains: a control module ST, a safety transformer and a power supply SR15-150-4/11.



Figure 42. Cassette of a surface station SP/DTSS

A receiver module OCGA is shown in Figure 43. It has been made on the basis of a single EURO (100 x 160) construction. A front plate of the module has a width of 4T in the cassette. The front plate contains four LED's. Every receiver OCGA operates with a pressure transmitter NSPG by means of one teletransmission line. It provides for intrinsically safe power supply of the transmitter and two-way digital transmission to and from the NSPG transmitter.



Figure 43. Receiver module OCGA

A very important element of the surface station is a couple-control module of the transmission ST/DTSS. This module is responsible for organizing a parallel operation of all transmission channels and it plays a role of a master processor with reference to receiver stations. The module makes timing which is required by intrinsically safe transmitting and receiving modules. Furthermore the module provides for transfer in real time of consecutive samples of digital records to PC, which makes detection and archiving of fast changes in pressure. The couple-control module of the transmission ST/DTSS is fitted with a manipulator, which contains a function keyboard and displayers of type LCD and LED which allow us to enter and display of operating and diagnostic parameters. Two segments of LED's serve for a control display of a current level of signals (a noise) in the channels specified by an operator. The LCD screen plays a role of a "dialog window".

Table 9. Technical data of the surface station SP/DTSS

| Data of intrinsic safe circuit | | |
|--|--|-------------------------------------|
| 1. | Max supply voltage | $U_m = 253V$ |
| 2. | Max output current | $I_o = 78mA$ |
| 3. | Max output voltage | $U_o = 35V$ |
| 4. | Max output power | $P_o = 1.98W$ |
| 5. | Max external capacity | $C_o = 2.5\mu F$ |
| 6. | Max external inductance | $L_o = 50mH$ |
| Operating data of the receiver OCGA | | |
| 1. | Min supply voltage of transmitter from the surface by means of transmission lines | 13 VDC |
| 2. | Voltage at transmission line when the underground transmitter disconnected (open line) | ≤ 35 VDC |
| 3. | Number of channels | 6 (max. 16) |
| 4. | Type of transmission | digital. two-way |
| 5. | Kind of signal transmission | serial in real time |
| 6. | Signalling transmission errors | for both directions of transmission |
| Working conditions | | |
| 1. | Temperature | $+5^{\circ}C \div 40^{\circ}C$ |
| 2. | Humidity | < 98% at temp. $35^{\circ}C$ |
| 3. | Mark of protection concept | I M1 Exia I Ma |

Description of the transmitter NSGP

The main task of the transmitter NSGP is a measurement of pressure from an external pressure sensor, analogue-digital conversion of a signal and transmission to the surface station. A block diagram of the transmitter NSGP is presented in Figure 44.

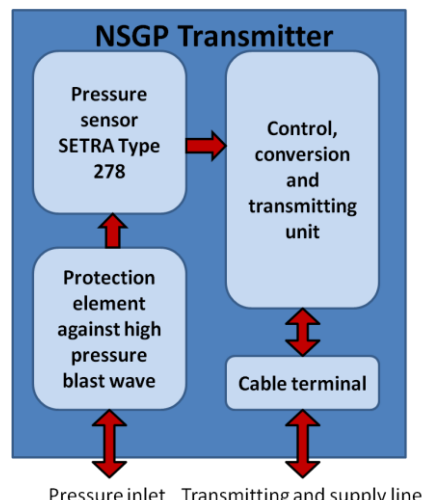


Figure 44. Block diagram of NSGP transmitter

The following elements have been mounted in a casing made of ZnAl alloy:

- a protective element from effects of a shock wave of explosion; a miniature pressure regulator made by Festo company;
- detector of absolute pressure SETRA Type 278;
- electronic circuit for analogue-digital conversion of a signal from pressure detector and for measuring data transmission to the surface station;
- terminal chamber which contains a connecting socket of a supply-transmission line and a suitably protected air inlet for a pressure detector.

Figure 45 presents the NSGP transmitter including its components.



Figure 45. View of the NSGP transmitter

A converter A/C is responsible for conversion of an analogue signal into digital signal from a sensor. The converter converts samples with a frequency of 500 Hz and resolution of 16 bits. The converted digital data are transferred to micro-controller, which forms a data frame DTSS and sends it to the receiver OCGA. Every data frame contains additionally – besides a measured value of pressure – 32 bit number of sequence indicating a time of making a given measurement. The transmitter NSGP has been fitted with a super-capacitor designed for a short time standby of operation in case of cut-off of a supply-transmission line. If the micro-controller detects a loss of supply, then it starts to record measuring data to permanent storage F-RAM. A recording time is 2040 ms. which is sufficient for recording 510 measuring samples. Every disconnection of the transmitter from the line initialises a new data record to the storage and the previous data are overwritten with new current data. The measuring data stored in F-RAM can be read out by means of interface Z2 UART. The technical data of the transmitter NSGP have been presented in Table 10.

Table 10. Technical data of the transmitter NSGP

| Data of intrinsic safe circuit | | |
|---|--|---------------------------|
| 1. | Max input current | $I_i = 78\text{mA}$ |
| 2. | Max input voltage | $U_i = 35\text{V}$ |
| 3. | Max input power | $P_i = 2\text{W}$ |
| 4. | Max internal capacity | C_i – negligible |
| 5. | Max internal inductance | L_i – negligible |
| Operating data of the transmitter NSGA | | |
| 1. | Min supply voltage of a transmitter | 16VDC |
| 2. | Current consumption of a transmitter NSGP | $\leq 25\text{ mA}$ |
| 3. | Type of transmission | Digital transmission DTSS |
| 4. | Number of input channels | 1 |
| 5. | Frequency of data transmission | 250 Hz |
| 6. | Range of voltage of measuring signal (input) | 0-2.5V |
| 7. | F-RAM memory | 8192 KB |
| 8. | Charging time of a super-capacitor | 2 hours |
| 9. | Measurement of absolute pressure | 800 \div 1300 hPa |
| 10. | Accuracy | $\pm 0.3\text{ hPa}$ |
| Working conditions | | |
| 1. | Temperature | $0 \div 50^\circ\text{C}$ |
| 2. | Humidity | $0 \div 100\%$ |
| 3. | Mark of protection concept | I M1 Exia I Ma |

To read out the recorded data in the F-RAM memory, it should be connected an appropriate cable FTDI (output voltage 3.3V. logic levels 3.3V). The parameters of the UART interface are: 115200b/s without control of flow and without memory parity bit. In order to start reading out the data, it should be sent a read-out command (a byte of value 0x78). A correct reception of this byte is signalled by shining LED. In this moment the transmitter starts to transmit of all contents of the F-FAM memory. During every read-out there are transferred 1020 measuring samples of pressure and 510 numbers of sequences.

Conclusions

As a result of the works carried out within the Task T3.1 there have been developed the modified pressure sensors which met the assumed requirements. There has been developed a measuring system consisting of surface devices (a central station of the SP/DTSS system) and underground equipment (NSGP sensors). A complete measuring system was tested during experiments of explosions carried out in the EM "Barbara" and under conditions of normal work in a mine. All devices included in the system have appropriate ATEX certificates which allow us to use the system for operation in underground mines.

Task 3.2 – Analysis of obtained data

The modified monitoring devices, developed in the previous task, was installed underground in a PGG mine in order to validate its operation and gain knowledge about the transients that can be observed in the air pressure values during a normal situation, taking also into account the usual changes that can happen in the ventilation system of an operative mine.

The obtained data were analysed, in order to determine the limits between a normal operation of the ventilation system and what can be considered as an anomaly. The outcome of this analysis were the basic specifications of the software developed in the next task.

Work Undertaken

After the ATEX certificates for the NSGP transmitters were obtained and the system for rapid pressure measurements had been completed, the system was installed in the hard coal mine "Ruda" Ruch Halemba (owned by PGG). Within the program of this stage of the project there were carried out the trials of the system in the underground conditions. The NSGP transmitters (pressure sensors) were installed in the excavation 414/1/H driven by blasting operations. The excavation has been ventilated by separate forced ventilation with use of an air pipe. For the trials there were used three pressure sensors (in total made 6 sensors to provide a replacement of sensors in case of any malfunction of them). The sensors were installed along the excavation. At the beginning of the trials the first sensor was located in a distance of 110 m from the working face and the following sensors were installed at 176th and 309th m. The sensors were not displaced during the trials due to quite low drifting rate (about 1.5 m daily). A map with layout of the sensors is shown in Figure 46.

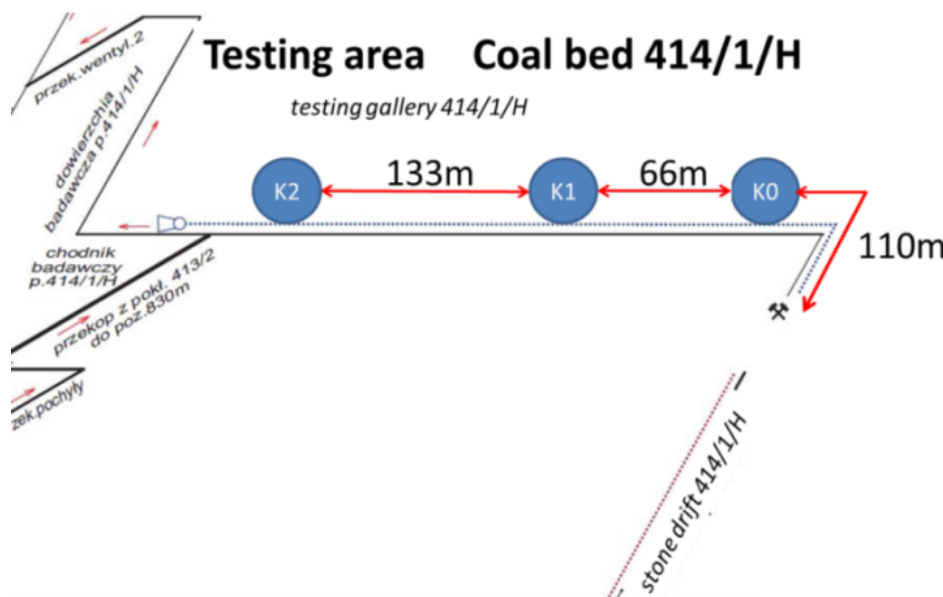


Figure 46. Layout of the pressure sensors in the excavation 414/1/H

The trials were carried out in August 2016. The choice of the place of trials was based on possibility to verify the operation of the system designed for measurements of rapid changes in pressure in conditions of a normal work of a ventilation system of a mine as well as to record the changes in pressure caused by use of explosives.

Results

The NSGP transmitters (pressure sensors) recorded continuously in the trials the changes in pressure occurring during a normal operation of the ventilation system in the mine as well as the rapid pressure increases caused by a blast wave induced by blasting operations. During the trials none of the sensors was damaged. The system recorded about 1.814.400.000 values of pressure. The measuring signals stored in the system allowed the assessment of operation of the sensors in the mining conditions. During a normal work of the ventilation system there were recorded in the excavation very low changes in pressure related to changes in atmospheric pressure characterized by very low dynamics of a few hPa a day. The sensors recorded also low changes in pressure induced by roughness of a fan used in a separate forced ventilation system (Figure 47).

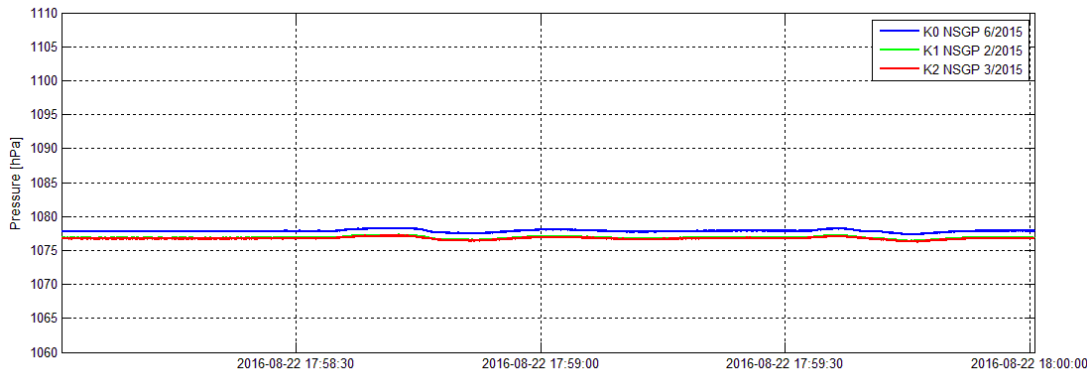


Figure 47. Changes in pressure in the tested excavation during a normal operation of the ventilation system

Due to drivage with blasting technique it was possible to record the changes in pressure caused by a blast wave after charge blasting in the driven excavation. Depending on a distance of the sensors from the face there were recorded rapid pressure jumps at a level from about 30 to 40 hPa. The selected courses of the changes in pressure caused by blast waves induced by charge blasting in the driven excavation are shown in Figures 48, 49, 50 and 51

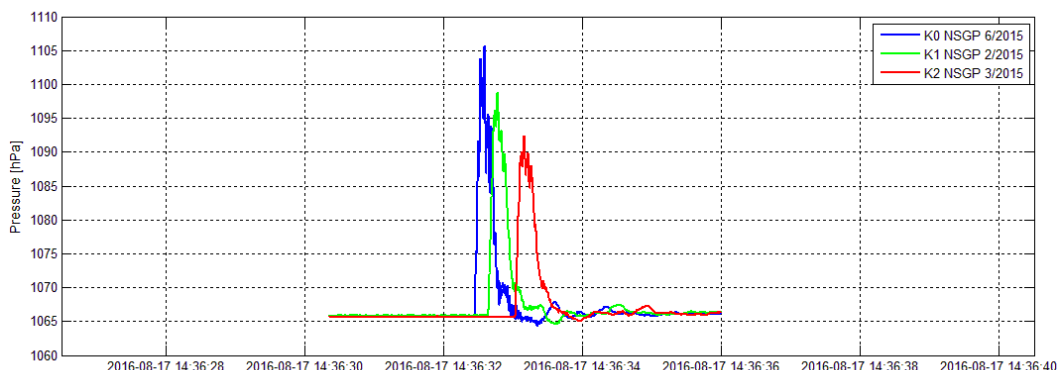


Figure 48. Changes in pressure in the excavation induced by a blast wave on 17.08.2016

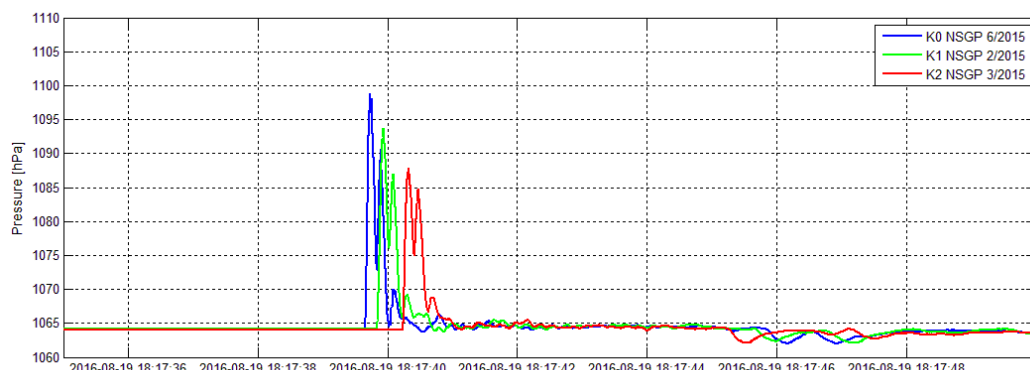


Figure 49. Changes in pressure in the excavation induced by a blast wave on 19.08.2016

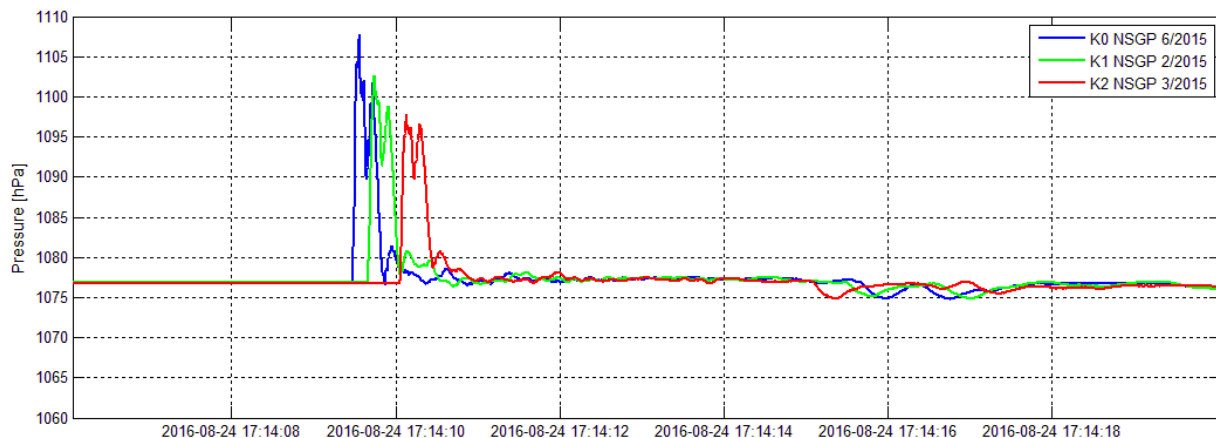


Figure 50. Changes in pressure in the excavation induced by a blast wave on 24.08.2016

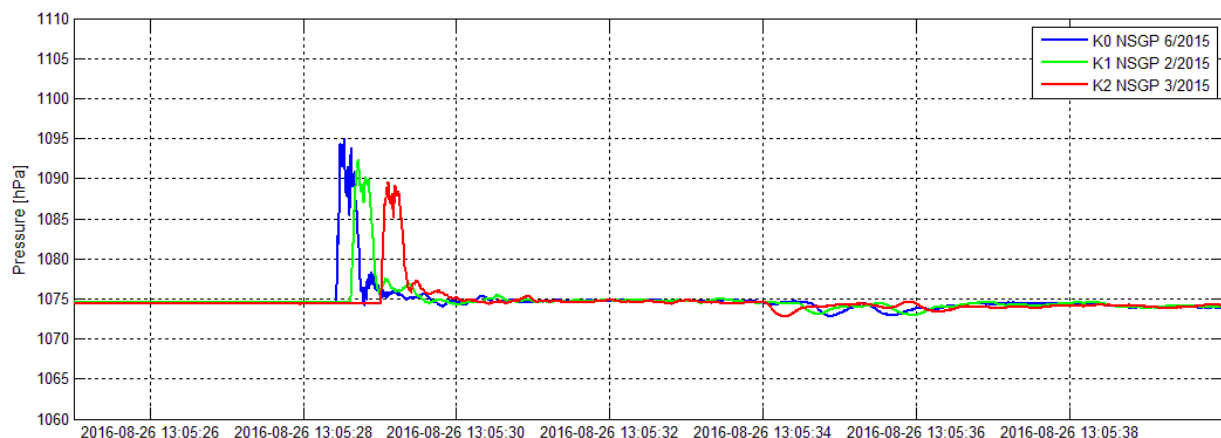


Figure 51. Changes in pressure in the excavation induced by a blast wave on 26.08.2016

Main problems encountered and correction actions

In the process of trials in the mine no particular technical problems were raised. The tele-technical infrastructure of the mine and the equipment included in the system worked correctly in accordance with the assumptions. The completion of the Task T3.2 was behind the schedule planned in the project. It was caused by delayed obtaining the ATEX certificate for the NSGP transmitters than it was expected previously. The next reason for delay was late beginning works by the mine "Ruda Ruch Halemba" in the gallery 414/1/H. This delay did not affect significantly the start of works on software planned within the Task T.3.3 and on the next works in the project.

Conclusions

The trials carried out in the mine allowed to collect sufficient measuring data enabling to continue further works on development of system software. The trials allowed us also to check functioning methods of the individual elements of the system in the mine conditions. On the basis of the stored changes in pressure during explosions there were calculated velocities of blast waves and response times of the pressure sensors. The measuring results are presented below in the Table 11.

Table 11. Velocity of a blast wave and response times of the sensors

| No. | Date of explosion | Velocity [m/s] | Response time [ms]/[Hz] |
|-----|-------------------|----------------|-------------------------|
| 1 | 17.08.2016 | 350.48 | 29.1 / 34.4 |
| 2 | 19.08.2016 | 342.76 | 28.8 / 34.7 |
| 3 | 24.08.2016 | 347.56 | 27.9 / 35.8 |
| 4 | 26.08.2016 | 347.56 | 27.9 / 35.8 |

The response times of the sensors to rapid pressure jumps are very close to the response times determined in the laboratory within the Task T3.1 (35.7Hz). They confirm that the sensor SETRA Typ 278 meet the assumptions and technical requirements.

Task 3.3. – Software development

A software package was developed to perform the analysis of air data pressure in an automatic way. This software followed the specifications defined in the previous task and is able to detect important anomalies in the ventilation system that could be an indication of incidents or high explosion risk situations.

Software of the system designed for fast measurements of pressure consists of three modules which are actually the separate computer programs operating with each other. A block diagram of this software is shown in Figure 52.

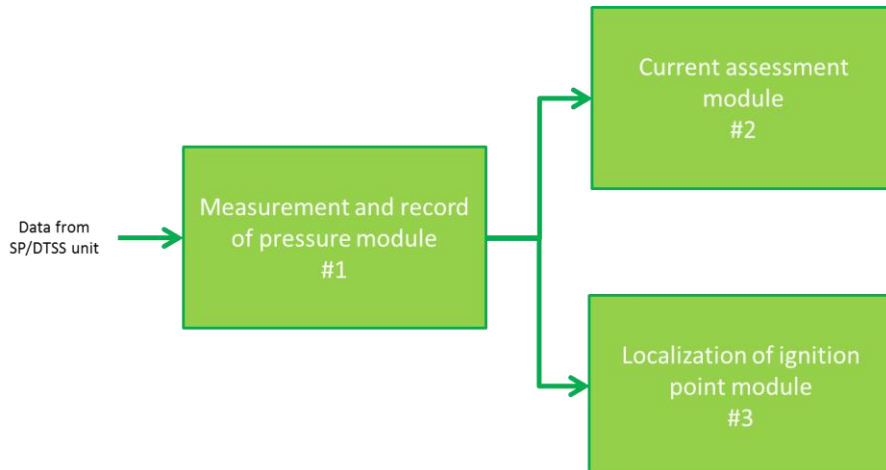


Figure 52. Block diagram of system software

Results

Module of measurement and record of pressure

The aim of the implemented program *CisK6* in the *LABView* environment is acquiring and archiving the values of absolute pressure available from the NSGP sensors. The program receives the measuring values from a central station of the system, integrates and decodes them and displays their binary values; next they are also archived in binary form. The application displays histograms for each channel as well. For purposes of a current analysis of measuring data sent from the NSGP sensors, the program saves to file csv in 3 seconds intervals the current values of pressure from all channels of the system including additional information relating to correctness and time of measurement.

The additional *DecodeCisK6* module allows the archival measuring data base to be processed and the measuring values from the selected sensors to be stored in file csv for a given period; the data are used for further processing. The measurements from selected channels are stored in packets of 256 measuring values and in 512 ms intervals.

The window of the program *CisK6* during normal work is shown in Figure 53.



Figure 53. CisK6 Module – integration, decoding and archiving the measurements

Module of a current assessment of pressure measuring

Figure 54 shows the window of the program *Cisnienie*. The aim of the program implemented in the *MATLAB* environment is current processing and visualising the values of pressure on the basis of indications of the NSGP sensors available in the system. The window of the program is divided into two parts. In the first part there are shown diagrams of the current and just processed indications of pressure obtained from the system. The program for each of six channels (K0 – K5) displays the measuring values of pressure from the last 15 minutes and a trend of values with use of combination of linear regression and weighted average of the last measurements. Additionally in case of the selected box *Kalibracja* the program recalculates the values of pressure according to the delivered characteristics of calibration of the NSGP sensors stored in text files. The second part of the window supervises the operation of the whole system. The pushbuttons *START* and *STOP* are responsible for activating and deactivating the measuring data processing of the system. The pushbutton *OBLICZANIE MIEJSCA WYBUCHU* opens the window *Lokalizacja* of the program.

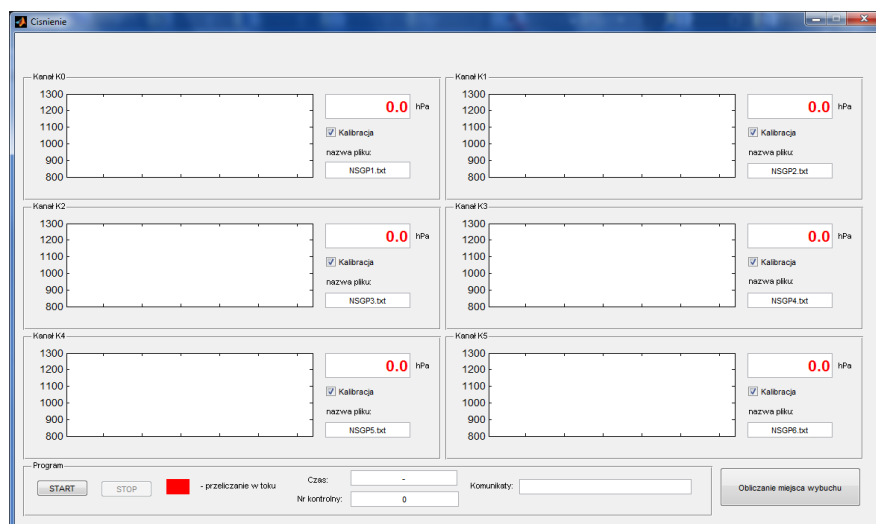


Figure 54. A window of the program *Cisnienie*

When the system is operating then the values of pressure are downloaded from the file *CisBin.csv* updated by the *CisK6* program in about 3 seconds intervals. The algorithm checks a correctness of the file structure. A correctness marker of every operating NSGP sensor is also a subject to control. Next the binary values of pressure are converted into numbers from the range of $800 \div 1300$ hPa according to the following formula:

$$P = \frac{pom}{32768} * 500 + 800 [hPa]$$

where:

pom – binary value of the absolute pressure from the range of $0 \div 32768$.
Figure 55 shows the window of the program *Cisnienie* during a work.

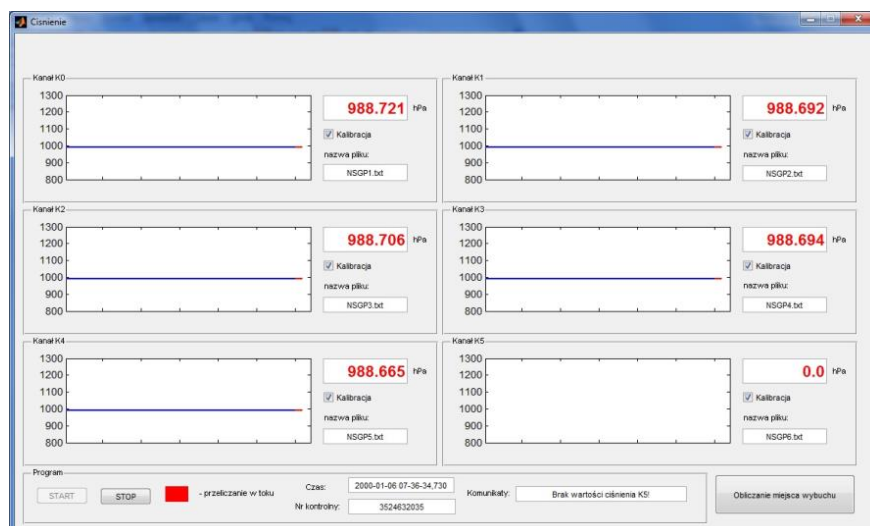


Figure 55. Program *Cisnienie* – estimation of the current values of pressure

Program for location of an explosion at a working face area

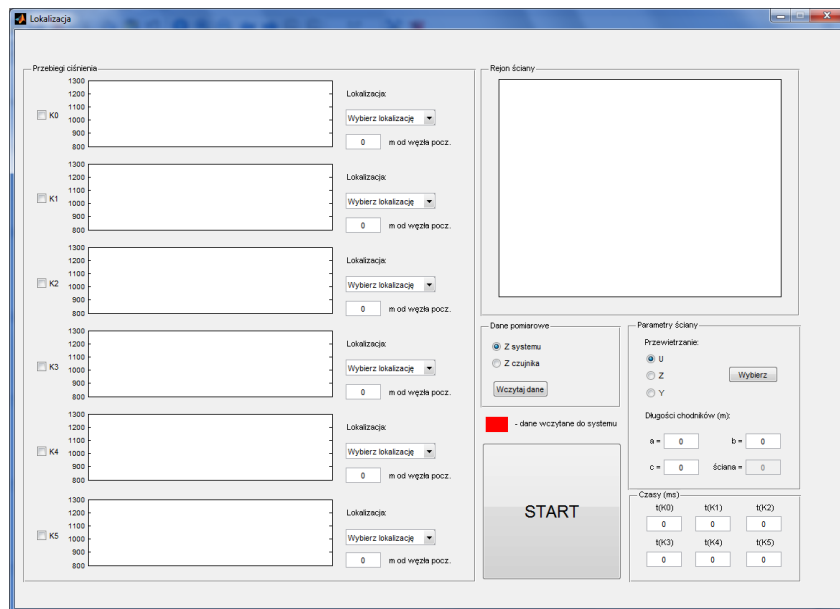


Figure 56. A window of the program *Lokalizacja*

The aim of the program *Lokalizacja* implemented in the *MATLAB* environment is a determination of a source of methane explosion on the basis of the measured values of absolute pressure given by the NSGP sensors installed at a working face area. The data readout from an internal memory of a sensor or from the archiving program *DecodeCisK6* are downloaded by the program as a file *csv*.

In order to determine a source of methane explosion in workings it is necessary to define their all parameters such as a method of ventilation of a longwall, length of all galleries at this area and places of installation of pressure sensors. The calculations are done on the basis of the downloaded files containing measurement values of pressure. After activating the program, the algorithm calculates a pressure increase for respective sensors and selects of them the sensors which have a decisive influence on determination of a location of explosion. On the basis of the estimated time values the algorithm determines a location of explosion. In the diagram there are generated the following information: a structure of workings, location of pressure sensors as well as a message about a probable place of a methane explosion.

A window of the program *Lokalizacja* is shown in Figure 56. It consists of the following elements:

- **Courses of pressure.** This box contains diagrams of six channels K0 – K5 of the system for pressure measuring. By means of a drop-down menu it is selected for each channel a section of a working in which a sensor has been installed and it is also selected a distance of the sensor from the beginning of the given section. Additionally every sensor has a check box which allows choosing the sensors involved in the process of location of the source of methane hazard.
- **Working face area.** This field is used to visualize a structure of a working face area during operation of the program. After selecting a ventilation method ("U", "Y", "Z"), it is drawn in the diagram a structure of workings. Next during operation of the algorithm it is also marked location of sensors and location of possible place of explosion or ignition of methane.
- **Measuring data.** This box is used for downloading the measuring data necessary for calculations. The measuring values can be downloaded directly from the measuring system i.e. from the file *csv* by means of the archiving program *DecodeCisK6* or from the internal memory file of a pressure sensor. After downloading the data, the courses of pressure in a respective time period are displayed in diagrams.
- **Parameters of a working face.** This field is used to define a structure of a working face area where the system for pressure measuring has been installed. In the check box there are set: a method of ventilation ("U", "Y", "Z") and length of individual sections of workings in the given structure including the length of the longwall. The pushbutton *Wybierz* saves settings of the changes and next the program draws in diagram a structure of workings basing on the defined parameters.
- **Times.** This field is used to display the calculated rise times of pressure in a given time period.

Algorithm of operation of the program Lokalizacja

Figure 57 shows a flowchart of the algorithm of analysis of the measuring data downloaded from the pressure sensors NSGP.

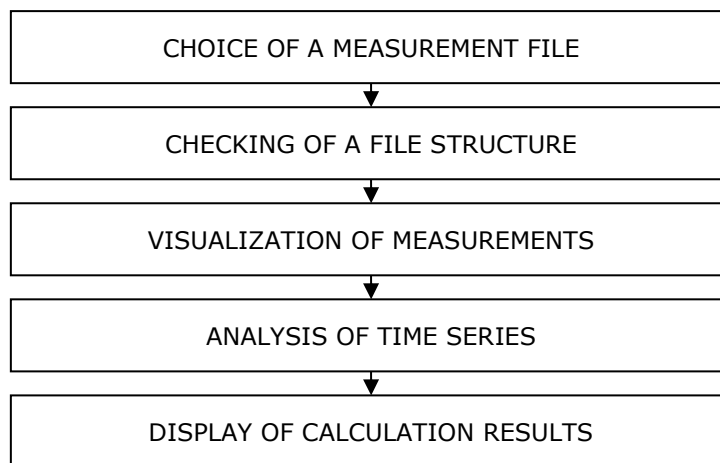


Figure 57. Flowchart of the algorithm of data analysis

The algorithm starts with display of a window of selection of a file to be downloaded. After saving (confirming) the file, its structure is checked. When a file downloaded from the archiving program *DecodeCisK6* is selected then it is checked a correctness of content of the file header (a list of the archived channels) and the time footer recorded with accuracy up to 1 ms. Then a format of the measuring data is checked. The time footers are stored in packets of 256 measuring values therefore the time vector is completed as well. Similarly to the program *Cisnienie*, the pressure values are converted from the binary form into the numbers from the range of 800 ÷ 1300 hPa according to the formula:

$$P = \frac{pom}{32768} * 500 + 800 [hPa]$$

where:

pom – binary value of the absolute pressure from the range of 0 ÷ 32768

After doing all operations, there are displayed the diagrams of pressure measurements in the range of 800 ÷ 1300 hPa respectively for every channel saved in file.

The next step is data analysis regarding determination of rise times in pressure. The measurements of every channel are subjected to filtering. It is determined a maximum value for every channel. Next it is created a vector of changes in values and on this basis it is defined a start point of increase in pressure of every sensor. A rise time which occurs at the earliest stage is chosen as a general start point. The rise times are calculated for every channel and saved in edition boxes of the program window.

The procedure described above is performed when the data are downloaded from the internal memory of a sensor; however in this case before data downloading from file, it is necessary to mark the channels for which the data are downloaded. The algorithm activates procedures successively for each channel marked in the window.

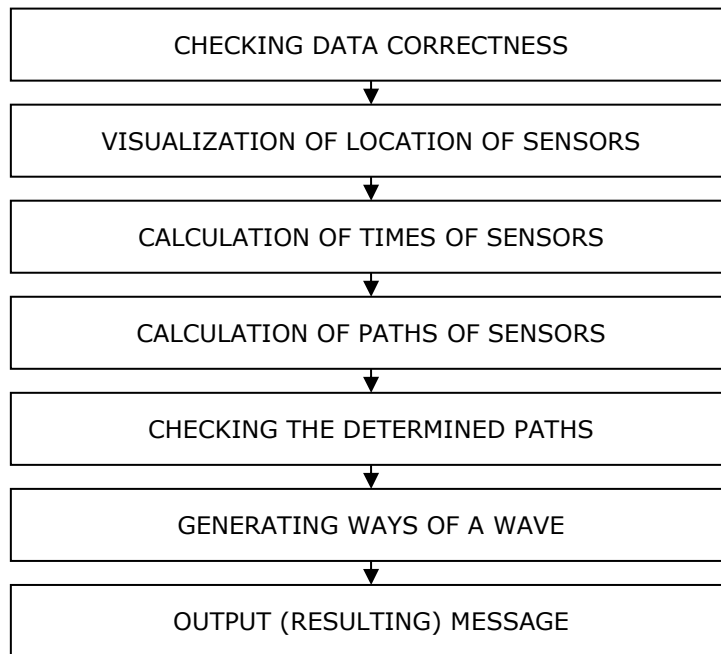


Figure 58. Flowchart of a location algorithm

Figure 59 presents a flowchart of a location algorithm based on indications of measurements obtained from the pressure sensors NSGP. The algorithm begins the operation with checking a correctness of configuration of workings in which the pressure monitoring system has been installed – i.e. lengths of galleries, layout of the pressure sensors. Then the rise times calculated in the process of data downloading are saved in the time table. The program marks the places of installation of the sensors NSGP in the plan of workings.

For calculations there have been used the pressure sensors which recorded the event at the earliest. For this purpose the program creates an operating table including the times of all sensors sorted according to a moment of response to increase in pressure. Next for the previously selected channels it has been created a network of paths among individual sensors according to defined parameters of a working. The table including the lengths and times has been supplemented on the basis of the created network. The paths proportional to every sensor have been determined according to the following formula:

$$s_{ix} = \frac{t_i}{t_i + t_j} \cdot s_{ij} \quad [m]$$

where:

t_i – response time of a sensor [ms];

t_j – response time of a sensor on a given path of the network [ms];

s_{ij} – a distance between sensors on a given path of the network [m].

For the paths of the sensors calculated in such a way, it is checked a conformity of individual pairs with a real distance between the sensors. Therefore the sums of the paths for each combination of the ways are calculated and it is checked which combinations give a value equal to the path between respective sensors. Positively verified paths are saved in the conformity table. On this basis there are generated the resulting paths from individual sensors to the place of explosion.

The final stage in the operation of the program is visualization on the scheme of location of a potential methane explosion. The algorithm follows the path saved in the conformity table to the point indicated by the calculated proportional paths. The program ends and displays a message about distances among respective sensors and a source of methane explosion.

Example of operation of the program

The operation of the program has been presented on the basis of an experiment carried out on in the Experimental Mine "Barbara". The experiment consisted in gas delivery into a working by means of a sack made of polyethylene. The gas volume was 50 m³. After the sack had been filled with gas, it was broken then (bursting) by a detonating fuse. This released methane into the working space. Next it was initiated an explosion by means of igniters mounted at the roof

of the main gate. Three pressure sensors NSGP were installed in the working. On the surface it was installed a central station of the pressure measuring system. The sensors were connected to the measuring system on the following channels:

- K0 – located in the inset on side; 22 m from the main gate;
- K1 – located in the main gate in a distance of 200 m from its entry and 170 m from the inset with installed pressure sensors K0 and K2;
- K2 – located in the inset directly opposite 20 m from the main gate.

As a result of the experiment it was obtained a record of changes in pressure in the workings of the experimental mine. After the module *DecodeCisK6* had been configured, it was obtained storage of the pressure measurements in the file csv.

In order to determine a place of the methane explosion there were defined the parameters of the working in the program *Lokalizacja*. It was defined a ventilation system as "Y" method, the lengths of galleries and the places of installation of the pressure sensors were determined.

Next the file with measuring data generated by the system was downloaded. The pressure diagrams were displayed in the diagrams of the channels K0, K1 and K2. The rise times of pressure were determined during experiment in the text boxes. Figure 59 shows the window of the program *Lokalizacja* after defining a working and downloading the measuring data.

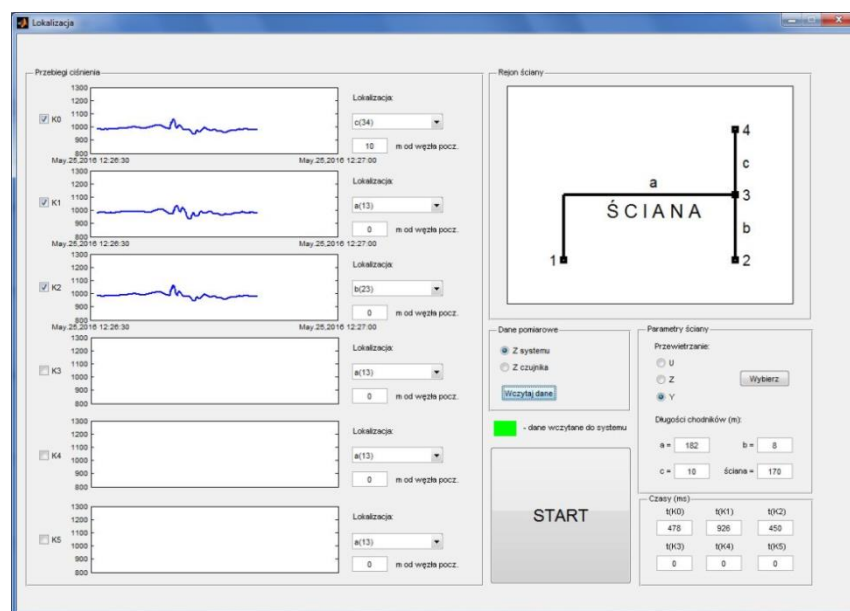


Figure 59. A window of the program *Lokalizacja* – measuring data and configuration of workings

Before starting the calculations, it was decided which pressure sensors would be taken as a base for determination of the place of explosion. The rise times of measuring signals were:

- $t(K0) = 478 \text{ ms}$;
- $t(K1) = 926 \text{ ms}$;
- $t(K2) = 450 \text{ ms}$.

After all parameters had been defined, the location algorithm was activated. The program marked the location of the pressure sensors in the plan of the working. Next it was calculated the place of explosion and it was marked in the plan of the working face area; it has been shown in Figure 60.

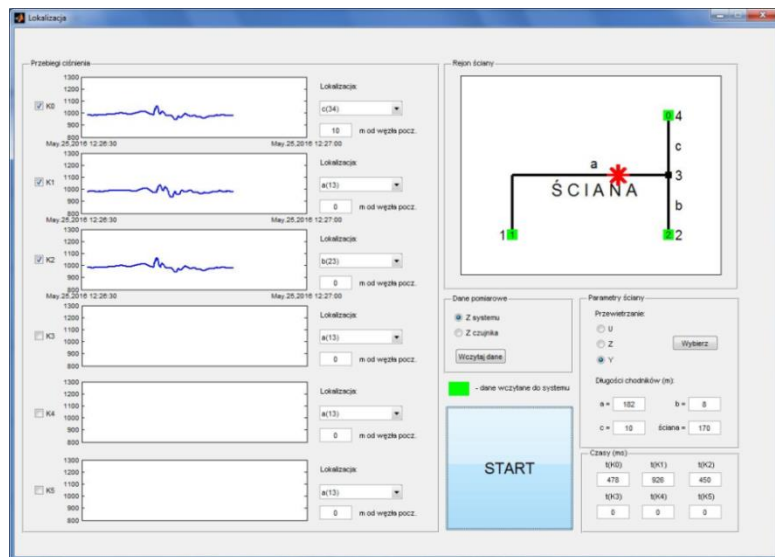


Figure 60. A window of the program Lokalizacja – determination of the place of the potential methane explosion

After the calculations had been terminated, the program displayed a summary message of the calculations (Figure 61). The source of hazard has been determined at a distance of about 65 m from the sensor K0, about 127 m from the sensor K1 and about 62 m from the sensor K2. The data showed that the source of the explosion was on 73 m of the experimental main gate. According to the information presented by the Experimental Mine "Barbara", the explosion happened on about 80 m of the main gate. It follows that during the experiment the algorithm determined the source of hazard with high accuracy.



Figure 61. A window of the program Lokalizacja – message showing a potential place of methane explosion

Conclusions

Software developed within the project allows archiving the measuring data and allows for on-going assessment and analysis of pressure levels in a given area of a mine. It allows also to detect with high accuracy a place of a possible explosion on the basis of indications of the sensors.

Task 3.4. – Validation tests

The validation of the system performance was carried out at two levels:

- Firstly the system was tested during some of the explosion tests planned at Experimental Mine Barbara (GIG), in order to check its capacity to detect and record the transients in air pressure values occurring during an explosion and the possibility to determine the ignition point of the explosion upon the base of such data.
- Secondly the system was installed at a PGG mine and tested during a reasonable long period of time, in order to validate its functionality and its performance.

Work Undertaken

Explosion tests at Experimental Mine Barbara

The experiments which consisted in delivering methane into a working and next initiating an explosion were carried out in the main gate 400 m at the level 46 m in the underground of the Experimental Mine "Barbara". The blowing ventilation stream velocity for methane distribution was 0.2-0.3 m/s in all experiments in the working. The total number of the experiments was 9; however the system for rapid changes in pressure was used in 6 experiments. The layout of the sensors in the experimental gallery (numbers Ex-03 to Ex-07) is shown in Figure 62.

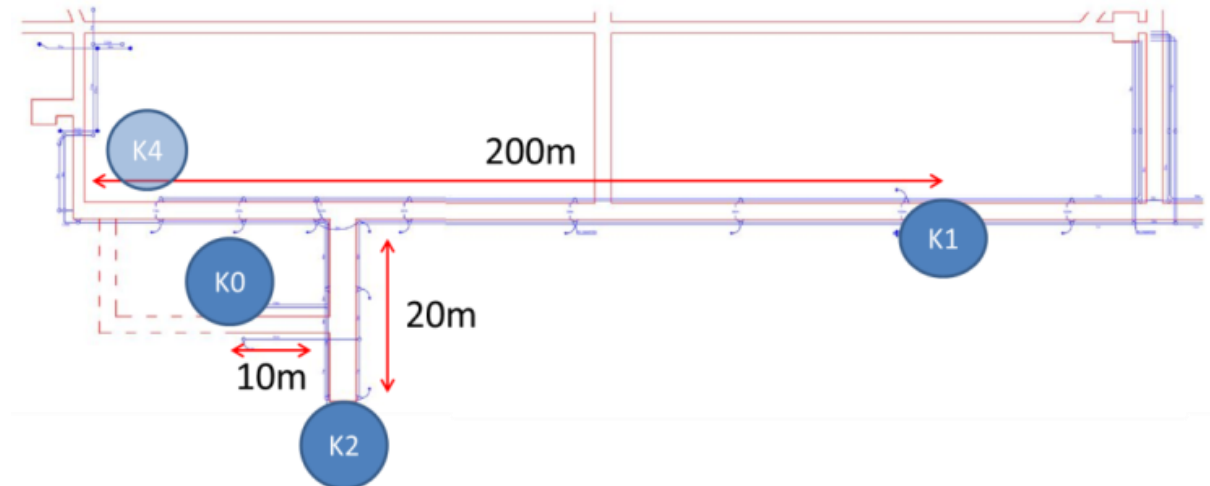


Figure 62. Layout of pressure sensors during experiments

Tests at KWK "Ruda-Ruch Halemba" mine

The trials were performed in the coal mine "Ruda-Ruch Halemba" that belongs to PGG. The miners of the coal mine, appointed by PGG to carry out the project, made available for trials the working face area No 4a in the seam 402/K and necessary telecommunication infrastructure designed for data transmission to the surface. The trials were carried out in the period 01.12.2016 ÷ 15.01.2017. Four transmitters NSGP (pressure sensors) were installed in the working face area:

- K0 – in the gallery 5, 20 metres from the crossing with the raise 5,
 - K1 – in the gallery 5, 1300 metres from the crossing with the raise 5,
 - K2 – in the gallery 4, 1200 metres from the crossing with the raise 5,
 - K3 – in the gallery 4, 20 metres from the crossing with the raise 5,

The map of area, where the trials were carried out, including the location of the sensors is presented in Figure 63.

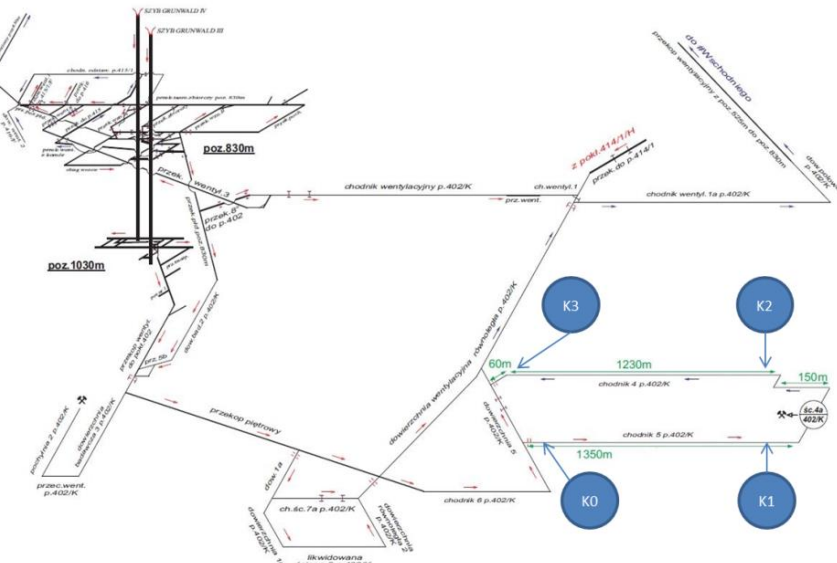


Figure 63. Location of transmitters in the working face area No 4a

The sensors K1 and K2 installed in the working face area were in the middle of the period of the trials relocated of 50 m towards the raise 5.

Results

Results of Explosion tests at Experimental Mine Barbara

Figure 64 shows the recorded changes in absolute pressure caused by detonation of a detonating fuse cutting a balloon (a sack) filled with methane.

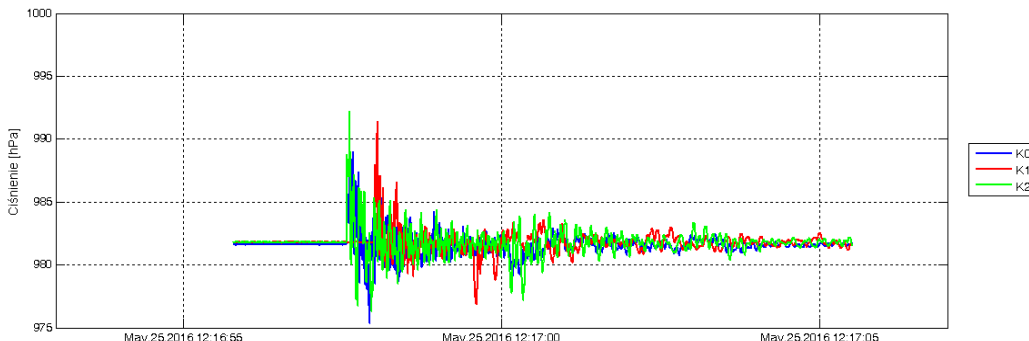


Figure 64. Changes in absolute pressure caused by detonation of fuse

Figure 65 presents the changes in pressure caused by attempt at initiation of methane explosion in the excavation.

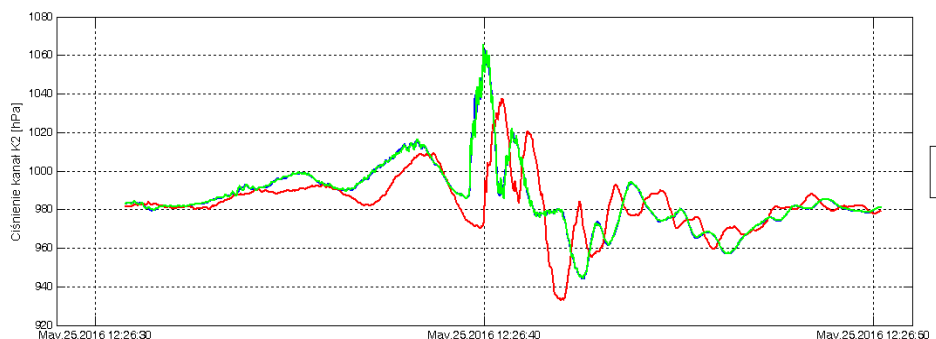


Figure 65. Changes in absolute pressure caused by attempt at initiation of methane explosion

The courses of pressure shown in Figure 65 may prove that during this experiment there was not methane explosion but methane ignition. The recorded courses of pressure allowed us to calculate a place of initiation of this event (explosion/ignition) which was located at 73rd meter of the main gate.

Figure 66 presents the changes in pressure caused by attempt at initiation of methane explosion in the excavation.



Figure 66. Changes in absolute pressure caused by attempt at initiation of methane explosion

The courses of pressure shown in Figure 66 may prove that during this experiment there was not methane explosion but it happened methane ignition like in the previous experiment. The recorded courses of pressure allowed us to calculate a place of initiation of this event (explosion/ignition) which was located at 99th meter of the main gate.

Figure 67 presents the changes in pressure caused by initiation of methane explosion in the excavation.

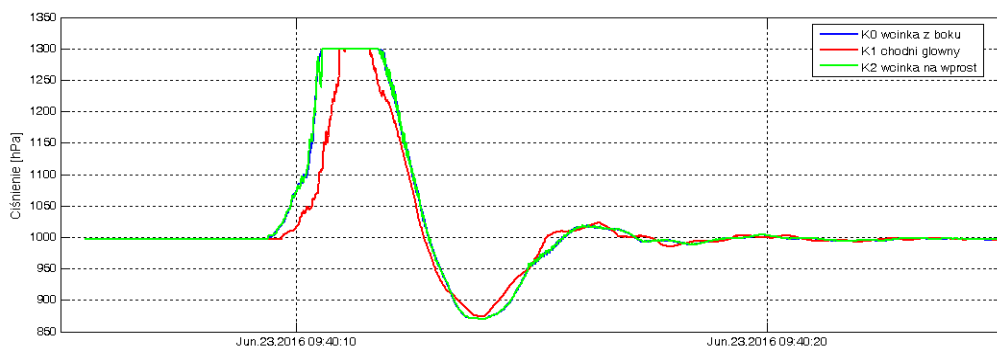


Figure 67. Changes in absolute pressure caused by methane explosion

The courses of pressure shown in Figure 67 may prove that during this experiment methane explosion happened. The values of the recorded pressure exceeded considerably the maximum measuring range of the pressure sensors (1300 hPa). Even though the measuring range of the pressure sensors was so much exceeded, they recovered after a short while to operating measuring efficiency. The main reason for that was activation of a protective system of detection elements of the sensors. There have been used pressure regulators installed in the NSGP sensors.

The recorded courses of pressure allowed us to calculate a place of explosion which was located in accordance with calculations at 74th meter of the main gate.

Figure 68 presents the changes in pressure caused by initiation of methane explosion in the excavation.

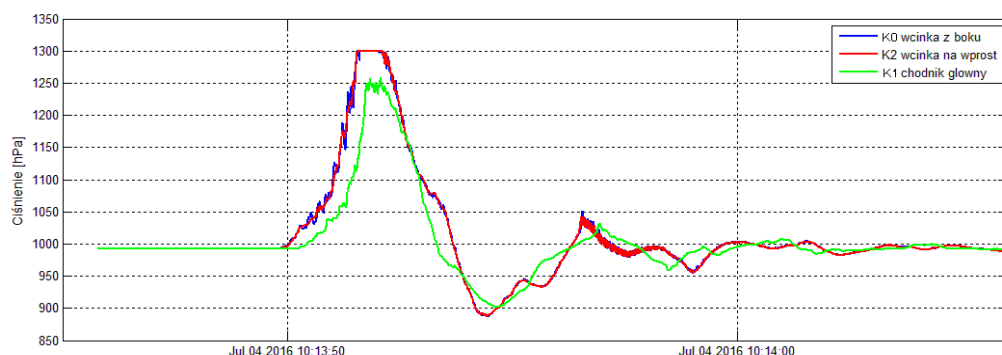


Figure 68. Changes in absolute pressure caused by methane explosion

The courses of pressure shown in Figure 68 may prove that during this experiment methane explosion happened. The values of the recorded pressure in two cases exceeded considerably the maximum measuring range of the pressure sensors (1300 hPa). Even though the measuring range of the pressure sensors was so much exceeded, they recovered after a short while to operating measuring efficiency. The main reason for that was activation of a protective system of detection elements of the sensors. There have been used pressure regulators installed in the NSGP sensors.

The recorded courses of pressure allowed us to calculate a place of explosion which was located in accordance with calculations at 66th meter of the main gate.

Figure 69 presents the changes in pressure caused by initiation of methane explosion in the excavation.

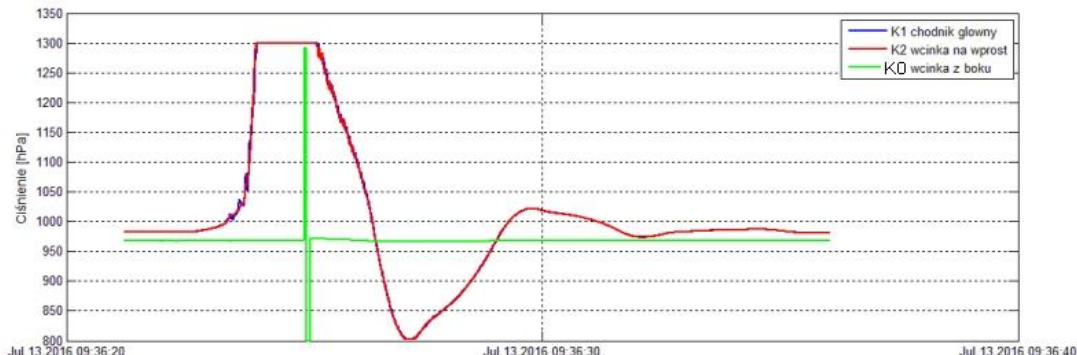


Figure 69. Changes in absolute pressure caused by methane explosion

The courses of pressure shown in Figure 69 may prove that during this experiment methane explosion happened. The values of the recorded pressure in two cases exceeded considerably the maximum measuring range of the pressure sensors (1300 hPa). Even though the measuring range of the pressure sensors was so much exceeded, they recovered after a short while to operating measuring efficiency. The main reason for that was activation of a protective system of detection elements of the sensors. There have been used pressure regulators installed in the NSGP sensors. One of the pressure sensors was damaged during this experiment. After the damaged sensor had been diagnosed, it was noticed that the reason for the damage was breaking electric connection in one connector mounted on pcb. It could be caused by high temperature occurring during explosions and vibrations induced by blast wave of explosion. The connections were repaired (soldered) and the sensor was re-installed in the working. Other sensors worked without interruption.

The recorded courses of pressure did not allow to calculate a place of explosion due to the damage of one sensor.

Figure 70 presents the changes in pressure caused by initiation of methane explosion in the excavation. During this experiment it was installed an additional (the forth one) pressure sensor at 10th m of the main gate (K4).

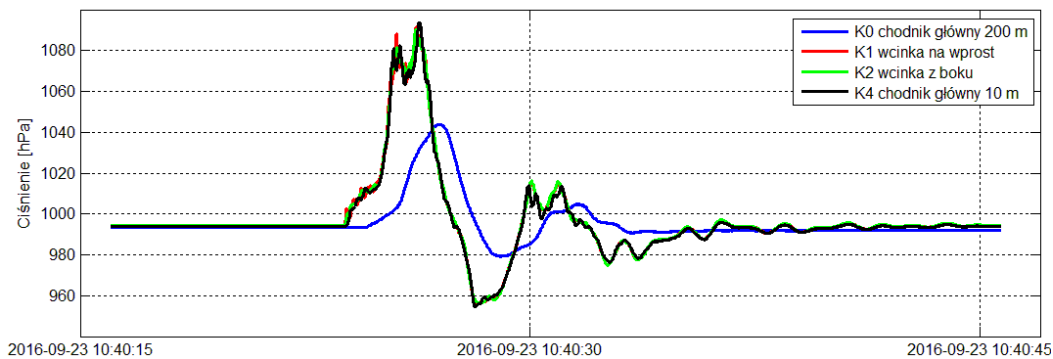


Figure 70. Changes in absolute pressure caused by methane explosion

The courses of pressure shown in Figure 70 may prove that during this experiment there was not methane explosion in the excavation but it happened methane ignition like in the previous experiments.

The recorded courses of pressure allowed to calculate a place of initiation of explosion which was located in accordance with calculations at 30th meter of the perpendicular crosscut at the crossing with the gallery located parallel to the main gate.

Results of tests at KWK "Ruda-Ruch Halemba" mine

During the trials in the tested area there has not been noted any situation which could occur of any aerologic hazard. The recorded changes in pressure were caused by a normal operation of the ventilation system of the mine. The diagrams shown below present the selected pressure courses recorded in the system. The changes in pressure result from:

- opening and closing the air dam in the raise 5 in particular measured by means of the sensors K0 and K3 (Figure 71);
- changes in pressure caused by operation of a shearer and a powered support measured by means of the sensors K1 and K2 (Figure 72);
- changes in pressure caused by changes in atmospheric pressure recorded by all sensors (Figure 73).

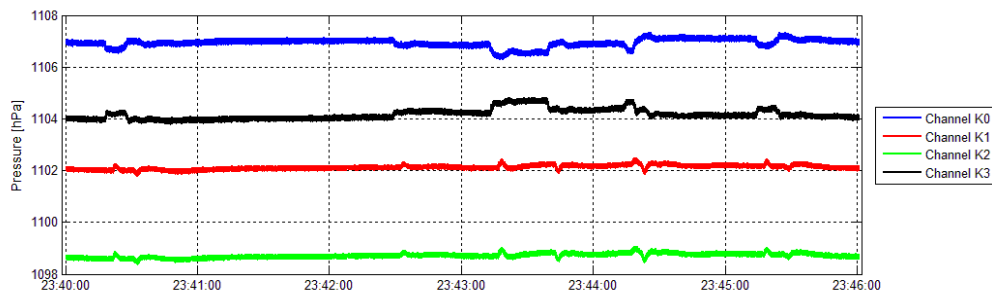


Figure 71. Changes in pressure caused by operation of the air dam installed in the raise No. 5

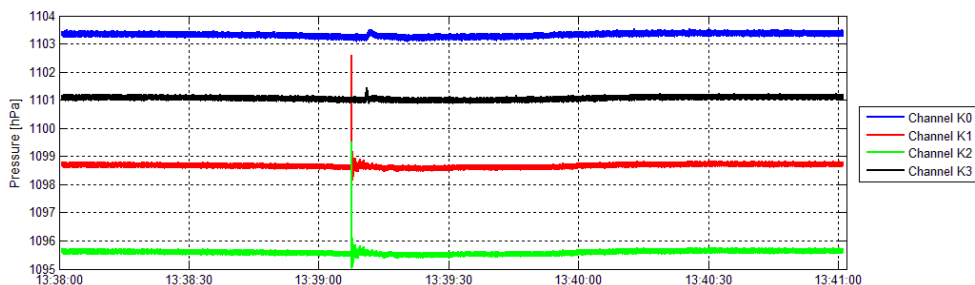


Figure 72. Changes in pressure caused by operation of a shearer and a power support

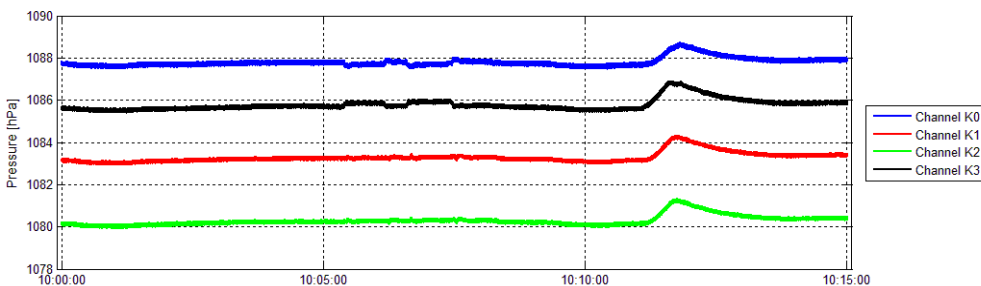


Figure 73. Changes in pressure caused by a change of atmospheric pressure

The trials in the mine have shown that the system for fast measurements of pressure was working properly from the technical point of view. The measuring data from the sensors were transmitted smoothly at a distance of more than 6 km and then were recorded in the system located on the surface. All measuring data collected during the trials were analysed.

The analysis of tolerable and non-tolerable levels of changes in pressure

Six measuring results selected from the recorded changes in pressure were analysed. i.e.:

- three cases of changes in pressure caused by opening the air dam located in the raise 5 in the seam 402, between the roads 5 and 4;
- two cases of changes in pressure caused by operation of a shear and movement of a power support;
- one case of changes in pressure in the face area caused by a change in atmospheric pressure.

The analysis was made according to the method described previously. The following assumptions were applied for calculations:

- a reference (base) value of the pressure difference ΔP_B , between intake air ΔP_D (sensor K0) and return air ΔP_O (sensor K3) when the air dams were closed; the measurements were made in the period of stabilized, constant atmospheric pressure;
- it was determined a minimum value of pressure difference ΔP_A between intake air ΔP_D (sensor K0) and return air ΔP_O (sensor K3) during emergency state of ventilation (the air dams opened, operation of the shearer, change in atmospheric pressure) made in the same period of stabilized, constant atmospheric pressure;
- it was calculated a reference value of the pressure as a difference between a base difference of changes in pressure ΔP_B and a minimum value of pressure difference ΔP_A . This value is a reference point for determining the tolerable, non-tolerable and critical changes in pressure;
- it was defined a range of tolerable changes in pressure ΔP_T up to 20% difference between the base and minimum values.

Depending on a level of hazards occurring in a given area, it is required to develop procedures on dynamic changes in barometric pressure:

- non-tolerable ΔP_N , i.e. which exceed the tolerable changes, but which are below a value of 50% not exceeding the base difference ΔP_B and the minimum difference ΔP_A .
- critical ΔP_K , which exceed 50% of difference between the base difference ΔP_B and the minimum difference ΔP_A , as well as to inform the persons responsible for safety monitoring in the area about the above mentioned values.

Analysis of the measuring results of 20.12.2016

A change in pressure in the working face area caused by opening the air dam in the raise 5 was analysed. This change causes a step change in indications of the sensors K0 and K3 (the indications aim at equating), located close to the air dam. There were observed to a lesser extent the step changes in pressure measured by the sensors K1 and K2 (Figure 74).

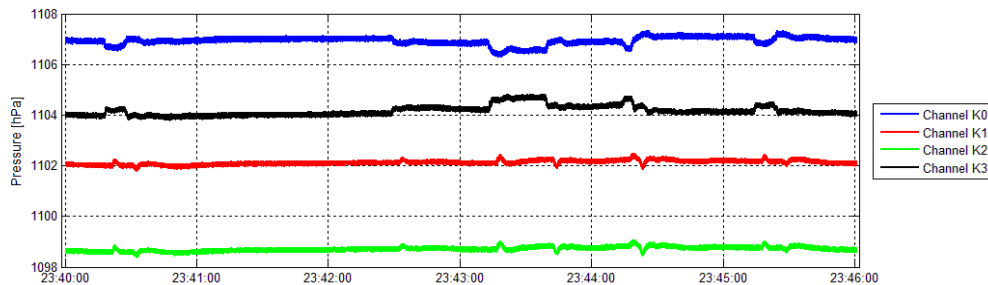


Figure 74. Analysed course of changes in pressure recorded in the face area caused by opening the air dam

Calculations:

$$\Delta P_B = K0 - K3 = 2.70 \text{ hPa}$$

$$\Delta P_A = K0 - K3 = 1.83 \text{ hPa}$$

$$\Delta P_B - \Delta P_A = 0.87 \text{ hPa}$$

$$\Delta P_T = <20\% (\Delta P_B - \Delta P_A) \Rightarrow < 0.174 \text{ hPa}$$

$$\Delta P_N = 20\text{-}50\% (\Delta P_B - \Delta P_A) \Rightarrow 0.174 - 0.435 \text{ hPa}$$

$$\Delta P_K = >50\% (\Delta P_B - \Delta P_A) \Rightarrow > 0.435 \text{ hPa}$$

The results of calculations are presented in Table 12.

Table 12. Results of calculations for the data recorded on 20.12.2016

| Measuring channel | Normal state [hPa] | Emergency condition [hPa] | Δ [hPa] |
|-------------------|--------------------|---------------------------|----------------|
| K0 | 1107.02 | 1106.61 | -0.41 P_N |
| K1 | 1102.18 | 1102.42 | +0.24 P_N |
| K2 | 1098.77 | 1099.07 | +0.30 P_N |
| K3 | 1104.32 | 1104.78 | +0.46 P_K |

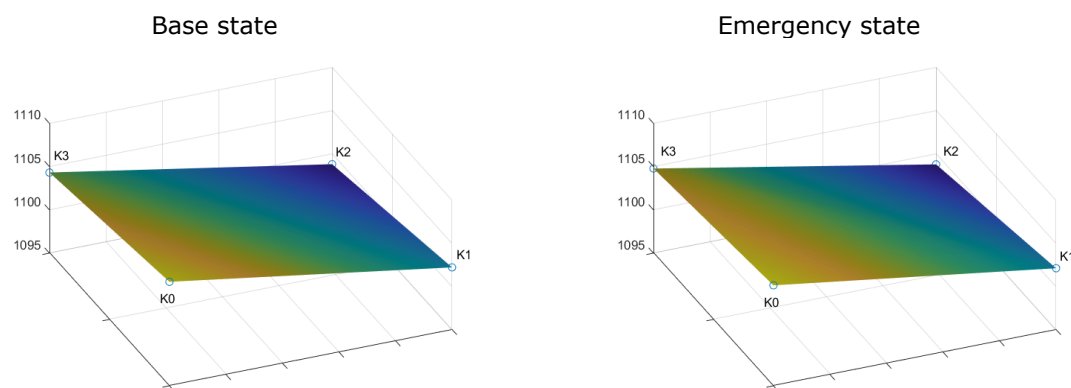


Figure 75. Visual summary of measuring results for a normal state and an emergency state during opening the air dam in the raise 5

Analysis of the measuring results of 06.12.2016

A change in pressure in the working face area caused by operation of a shearer and a power support was analysed. This change causes a step change in indications of the sensors K1 and K2, located close to the working face. There were observed to a lesser extent and time delayed the step changes in pressure measured by the sensors K0 and K3 (Figure 76).

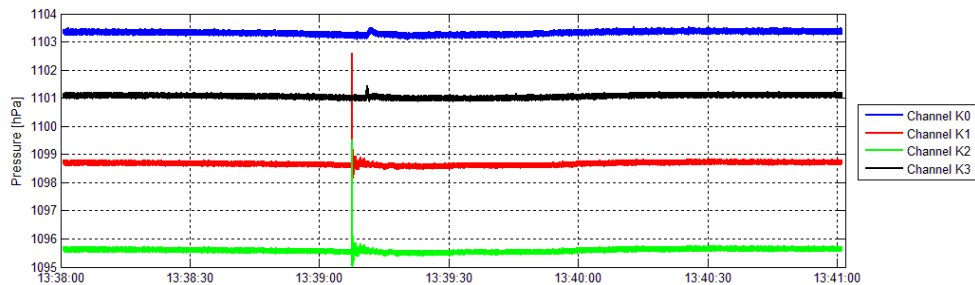


Figure 76. Analysed course of changes in pressure recorded in the face area caused by operation of a shearer and a power support

Calculations:

$$\Delta P_B = K0 - K3 = 2.23 \text{ hPa}$$

$$\Delta P_A = K0 - K3 = 2.12 \text{ hPa}$$

$$\Delta P_B - \Delta P_A = 0.11 \text{ hPa}$$

$$\Delta P_T = <20\% (\Delta P_B - \Delta P_A) \Rightarrow < 0.022 \text{ hPa}$$

$$\Delta P_N = 20\text{-}50\% (\Delta P_B - \Delta P_A) \Rightarrow 0.022 - 0.055 \text{ hPa}$$

$$\Delta P_K = >50\% (\Delta P_B - \Delta P_A) \Rightarrow > 0.055 \text{ hPa}$$

The results of calculations are presented in Table 13.

Table 13. Results of calculations for the data recorded on 6.12.2016

| Measuring channel | Normal state [hPa] | Emergency condition [hPa] | Δ [hPa] | |
|-------------------|--------------------|---------------------------|----------------|-------|
| K0 | 1103.34 | 1103.57 | +0.23 | P_K |
| K1 | 1098.69 | 1102.50 | +3.81 | P_K |
| K2 | 1095.65 | 1099.51 | +3.86 | P_K |
| K3 | 1101.11 | 1101.45 | +0.34 | P_K |

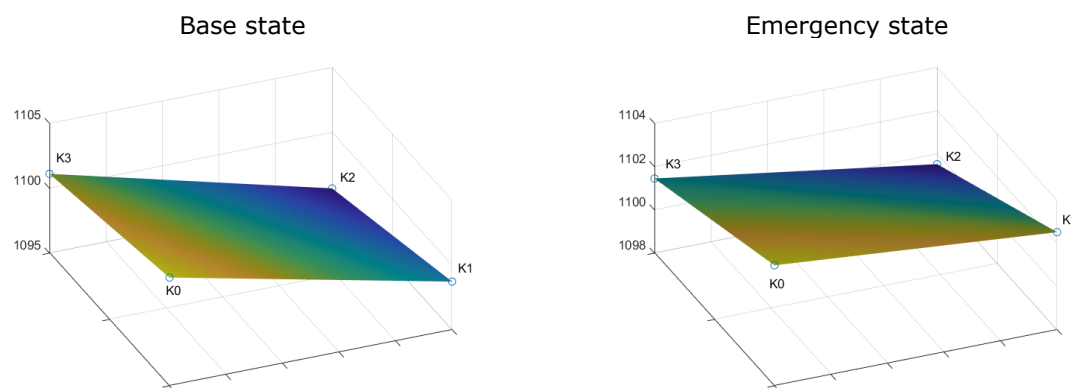


Figure 77. Visual summary of measuring results for a normal state and an emergency state during operation of a shearer and a power support

Analysis of the measuring results of 12.12.2016

A change in pressure in the working face area caused by a change in atmospheric pressure was analysed. This change causes a gradual increase and then a decrease in indications of all sensors. A value of increases is comparable for all sensors (Figure 78).

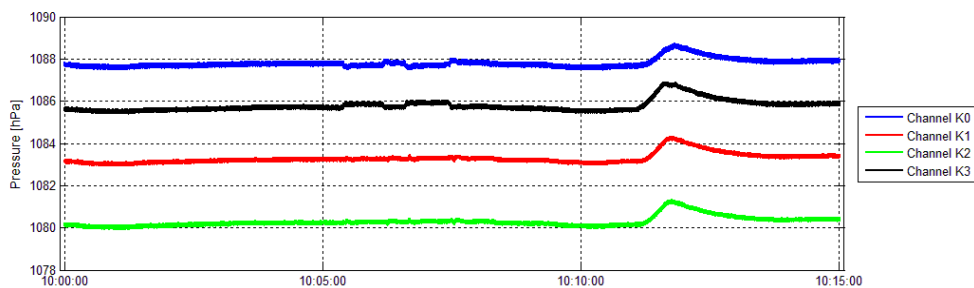


Figure 78. Analysed course of changes in pressure recorded in the face area caused by a change of atmospheric pressure

Calculations:

$$\Delta P_B = K0 - K3 = 1.97 \text{ hPa}$$

$$\Delta P_A = K0 - K3 = 1.84 \text{ hPa}$$

$$\Delta P_B - \Delta P_A = 0.13 \text{ hPa}$$

$$\Delta P_T = <20\% (\Delta P_B - \Delta P_A) \Rightarrow < 0.026 \text{ hPa}$$

$$\Delta P_N = 20-50\% (\Delta P_B - \Delta P_A) \Rightarrow 0.026 - 0.065 \text{ hPa}$$

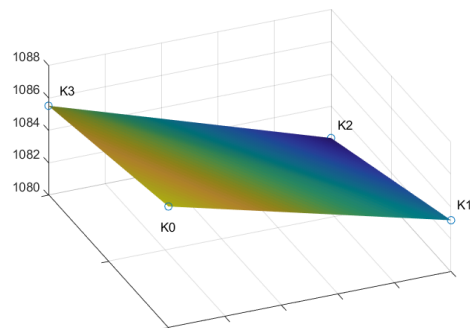
$$\Delta P_K = >50\% (\Delta P_B - \Delta P_A) \Rightarrow > 0.065 \text{ hPa}$$

The results of calculations are presented in Table 14.

Table 14. Results of calculations for the data recorded on 12.12.2016

| Measuring channel | Normal state [hPa] | Emergency condition [hPa] | Δ [hPa] | |
|-------------------|--------------------|---------------------------|----------------|-------|
| K0 | 1087.48 | 1088.74 | +1.26 | P_K |
| K1 | 1083.16 | 1084.48 | +1.32 | P_K |
| K2 | 1080.05 | 1081.34 | +1.29 | P_K |
| K3 | 1085.51 | 1086.90 | +1.39 | P_K |

Base state



Emergency state

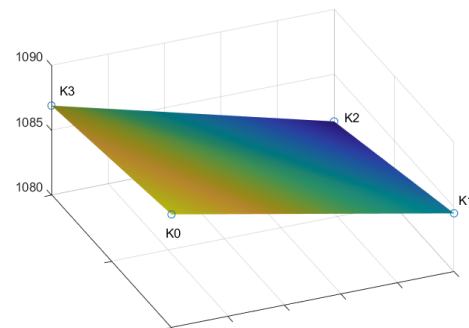


Figure 79. Visual summary of measuring results for a normal state and an emergency state during a change in atmospheric pressure

Conclusions

Explosion tests at Experimental Mine Barbara

The Table 15 shows the results of calculations of the initiation place of methane explosion generated by the Program. calculated on the basis of the recorded changes in pressure in comparison with the actual values defined in the experiment.

Table 15. Results of calculations of the initiation place of methane explosion

| Item | RESULT EMAG [m] | RESULT GIG [m] | DIFFERENCE [m] | COMMENTS |
|------|--|--|----------------|---|
| 1. | 73 | 80 | 7 | - |
| 2. | 99 | 100 | 1 | - |
| 3. | 74 | 60 | 14 | the range of the pressure sensor was exceeded |
| 4. | 66 | 40 | 26 | the range of the pressure sensor was exceeded |
| 5. | - | 30 | - | no indications from the sensor K4 |
| 6. | 30 in the perpendicular crosscut at the crossing with a gallery parallel to the main gate. | 30 in the perpendicular crosscut at the crossing with a gallery parallel to the main gate. | 1 | - |

In case of the measurements of pressure within the measuring range of the sensor Setra ($800 \div 1300$ hPa), the location of methane explosion is characterized by high accuracy – up to 10 m.

In case of the measurements of pressure made above the upper measuring range of the sensor Setra (more than 1300 hPa), the accuracy is good but worse than the accuracy in the measuring range of the Setra sensor. For the experiments carried out in the mine, the accuracy is at a level of 30 m.

This may be caused by:

- operation of the Setra sensor in the upper limit of the range.
- actuation of cut-off valves which were set to about 1200 hPa.
- estimated and not real maximum point of the pressure measurements.

Tests at KWK "Ruda-Ruch Halemba" mine

The trials in the mine showed that the system for fast measurements of pressure worked from the technical point of view correctly. The measuring data from the sensors were transmitted in the absence of any interference at a distance of more than 6 km and were recorded in the system at the surface. The analysis of measurements allowed to estimate the levels of pressure differences between intake and return air in the base and emergency state. Progressive or short-term stepwise changes in atmospheric pressure caused by operation of a shearer or a power support kept a comparable level of the pressure difference, while the analysis indicated possible occurrence of a dangerous change in pressure. In case of changes in pressure caused by opening/closing the dams, the determined levels of pressure differences showed which of them were contained in the allowable limits of changes in pressure and which of them should be treated as potentially dangerous situations.

Monitoring of the working face area with regard to changes in pressure in selected points and therefore between flowing over air stream and goaf including its significant vicinity, allows a rapid response to changes in equilibrium state. Due to continuous monitoring of aerodynamic potentials it is possible to update a potential diagram of a given area in normal conditions, as well as in hazardous situations.

Task 3.5. Definition of guidelines

Principles of use of pressure sensors

Location of installation of sensors

In order to evaluate properly the controlled working face area it is necessary to adjust the location of the sensors to the ventilation system. The principle is to locate an absolute pressure sensor PB in:

- workings with intake air – at a distance up to 20 m from a roadway crossing where the air stream is divided;
- workings with return air – at a distance up to 20 m from roadway crossing where the air stream is connected with another one.

See the examples shown in Figures 80, 81, 82 and 83.

The differential pressure sensor PR should be installed:

- in a working (in workings) with return air – at a distance up to 20 m from roadway crossing where the air stream is connected with another one. The examples in Figure 80, Figure 81, Figure 82 show this situation;
- in case of two workings behind the longwall – in each of them (the example in Figure 83).

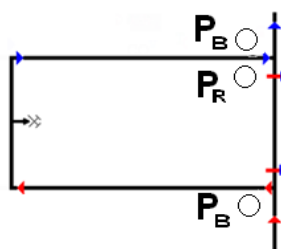


Figure 80. Example of location of absolute pressure sensors (PB) and differential pressure sensors (PR) for "U" ventilation system

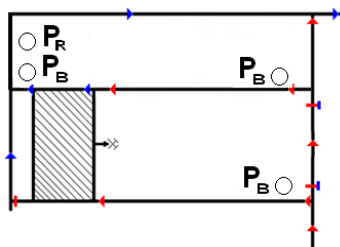


Figure 81. Example of location of absolute pressure sensors (PB) and differential pressure sensors (PR) for "Y" ventilation system

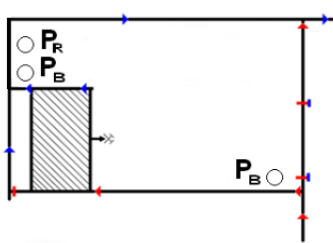


Figure 82. Example of location of absolute pressure sensors (PB) and differential pressure sensors (PR) for "Z" ventilation system

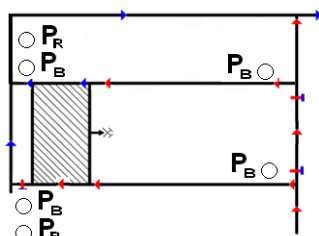


Figure 83. Example of location of absolute pressure sensors (PB) and differential pressure sensors (PR) for "H" ventilation system

Micro-barometric characteristic of a longwall area

When methane and spontaneous fire hazards co-occur, it is difficult to recognize a real level of danger. In the years 2003-2008, for 17 methane ignitions and explosions, 4 of them were caused by spontaneous fire and in two cases the spontaneous fire was one of the accepted reasons (Table 16).

Table 16. List of methane ignitions occurred in the years 2003-2013 caused by spontaneous fire in the mines in Poland

| No. | Name of mine | Date | Initializer | Place of event |
|-----|-------------------|-----------------|--|--|
| 1. | Bielszowice | 24.02.2003 | Spontaneous fire | Crossing of longwall and air roadway |
| 2. | Sośnica | 07.11.2003 | Spontaneous fire | Longwall goaf |
| 3. | Bielszowice | 12.02.2005 | Spontaneous fire | Longwall goaf |
| 4. | Halemba | 21.11.2006 | Reason for the event was not determined clearly (with 25% probability: caused by sparks of electrical devices. electrostatic discharges. spontaneous fire. sparking rocks) | Area of a liquidated longwall (including a part ventilated by separate ventilation) and main and tail gates |
| 5. | Mysłowice-Wesoła | 13.01.2008 | Spontaneous fire | Dammed roadway behind a face prepared for extraction |
| 6. | Borynia | 04.06.2008 | Reason for the event was not determined clearly (with 33% probability: a crack spontaneous fire. fire of polyurethane adhesives. earth fault) | Area of a working face (no winning operations at a production shift when the event happened) |
| 7. | Sośnica-Makoszowy | 09.05.2009 | Developing spontaneous fire in goaf of the longwall 412/1 | Longwall p43 in the seam 412/1 at the level of 850 m |
| 8. | Mysłowice-Wesoła | 16 i 17.05.2010 | Developing spontaneous fire in goaf of the longwall 565 | Eastern gallery I at the area of crossing with the longwall 565 in a seam layer 510 close to roof at the level 665 m |
| 9. | Sośnica-Makoszowy | 13.12.2013 | High temperature cause by self-heating of coal left in goaf of the longwall | Tail gate I101 of the longwall I101 in the seam 408/1 at the level of 950 m |

Implementation of recommendations of post-accidents commissions within barometric and differential pressure monitoring allow to determine the levels of tolerable and non-tolerable changes in pressure in a given area. On the other hand the development of knowledge about distribution of field of aerodynamic potentials in a given area allow to analyse and evaluate a flow of gases through goaf. Mainly it is a migration of oxygen that is significant for development of self-heating process; a migration of carbon monoxide (products of self-heating) that is significant for workings with flowing over air stream; and a migration of methane that is significant due to its possible outflow to flowing over air stream, as well as its movement to the place (a source) of self-heating process that may lead to the risk of methane ignition and explosion. Therefore the works have been undertaken on a barometric system which consists of:

- in the first place –an absolute pressure and optionally a differential pressure monitoring;
- in the long term – monitoring a distribution of field of aerodynamic potentials in area of a given longwall.

A field of aerodynamic potentials is changing due to the changes in air parameters and the changes in structure of a ventilation network or values of resistances of workings. The distribution of field of potentials is determined by measurements of an absolute pressure and temperature (dry and wet bulb) in selected points (nodes) of the ventilation system and at a pit-bank level. The measurements are made relatively rarely by means of hand-held instruments.

The values of potentials calculated on the basis of measurements made by means of hand-held instruments are affected by some uncertainty resulting from non-simultaneous measurements and dynamic changes in a ventilation network as well as from a human error. Implementation of continuous monitoring of aerodynamic potentials eliminates such errors and allows to update a potential diagram of a given area both in normal conditions and in hazardous situations.

Method of determination of the levels of changes in tolerable and non-tolerable pressures

Monitoring of the area as regards the changes in pressure in selected points and therefore between flowing over air stream and goaf and its significant vicinity allows a quick response to such change in steady-state. However not every change requires an intervention. Therefore it is important to determine for a given area the levels of changes in tolerable and non-tolerable pressure. This requires following actions:

- determining a base value of pressure difference ΔP_B between intake air stream (streams) ΔP_D and return air stream (streams) ΔP_O assuming a stabilization of a direction of flow and air stream volume (functional and closed air dams in the working face area) to be made during stabilized. constant atmospheric pressure;
- determining a base value of pressure difference ΔP_A between intake air stream (streams) ΔP_D and return air stream (streams) ΔP_O for emergency condition of ventilation (air dams opened) to be made in the same time of stabilized. constant atmospheric pressure;
- determining a range of tolerable changes in pressure ΔP_T between up to 10% or up to 20% of a difference between a reference base value and a minimum value.

According to a level of hazards occurring in a given zone it is required to develop procedures (by ventilation department officer) with regard to the dynamic changes in barometric pressure:

- non-tolerable ΔP_N , it means more than the tolerable changes and less than a value below 50% between the values of the base difference ΔP_B and the minimum difference ΔP_A .
- critical ΔP_K , i.e. which exceeds 50% of the difference between the values of the base difference ΔP_B and the minimum difference; and to inform of the procedures the persons responsible for monitoring of safety in a given area.

3.3.3 WP4 – Validation of explosion mitigation systems

WP Leader: **GIG**

Partners: **AITEMIN INERIS**

Task 4.1. Review of experiences

The Deliverable D11 was prepared. The objective of this document was to review and summarize the experiences held with triggered barriers at European level. It was mainly based on the activities in which the EXPRO partners AITEMIN, DTEK, GIG and INERIS have been directly involved, but it made also references to works carried out by other organizations.

There have been a series of experiences with different types of triggered barriers in the main coal mining regions in the world, but the results obtained are not fully satisfactory, and the actual fact is that the use of these systems is not a current practice today in most countries. In particular, triggered barriers are not used in western European countries.

3.3.4 WP5 – Integration of results and dissemination

WP Leader: **GIG**

Partners: **AITEMIN INERIS EMAG FSB PGG**

Task 5.1 Integration of results

The Final Report that integrates contributions from all participants has been prepared. The Report was stored in the common disk space of the Project.

Task 5.2 Dissemination activities

Several publications have been prepared and is planned:

- M.Malachowski, The use of the monitoring system of rapid pressure changes to the location of the explosion in underground, Scientific Seminar in ITI EMAG, 20th June 2017,
- M.Malachowski, D.Felka, K.Szczerba, Research on changes in the absolute pressure in the mining excavations for the detection of ventilation faults and the location of the ignition point of explosion, IV Polish Mining Congress, 20th November 2017,
- J. Daubech, Ch. Proust, E. Leprette, G. Lecocq (2018), Further insight into the gas flame acceleration mechanisms in pipes. Part I: experimental work, accepted for XII ISHPMIE, August 12-17th, Kansas City,
- G. Lecocq, E. Leprette, J. Daubech , Ch. Proust (2018), Further insight into the gas flame acceleration mechanisms in pipes. Part II: numerical work, accepted for XII ISHPMIE, August 12-17th, Kansas City,

- K. Cybulski, Z. Dyduch, R. Hildebrandt, H. Kopton, Development of a methane explosions in the underground experimental facilities of GIG EM Barbara, IV Polish Mining Congress, 20th November 2017,
- Results of project were also presented during meeting organized for directors of the mines and for staffs of the mines responsible for safety.

3.4 CONCLUSIONS

WP1 – Project coordination

The general management of technical works was conducted during the whole Project. All, five coordination meetings and one internal meeting of the simulation group were organized. The project website was created and updated. No important problems have been found relating to this work package.

As AITEMIN could no longer participate in EXPRO project starting from 16.11.2016 GIG replaced AITEMIN on the position of Project Coordinator. Despite of the change management of technical work was conducted as planned, including coordination meetings and exchange of experimental and numerical results. To facilitate the exchange a common disk space was made available for all participants.

WP2 – Development and calibration of explosion numerical models

A series of large scale methane explosion tests carried out at three different locations (at INERIS, GIG and FSB) provided experimental data necessary for calibration and verification of the numerical models. Apart from that the results provided a new insight into the explosion in different geometries, as well as the explosion development in inhomogeneous mixtures.

The numerical model for solving large-scale problems has been verified. Sover b-Xi based on the development of Gülder was implemented and verified. The obtained values of flame propagation velocity in a large scale (400 m gallery) are comparable in size to the order of magnitude with the results obtained in experimental studies. This proves the usefulness of the numerical methods used to conduct a large-scale event case study. Nevertheless, the method used to describe the geometry (domain) - a geometric description directly – provides a sufficient representation of details, but requires time (is time-consuming) to receive a solution to the problem. There is a large dependence between the representation of geometric details of the analysed space and the time needed to obtain a solution. This is a limitation in the application of the method to the analysis of very large spaces.

An alternative approach, unverified in the project, is the Porosity Distributed Resistance (PDR) approach method. This method allows to limit the number of finite volumes with the simultaneous definition of flow parameters in the area to be spoiled. The simplified area is not defined directly by a detailed representation of the geometry, but by a set of physical parameters present in the area.

Nevertheless, the b-Xi flame propagation model used in the project can be effectively used with the PDR method.

In the developed solution, models for a non-homogeneous gas mixture were used effectively. This is particularly important because of the practical application possibilities. In real situations, subject to analysis, almost always is deal with heterogeneous mixtures.

The numerical models developed and their verified in large scale conditions confirm the usability of the b-Xi model of flame propagation.

WP3 – Development of fast air pressure monitoring system

As a result of the works within the WP3 there have been developed the modified pressure sensors which met the given requirements. There has been developed a measuring system consisting of surface devices (a central station of the SP/DTSS system) and underground equipment (NSGP sensors). All devices included in the system have appropriate ATEX certificates which allow to use the system for operation in underground mines. The system software was developed which allowed data communication, data processing and measuring data archiving, as well as locating initial places of a possible explosion based on the recorded pressure measurements. A complete measuring system was tested during experiments of explosions carried out in the EM "Barbara" and under conditions of normal work in a mine in two areas. The trials carried out in the mine allowed to collect sufficient measuring data enabling to continue further works on development of system software. The trials allowed also to check functioning methods of the individual elements of the system in the mine conditions. On the basis of the stored changes in pressure during explosions there were calculated velocities of blast waves and response times of the pressure sensors. The response times of the sensors to rapid pressure jumps are very close to the response times determined in the laboratory within the Task T3.1 (35.7Hz). They confirm that the sensor SETRA Typ 278 meet the assumptions and technical requirements.

Software developed within the project allows archiving the measuring data and allows for on-going assessment and analysis of pressure levels in a given area of a mine. It allows also to detect with high accuracy a place of a possible explosion on the basis of indications of the sensors.

The results of calculations of the initiation place of methane explosion generated by the Program, calculated on the basis of the recorded changes in pressure in comparison with the actual values defined in the experiment shows that the location of methane explosion is characterized by high accuracy – up to 10 m.

The trials in the mine showed that the system for fast measurements of pressure worked, from the technical point of view, correctly. The measuring data from the sensors were transmitted in the absence of any interference at a distance of more than 6 km and were recorded in the system at the surface. The analysis of measurements allowed to estimate the levels of pressure differences between intake and return air in the base and emergency state. Progressive or short-term stepwise changes in atmospheric pressure caused by operation of a shearer or a power support kept a comparable level of the pressure difference, while the analysis indicated possible occurrence of a dangerous change in pressure. In case of changes in pressure caused by opening/closing the dams, the determined levels of pressure differences showed which of them were contained in the allowable limits of changes in pressure and which of them should be treated as potentially dangerous situations.

Monitoring of the working face area with regard to changes in pressure in selected points and therefore between flowing over air stream and goaf including its significant vicinity, allows a rapid response to changes in equilibrium state. Due to continuous monitoring of aerodynamic potentials it is possible to update a potential diagram of a given area in normal conditions, as well as in hazardous situations.

WP4 – Explosion mitigation systems

The Workpackage was cancelled after preparing the *Review of European experiences in the use of triggered barriers* (Deliverable D11). In the Review the following general conclusion were formulated.

Developing a triggered barrier system capable to stop methane explosions at an early stage has been a common objective in most coal mining countries across Europe. There has been a significant number of research projects on this field, as well as many validation experiments in controlled conditions. The concept of all the systems developed so far has been very similar, although there are differences in the specific design and the technologies involved.

The results obtained in the different series of experimental tests carried out in the last two decades have been good in general terms, although it has not been possible to assure a 100 % of the reliability in the operation and efficiency of the barriers. The capacity of the triggered barriers to stop an explosion strongly depends on the explosion parameters and the gallery dimensions, and therefore it is not possible to find a general solution for all situations. Each specific explosion scenario requires an individual analysis.

All this, together with the high price of this type of equipment, and other practical constraints, such as their large size, and the difficulties to install, move and maintain the units underground, have probably prevented the general deployment of the triggered barriers at European level.

The practical experiences on the efficiency of triggered barriers to stop an explosion in real conditions is therefore very limited, and, according to the review made, is mainly concentrated in Ukraine. The experience in this country proves that the reliability of the triggered barriers is not as good as it should be.

In any case, the interest in finding a triggered barrier system that can provide a reasonable level of protection still continues, and in particular a new generation of devices is being developed in Ukraine. One of the objectives of the EXPRO project was to follow these new developments and in particular to carry out validation tests with these new systems.

WP5 – Integration of the results and dissemination

The Final Report that integrates contributions from all participants has been prepared. The Report was stored in the common disk space of the Project.

Several publications have been prepared and published. Some other have been accepted for the next ISPMIE Conference that will be held in August this year, in Kansas City, USA.

3.5 EXPLOITATION AND IMPACT OF THE RESEARCH RESULTS

WP1 – Project coordination

This Workpackage has no any impact.

WP2 – Development and calibration of explosion numerical models

The numerical models developed in the Project allow for at least qualitative prediction of the methane explosion development in large confined volumes. They allow modelling of the explosion both in a homogenous and inhomogeneous mixtures. They can also be used to predict distribution of methane concentration after its releases in different conditions. Therefore the model may be seen as a bridgehead for further development and adaptation to many practical applications.

Possible applications of the models include:

- Possibility to conduct post-factum event analysis, case scenario analysis.
- Analysis of events in underground gallery, excavations, tunnels etc.
- Analysis of possible flame propagation scenarios in various industry sectors where there is a risk of explosion.
- Educational application - for a better understanding of the phenomenon.

The large scale test of methane release and its subsequent explosion revealed several important phenomena:

- Abrupt release of large amount of methane in a mine working where an air flow is marginal, i.e. < 0.5 m/s, results in formation of a methane layer under the roof along a long distance. Ignited, the layer burns with the flame front speed of a few meters per second.
- Continuous release of large amount of methane into a mine working yields similar results.
- An increase of turbulence in the methane jet significantly improves mixing. The mixture, when ignited, develops into an explosion.
- Many factors influence the distribution of methane concentration and the explosion development.

Those information helps to better understand the development and consequences of methane explosions that occurred in underground mine workings.

WP3 – Development of fast air pressure monitoring system

During mining operations in the deep coal mines there may occur hazards which can cause emergency states (transient states) in the ventilation system.

The reasons for hazards (emergency states), disturbances and changes in ventilation conditions are mining operations and natural factors like:

- underground fires;
- methane and/or coal dust explosions;
- sudden gas emission;
- sudden outflow of gases (methane, coal monoxide, coal dioxide, nitrogen) from goaf;
- high power rock bumps (rock bursts);
- outbursts of gas and rock.

The aim of works was realization of one of few demands of after-accident commissions relating to investigation of circumstances and reasons for fires and explosions, as well as group accidents at work in the mines. The commissions have recommended extending automatic gasometry systems by measurements of absolute pressure at longwall areas with methane (II-IV categories), fire, methane and coal dust explosion, and rock burst hazards. It is very crucial to determine a place where an explosion occurred. This can be determined with sufficient accuracy by quick measurements of propagated waves of air pressure from a source of explosion or other sudden events. The area is very devastated after the explosion and the after-accident commissions are not able to determine a reason for explosion and a place of its initiation on the basis of the used monitoring methods. The aim of works within the project was to extend functions of monitoring systems designed for mine atmosphere by measurements and analyses of quick (rapid) changes in absolute air pressure in the underground mines for preventive purposes. The measurements allow to archive data and to use them for analyses of reasons for occurrence of disasters.

System for fast air pressure monitoring developed during the project is the first of its kind innovative system enabling continuous control of pressure parameters in mines. Its application allows not only for current control of ventilation conditions but also for post-accident analyzes and online determining for a given area the levels of changes in tolerable and non-tolerable pressure.

The results of work were presented on ITI EMAG seminar on 20.06.2017 "The application of a system for monitoring rapid pressure changes to the location of an explosion site in underground excavations" and on IV Polish Mining Congress in Cracow (20-22.11.2017) "Research on changes in the absolute pressure in the excavations for the detection of faults and the location of the place of explosion".

The developed solution of fast air pressure monitoring system was also presented in State Mining Authority and The Strata Mechanics Research Institute of Polish Academy of Sciences. Representatives of both organizations showed great interest in the system promotion and assistance in implementation.

WP4 – Explosion mitigation systems

The Workpackage was cancelled after the preparation of Review of European experiences in the use of triggered barriers. Therefore no research has been carried out.

WP5 – Integration of the results and dissemination

Several papers on both experimental results and numerical models have been prepared and are planned:

- M.Malachowski, The use of the monitoring system of rapid pressure changes to the location of the explosion in underground, Scientific Seminar in ITI EMAG, 20th June 2017.
- M.Malachowski, D.Felka, K.Szczerk, Research on changes in the absolute pressure in the mining excavations for the detection of ventilation faults and the location of the ignition point of explosion, IV Polish Mining Congress, 20th November 2017.
- J. Daubech, Ch. Proust, E. Leprette, G. Lecocq (2018), Further insight into the gas flame acceleration mechanisms in pipes. Part I: experimental work, accepted for XII ISHPMIE, August 12-17th, Kansas City.
- G. Lecocq, E. Leprette, J. Daubech , Ch. Proust (2018), Further insight into the gas flame acceleration mechanisms in pipes. Part II: numerical work, accepted for XII ISHPMIE, August 12-17th, Kansas City.
- K. Cybulski, Z. Dydych, R. Hildebrandt, H. Kopton, Development of a methane explosions in the underground experimental facilities of GIG EM Barbara, IV Polish Mining Congress, 20th November 2017.
- Presentation of EXPRO Project at GMI Coal Subcommittee Meeting and 12th Session of UNECE Group of Experts on Coal Mine Methane, Geneva, 23-25 October 2017.
- Results of project were also presented during meeting organized for directors of the mines and for staffs of the mines responsible for safety.

4 LIST OF ACRONYMS AND ABBREVIATIONS

A/C: Alternate current
AITEMIN: Asociación para la investigación y el desarrollo industrial de los recursos minerales (Spain)
ARAMIS M/E: Seismic system equipped with digital transmission of seismic signals
ASVP: Automatic Explosion Suppression System
ATEX: EU directives about explosive atmosphere. TEX derives its name from the French title of the 94/9/EC directive: Appareils destinés à être utilisés en ATMosphères EXplosibles.
Bit: Binary digit
CARDPAC: Card Packet System
CFD: Computational Fluid Dynamics
CIRCABC: Communication and Information Resource Centre for Administrations.
Businesses and Citizens
CMC: Computer-mediated communication
DAQ: Data Acquisition
DC: Direct Current
DPT sensor: Differential Pressure Transmitter sensor
DTEK: Energy company in Ukraine
DTSS: Digital Topographic Support System
EMAG: Instytut Technik Innowacyjnych (Poland)
EXPRO: Prediction and Mitigation of Methane Explosions Effects for Improved Protection of Mine Infrastructure and Critical Equipment
FLACS: FLame ACceleration Simulator
F-RAM: Ferroelectric Random Access Memory
FS: Full Scale
FSB: Fundación Santa Bárbara (Spain)
FTDI cable: Future Technology Devices International cable
GIG: Glowny Instytut Gornictwa (Poland)
GPS: Global Positioning System
IMG PAN: Instytut Mechaniki Górotworu Polskiej Akademii Nauk
INERIS: Institut National de l'Environnement industriel et des Risques (France)
IP: Ingress Protection
KISTLER: Manufacturer of Pressure sensors
KWK: Kopalnia Węgla Kamiennego (Poland)
LABView: Laboratory Virtual Instrumentation Engineering Workbench
LCD: Liquid crystal display
LED: Light-emitting diode
MATLAB: MATrix LABoratory
NITROCORD: penthrite detonating cords for rocks
NSGP transmitter: Gas Pressure transmitter
OCGA: Official Code of Georgia Annotated
PC: Personal Computer
PGG: Polska Grupa Górnicza (Poland)
RANS: Reynolds-averaged Navier-Stokes equations
RFCS: Research Fund for Coal and Steel
SLVA: Automatic Explosion containment System
SEMP: System Engineering Management Plan
SPI seismometer: Seismic Platform Interferometer
SETRA: USA manufacturer of pressure transducers, transmitters, capacitive pressure sensors and acceleration sensing devices.
St: Turbulent flame speed
TGC: Technical Group
THP-2 sensor: High pressure sensor
USA: United States of America
UART: Universal Asynchronous Receiver-Transmitter
WP: Work Package

5 LIST OF REFERENCES

1. "MINFIREX" Project Final Report RFCR-CT-2010-00005. "WP4 - Effective explosion protection". March 2014.
2. Aitemin. "Estudio y análisis de las Barreras Activas europeas. Aplicación a las explotaciones por sutiraje de la Cuenca Central Asturiana". Febrero 1993.
3. Aitemin. "Improving productivity by reducing explosion risks in special mining conditions". ECSC Agreement n° 7220-AC/759. October 1995 - September 1997.
4. Aitemin. "Sistema de Confinamiento de explosiones para explotaciones por subniveles". Proyecto OCICARBÓN C-13.423. Octubre 1998.
5. Budziszewski A., Mróz J., Szczygielska M., Stacjonarny czujnik do ciągłego pomiaru parametrów fizycznych powietrza i obliczania potencjałów aerodynamicznych. Mechanizacja i Automatyzacja Górnictwa. nr 12/2008. s. 41-45.
6. C. J. Lea. H. S. Ledin MSc PhD DIC. Fire and explosion group. "A Review of the State-of-the-Art in Gas explosion modelling" HSL/2002/02. Health&Safety laboratory. 2002.
7. Cybulski W. Badania nad przebiegiem wybuchu metanu w zależności od warunków zapoczątkowania wybuchu. Państwowe Wydawnictwo Techniczne. Katowice 1953.
8. DTEK. "ASVP-LV explosion suppression system. Internal document. 2015.
9. DTEK. "Automatic explosion isolation system SLVA.0. Operating manual. 1811.00.00.000RE. 2012.
10. Du Plessis. J.J., "Active barrier performance preventing methane explosion propagation". University of Pretoria. 2014.
11. Dyduch Z., Doświadczalny model przenoszenia wybuchu pyłu węglowego w wyrobiskach górniczych. Praca Doktorska GIG. Katowice 1995.
12. European Standard EN 14591:2007 "Explosion Prevention and Protection in Underground Mines - Protective systems".
13. Fuchs. Elmar. "Explosion protection and prevention in mining" 2007.
14. Goffart. P. R., "Arrêt Barrage a déclenchement. Système Belge". Convention CECA n° 7258-03/09/02. Rapport Final. 1993.
15. Goffart. P. R., "European Triggered Barrier – Experimental Results of the year 1994". December. 1995.
16. Goffart. P. R., "The Belgian Triggered Water Barrier – A summary". 1988.
17. Johannes Jacobus Labuschagne du Plessis and Helmut Späth. Uni9versity of Wollongong. "Active barrier performance preventing methane explosion propagation". 2014.
18. Kielar J., Wasilewski S., Pomiary ciśnienia bezwzględnego w kopalniach głębinowych. Mechanizacja i Automatyzacja Górnictwa nr 5/2001.
19. Lebecki K., Teoretyczna analiza przebiegu wybuchu pyłu węglowego w typowych warunkach górniczych. Praca Doktorska GIG. Katowice 1976.
20. Ljiljana Medic-Pejic a. Javier Garcia-Torrent. Nieves Fernandez-Añez a & Kazimierz Lebecki. "Experimental study for the application of water barriers to Spanish small cross section galleries. School of Mines and EnergyEngineering. Technical University of Madrid. Madrid. Spain. Official Laboratory of J.M. Madariaga Madrid. Spain. School of Occupational Safety. Katowice. Poland.
21. L. Medic Pejic; J. García Torrent; E. Querol Aragón; L. Montenegro Mateos. Departamento de Ingeniería Química y Combustibles. Universidad Politécnica de Madrid. Laboratorio Oficial J.M. Madariaga. C/ Eric Kandel. 1 - (TECNOGETAFE). Parque Científico y Tecnológico de la UPM. 28906 Getafe (Madrid). "Application of protection means against explosions in underground mines". 2012.
22. Miernik ciśnienia BAR. Materiały informacyjne Instytutu Mechaniki Górotworu PAN.
23. Mine Safety Operations Division. New South Wales Department of Primary Industries "Guideline for coal dust explosion prevention and suppression". 2001
24. Opracowanie modelu urządzenia do pomiaru ciśnienia bezwzględnego zbudowanego w oparciu o nową generację czujników oraz oprogramowania niezbędnego do opracowania wyników pomiarów. Praca statutowa Centrum EMAG (2007-2008).
25. Pritchard. D. K., "Review of explosion mitigation measures for platform legs". Health and Safety Laboratory (HSL/2006/64). 2006.
26. Proust Ch., Postic J., "Efficacité des arrêts-barrages déclenchés contre les explosions en cul-de-sac". convention CECA n° 7258/03/152/03. rapport INERIS EXI-CPr/DG F41c/43 (in French). 1991.
27. Rae. D. "Experimental coal-dust explosions in the Buxton full-scale surface gallery, IX- Assymetry in water and stone-dust barriers and in coal-dust deposits". Health and Safety Executive.
28. Rae. D., West. L.C. and Brookes. D.E. "Experimental coal-dust explosions in the Buxton full-scale surface gallery. X-tess during the development of the Mark II water dispersers for triggered Barriers". Health and Safety Executive.
29. Riebuck. B. and Rooker. K. "An automatic system for coal-dust explosions" Health and Safety Executive.
30. Roux P., Proust Ch., "Protection des culs de sac contre les explosions par arrêt barrage déclenchés". convention CECA n° 7262/32/226/03. rapport INERIS EXI-PRO/DG F41c/60 (in French). 1995.

31. Roux P., Proust Ch., "Recherche de la meilleure efficacité de la dispersion d'eau des arrêts-barrages déclenchés dans des conditions particulières". convention CECA n° 7220-1C/759. rapport INERIS EXI-Pro-CPr/MCh/DG-98-15 AP03/HBL (in French). 1998.
32. Sapko. M.J. Furno. A.L. and Kuchta. J.M. "Quenching methane-air ignitions with water sprays. U.S Bureau of Mines report of Investigations 8214.
33. Sprawozdanie Komisji powołanej decyzją Prezesa Wyższego Urzędu Górnictwa z dnia 5 czerwca 2008 r. dla zbadania przyczyn i okoliczności zapalenia i wybuchu metanu oraz wypadku zbiorowego. zaistniałych w dniu 4 czerwca 2008 r. w Jastrzębskiej Spółce Węglowej S.A., Kopalni Węgla Kamiennego „Borynia” w Jastrzębiu Zdroju".
34. System ARAMIS M/E. Materiały informacyjne Centrum Transferu Technologii EMAG.
35. Trenczek S., Rozszerzenie kontroli w rejonach ścian wydobywczych o pomiary ciśnienia w aspekcie zagrożenia wybuchowego. Mechanizacja i Automatyzacja Górnictwa. Nr 1/2010.
36. Wasilewski S., Nowoczesne przyrządy do pomiarów i rejestracji parametrów procesu wentylacji. Materiały seminaryjne XXII Dni Techniki ROW'96 – 10.1996.
37. Wytyczne stosowanie czujników pomiaru ciśnienia. Opracowanie Centrum Elektryfikacji i Automatyzacji Górnictwa EMAG. Katowice 2009. niepublikowane.
38. Zou D.H., Panawalage. S. "Passive and Triggered Explosion Barriers in Underground Coal Mines. A literature review of recent research". CANMET. Natural Resources Canada. 2001.
39. Investigation of flame emission and absorption spectroscopy using the HITRAN/HITEMP database and simulations for concentration and temperature determination in combustion environments. Lindecrantz. Susan. Master of Science Thesis - May. 2010. Lund Report on Combustion Physics. LRCP-140. Lund. Sweden.
40. Miniature infrared emission based temperature sensor and light-off detektor. Sivathanu. Yudaya R., Gore Jay P. and Yingjie Zhu. 1999. ATS program (Contract no. 96-01-SR044). 1003 Chafee Hall. Thermal Sciences and Propulsion Center Purdue University. West Lafayette. IN 47906.
41. PDA20H EC. Thorlabs. 2015. (www.thorlabs.com).
42. Combustion Model to a Turbulent Mixing Layer. Twenty-Seventh Symposium (International) on Combustion/ The Combustion Institute.
43. O.L. Gülder. 1990. Turbulent Premixed Flame Propagation Models for Different Combustion Regimes. Twenty-Third Symposium (International) on Combustion. The Combustion Institute.
44. ECSC RESEARCH N` 7262/03/312. European triggered barrier. Experimental Results of the year 1988 referring to the Final Report of the ECSC RESEARCH N` 7258/03/099/02. by P.R. Goffart (Belgium).
45. ECSC RESEARCH N` 7262/03/312. European triggered barrier. Experimental Results of the year 1994 and 1995. by P.R. Goffart (Belgium).
46. ECSC RESEARCH N` 7262/03/312. European triggered barrier. Experimental Results of the year 1994 and 1995. by P.R. Goffart (Belgium).
47. F.R. Menter, M. Kuntz, and R. Langtry. Ten years of industrial experience with the SST turbulence model. In *Proceedings of the fourth international symposium on turbulence, heat and mass transfer*, pages 625–632, Antalya, Turkey (2003). Begell House.
48. C. Madhav Rao Vendra, J.X. Wen, V.H.Y. Tam(2013). Numerical simulation of turbulent flame-wall quenching using a coherent flame model. Journal of Loss Prevention in the Process Industries, 26, 363-368.
49. F. Liu. A thorough description of how wall functions are implemented in OpenFoam. Chalmers university (2017).
50. H. Xiao et al., Experimental and numerical investigation of premixed flame propagation with distorted tulip shape in a closed duct, Combust. Flame 159 (2012) pp. 1523-1538.
51. Combustion Model to a Turbulent Mixing Layer, Twenty-Seventh Symposium (International) on Combustion/ The Combustion Institute.
52. O.L. Gülder. 1990. *Turbulent Premixed Flame Propagation Models for Different Combustion Regimes*, Twenty-Third Symposium (International) on Combustion. The Combustion Institute.
53. KERAMPRAN S. (2000), "Etude des mécanismes d'accélération des flammes se propageant depuis l'extrémité fermée vers l'extrémité ouverte de tubes horizontaux de longueur variable", thèse de docteur de l'Université de Poitiers soutenue le 14 décembre 2000 à Poitiers.
54. <http://www-ccrt.cea.fr/>.

Getting in touch with the EU

In person

All over the European Union there are hundreds of Europe Direct information centres. You can find the address of the centre nearest you at: https://europa.eu/european-union/contact_en

On the phone or by email

Europe Direct is a service that answers your questions about the European Union. You can contact this service:

- by freephone: 00 800 6 7 8 9 10 11 (certain operators may charge for these calls),
- at the following standard number: +32 22999696 or
- by email via: https://europa.eu/european-union/contact_en

Finding information about the EU

Online

Information about the European Union in all the official languages of the EU is available on the Europa website

at: https://europa.eu/european-union/index_en

EU publications

You can download or order free and priced EU publications at:

<https://publications.europa.eu/en/publications>. Multiple copies of free publications may be obtained by contacting Europe Direct or your local information centre (see https://europa.eu/european-union/contact_en).

EU law and related documents

For access to legal information from the EU, including all EU law since 1952 in all the official language versions,

go to EUR-Lex at: <http://eur-lex.europa.eu>

Open data from the EU

The EU Open Data Portal (<http://data.europa.eu/euodp/en>) provides access to datasets from the EU. Data can be downloaded and reused for free, for both commercial and non-commercial purposes.

This report summarizes the work undertaken and the results obtained in the Project from its beginning on 01/07/2014 to the end on 31/12/2017.

The work in Task 2.2 *Model development* was delayed because of a large computer runtime of the models developed. That was the primary reason for applying for time extension of the Project. By Amendment No. 2 of European Commission Project duration was modified. New duration was 42 months.

All activities planned in the Project have been completed with the exception of WP4. As DTEK was not able to participate in the Project it was agreed by European Commission to cancel further activities in WP4 after finishing Task 4.1 *Review of experience*. The Task was concluded with Deliverable D11 *Report on the review of European experiences in the use of triggered barriers*.

During the project, the project team was altered. As AITEMIN was not able to continue its activities in the Project, from the 16/11/2016 it was withdrawn as a coordinator and GIG was approved as a new Project coordinator. Also, GIG took over the position of WP1, WP2 and WP5 leader.

The most important results of the Project are:

- Development of the fast air pressure monitoring system, the software that controls the system and validation tests performed in large scale methane explosions and in real mining condition.
- Numerical models of methane explosions.
- Experimental data gathered in large scale tests performed at three different test sites: INERIS, GIG and FSB.

Studies and reports

